

WATER POLLUTION POTENTIAL OF RAINFALL ON  
SPENT OIL SHALE RESIDUES

by

J. C. Ward  
G. A. Margheim  
G. O. G. Löf

Sanitary Engineering Program  
Department of Civil Engineering  
Colorado State University  
Fort Collins, Colorado 80521

for the

WATER QUALITY OFFICE  
ENVIRONMENTAL PROTECTION AGENCY

Grant No. 14030EDB  
August, 1971

## EPA Review Notice

This report has been reviewed by the Water Quality Office, EPA, and approved for publication. Approval does not signify that the contents necessarily reflect the views and policies of the Environmental Protection Agency, nor does mention of trade names or commercial products constitute endorsement or recommendation for use.

## ABSTRACT

Physical properties, including porosity, permeability, particle size distribution, and density of spent shale from three different retorting operations, (TOSCO, USBM, and UOC) have been determined. Slurry experiments were conducted on each of the spent shales and the slurry analyzed for leachable dissolved solids. Percolation experiments were conducted on the TOSCO spent shale and the quantities of dissolved solids leachable determined. The concentrations of the various ionic species in the initial leachate from the column were high. The major constituents,  $\text{SO}_4^{=}$  and  $\text{Na}^+$ , were present in concentrations of 90,000 and 35,000 mg/l in the initial leachate; however the succeeding concentrations dropped markedly during the course of the experiment. A computer program was utilized to predict equilibrium concentrations in the leachate from the column. The extent of leaching and erosion of spent shale, and the composition and concentration of natural drainage from spent shale has been determined using oil shale residue and simulated rainfall.

Concentrations in the runoff from the spent shale have been correlated with runoff rate, precipitation intensity, flow depth, application time, slope, and water temperature.

This report was submitted in fulfillment of Grant No. 14030EDB under the sponsorship of the Water Quality Office, Environmental Protection Agency.

## CONTENTS

<u>Section</u>		<u>Page</u>
I	CONCLUSIONS . . . . .	1
II	RECOMMENDATIONS . . . . .	3
III	INTRODUCTION . . . . .	5
	Production of Shale Oil . . . . .	5
	Oil Shale Activities in the United States . . . . .	5
	Future Petroleum Demands . . . . .	9
	Oil Shale Residues . . . . .	10
	Erosion of Spent Shale Piles . . . . .	10
	Stabilization of Spent Shale Piles . . . . .	10
	Purpose and Scope of Report . . . . .	11
IV	WATER POLLUTION CONSIDERATIONS . . . . .	15
	Hydrologic Aspects . . . . .	15
	Surface Runoff Water Quality . . . . .	18
	Percolation Water Quality . . . . .	20
	Exchange Phase - Solution Phase Relationships . . . . .	20
	Crystalline Salt Phase - Solution Phase Relationships . . . . .	22
V	PROCEDURE AND EQUIPMENT . . . . .	25
	Bench Scale Studies . . . . .	25
	Pilot Studies . . . . .	27
	Chemical Analyses . . . . .	29
VI	EXPERIMENTAL DATA AND RESULTS . . . . .	37
	Bench Scale Studies . . . . .	37
	Rainfall Pilot Studies . . . . .	53
VII	DISCUSSION OF RESULTS . . . . .	71
	Physical Tests . . . . .	71
	Pilot Study . . . . .	73
VIII	ACKNOWLEDGEMENTS . . . . .	77
IX	REFERENCES . . . . .	79
X	SYMBOLS AND ABBREVIATIONS . . . . .	83
XI	APPENDICES . . . . .	87

## FIGURES

		<u>Page</u>
1	DISTRIBUTION OF OIL SHALE IN THE GREEN RIVER FORMATION, COLORADO, UTAH, AND WOMING (3) . . . . .	6
2	CRUSHED RAW SHALE . . . . .	12
3	SPENT SHALE FROM UOC RETORTING PROCESS . . . . .	12
4	SPENT SHALE FROM USBM RETORTING PROCESS . . . . .	13
5	SPENT SHALE FROM TOSCO RETORTING PROCESS . . . . .	13
6	SEGMENT OF COLUMN AND PORTION OF TOSCO SPENT SHALE USED IN COLUMN STUDY . . . . .	28
7	OVERALL LAYOUT OF RAINFALL FACILITY . . . . .	30
8	CLOSE-UP OF EXCAVATION . . . . .	31
9	INSTALLATION OF PLASTIC LINER . . . . .	31
10	SAND DRAIN UNDERLYING SPENT SHALE . . . . .	32
11	COLLECTION LINE FOR PERCOLATION WATER . . . . .	32
12	BACKFILLING OF FACILITY WITH 68 TONS OF FRESH TOSCO OIL SHALE RETORTING RESIDUE . . . . .	33
13	PARTIALLY BACKFILLED FACILITY . . . . .	33
14	COMPLETED FACILITY . . . . .	34
15	COMPLETED FACILITY WITH SIMULATED 1 1/2" RAIN OCCURRING	34
16	ORION SPECIFIC ION EQUIPMENT USED FOR CHEMICAL ANALYSES	35
17	LOGARITHMIC PROBABILITY PLOT OF SIZE DISTRIBUTION OF TOSCO SPENT OIL SHALE . . . . .	40
18	LOGARITHMIC PROBABILITY PLOT OF SIZE DISTRIBUTION OF USBM SPENT OIL SHALE . . . . .	41
19	VARIATION OF THE PERMEABILITY OF TOSCO AND USBM SPENT SHALES WITH TIME . . . . .	42
20	CAPILLARY PRESSURE VERSUS RELATIVE PERMEABILITY FOR TOSCO SPENT OIL SHALE . . . . .	45
21	FLOW CHART FOR COMPUTER PROGRAM . . . . .	49
22	CALCULATED AND OBSERVED VALUES OF $\text{Na}^+$ , $\text{SO}_4^-$ , and $\text{Mg}^{++}$ VERSUS VOLUME OF WATER LEACHED . . . . .	51
23	CALCULATED AND OBSERVED VALUES OF $\text{Ca}^{++}$ AND TDS VERSUS VOLUME OF WATER LEACHED . . . . .	52
24	RELATIONSHIP OF TDS IN SPENT SHALE RUNOFF WATER TO INDEPENDENT PARAMETERS . . . . .	56
25	SURFACE DEPOSIT ON TOSCO SPENT OIL SHALE . . . . .	57
26	PERCENTAGE COMPOSITION OF CATIONS IN SURFACE RUNOFF FROM SPENT SHALE AS RELATED TO INDEPENDENT PARAMETERS	60
27	SEDIMENT YIELD FROM SPENT SHALE FOR THREE HOUR PERIOD OF SIMULATED RAINFALL . . . . .	63
28	MOISTURE CONTENT OF SPENT SHALE VERSUS TIME FOR ONE FOOT DEPTH . . . . .	67
29	MOISTURE CONTENT OF SPENT SHALE VERSUS TIME FOR ONE FOOT, SIX INCH DEPTH . . . . .	68
30	TDS VERSUS CONDUCTANCE FOR SPENT SHALE SURFACE RUNOFF .	74
31	TDS VERSUS $\text{me}/\ell$ OF CATIONS FOR SPENT SHALE RUNOFF . . .	75
32	MEASURED CONCENTRATION VERSUS CALCULATED CONCENTRATION OF CATIONS IN SURFACE RUNOFF FROM SPENT SHALE . . . . .	76

TABLES

<u>No.</u>		<u>Page</u>
I	Major Shale Oil Reserves . . . . .	7
II	Empirical Constants for Equation 12 . . . . .	18
III	Sieve Analysis of Bureau of Mines Spent Oil Shale Residue . . . . .	38
IV	Sieve Analysis of TOSCO Spent Oil Shale Residue . . . . .	39
V	Physical Properties of the Various Oil Shale Residues .	43
VI	Results of the Blender Experiment . . . . .	46
VII	Results of the Shaker Experiment . . . . .	46
VIII	Experimental Results of the Percolation Experiment Conducted on TOSCO Spent Oil Shale Retorting Residue.	48
IX	Definition of Terms Used in Computer Program for Predicting the Quality of Spent Oil Shale Percolation Water . . . . .	50
X	Chemical Analysis of Surface Salt Evaporation Deposit .	61
XI	Calculated Sediment Yield in 3 Hour Period from Simulated Storms . . . . .	61
XII	Size Distribution of Sediment in Runoff . . . . .	64
XIII	Jar Test Data for Sediment in Runoff from Oil Shale Residue . . . . .	66
XIV	Water Balance Data for Simulated Rainfall . . . . .	66
XV	Concentrations of Minor Constituents . . . . .	69
XVI	Carbon and Nitrogen Content of Selected Samples . . . . .	70
XVII	Mass of Various Ions Leached Per 100 Grams of TOSCO Spent Shale . . . . .	71
XVIII	Chemical Analyses of Filtrate from Blender Experiments Conducted on Surface Soil Samples . . . . .	72

## SECTION I

### CONCLUSIONS

1. Leaching tests show that there is a definite potential for high concentrations of  $\text{Na}^+$ ,  $\text{Ca}^{++}$ ,  $\text{Mg}^{++}$ , and  $\text{SO}_4^-$  in the runoff from spent oil shale residues. However, with proper compaction, the piles become essentially impermeable to rainfall. On the other hand, snowfall eliminates the compaction in the top foot or so, and at least the top 2 feet of the residue becomes permeable to water.
2. Soluble salts are leached readily from spent shale columns.
3. Chemical concentrations of the effluent from spent shale columns may be predicted by using the relationships developed between soluble and exchangeable ions in soils which are in equilibrium with a water solution.
4. Sediment contained in runoff water from spent oil shale residue will be detrimental to water quality unless removed by settling.
5. Sediment in the runoff water from spent oil shale residue may be efficiently settled by the addition of small amounts of aluminum sulfate and/or by long periods of quiescent detention.
6. The chemical quality of surface runoff water from oil shale residue may be estimated by procedures developed within this report.
7. This list of conclusions is necessarily incomplete until the water pollution potential of snowfall on spent oil shale residues has been determined. This work is now (August, 1971) nearing completion.

## SECTION II

### RECOMMENDATIONS

This project was limited to the study of the quality and quantity of runoff from spent oil shale residue due to rainfall. However, in the oil shale area, more than half the total annual precipitation falls as snow. Annual precipitation is about 12 inches on valley floors and less than 20 inches on mesa tops. Natural snow that fell during the last of the rainfall experiments caused changes which indicate that percolation in the top few feet is going to be much more important in the case of snow because of the longer contact time. Water quality of runoff from snow melt is being investigated in another project sponsored by the U.S. Bureau of Mines.

The problem of water runoff will require close attention with regard to flash-floods that occasionally occur. In order to handle the runoff from the areas that drain into the canyons (where the oil shale residue is to be placed), it is recommended that the water be channeled away from the canyons containing the spent oil shale residue.

Because this project has demonstrated that, even on a very flat slope, sediment will be in the runoff, it is recommended that erosion control measures be studied. One possible erosion control measure would be to collect the surface runoff in ponds downstream of the residue pile. This project has demonstrated that this approach is technically feasible, but the economic practicality was not investigated.

Wetting to the optimum moisture and compaction of the spent shale piles to 90 percent Proctor density is recommended to insure minimum permeability and maximum stability of the piles.

It is recommended that the top surface of the shale piles not be left bare and exposed directly to the elements because of surface runoff leaching, erosion, and possible difficulties in revegetation. Studies should be made to determine the most suitable and economic methods for accomplishing this recommendation. One possibility that should be investigated is the use of local topsoil material to cover exposed sections of the oil shale residue.

Additional research, similar to that reported herein, should be carried out on revegetated spent shale residue and/or native surface soils.

The foregoing recommendations are necessarily incomplete until the water pollution potential of snowfall on spent oil shale residues has been determined. This work is now (August, 1971) nearing completion.



## SECTION III

### INTRODUCTION

One of the largest undeveloped natural resources in the United States is the more than 11 million acres of oil shale land located in Colorado, Utah, and Wyoming in the Green River Formation (see Figure 1). Shale strata that yield from a few to about 65 gallons of crude oil per ton of raw shale are distributed throughout much of the Green River Formation.

The oil shale ranges in thickness from a few feet to about 7,000 feet, and represents the equivalent of about two trillion barrels of oil in place, a quantity greater than that of the world's entire petroleum reserve plus the total petroleum production to date (1). Competent authorities estimate that an average yield of 75,000 barrels of crude oil per acre is recoverable by demonstrated mining and retorting methods (2). This would represent over 82 billion barrels of recoverable shale oil.

The most extensive known world deposits of shale are listed in Table I.

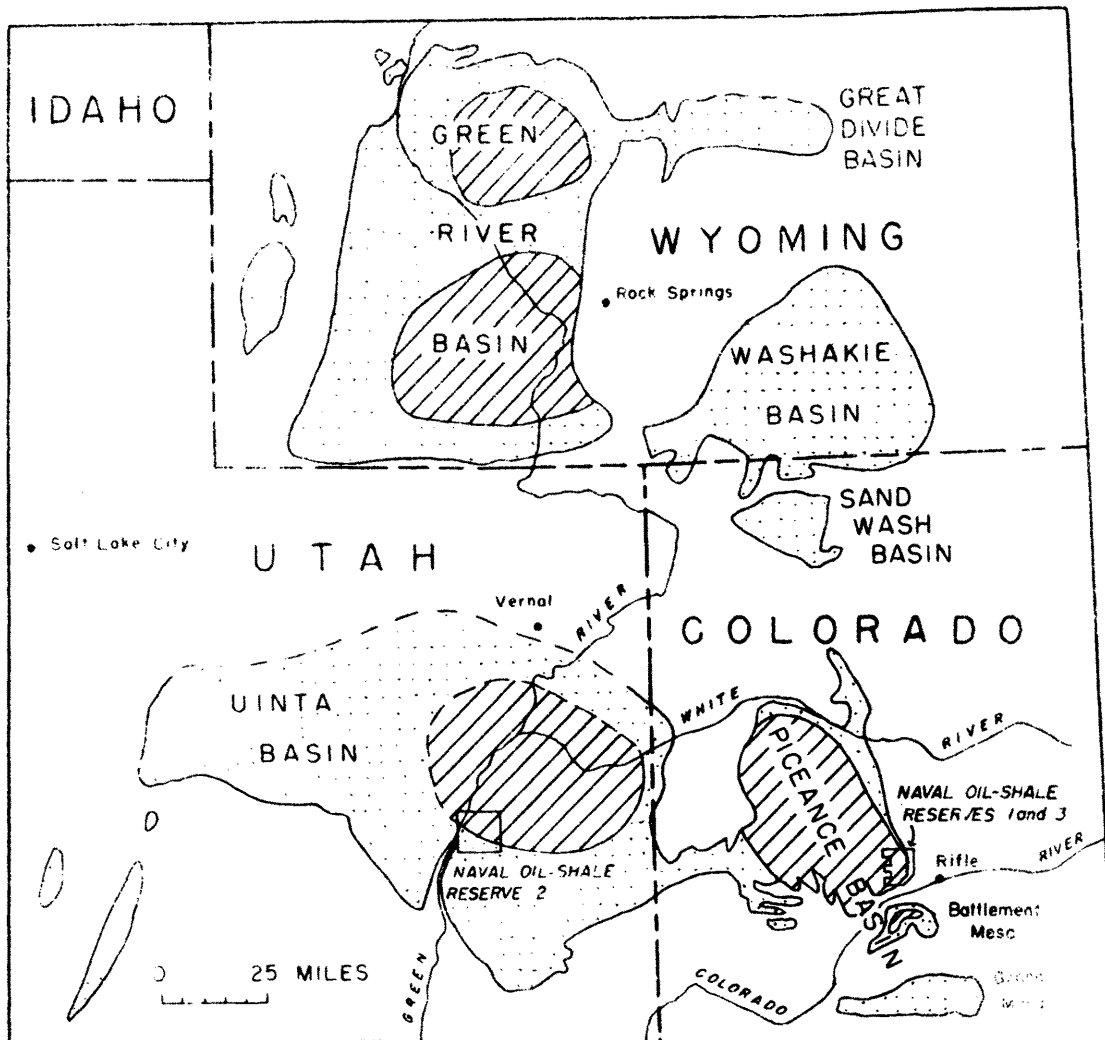
PRODUCTION OF SHALE OIL -- Production of oil from oil shale on a commercial scale dates back to the 1850's when operations were begun in Scotland and France. In the early 1900's, oil shale industries were established in New Zealand (1900), Switzerland (1915), Sweden (1921), Estonia (1921), Manchuria (1929), and later Russia, Germany, Spain, and South Africa.

By the end of 1961, the principal production of oil from oil shale had been from deposits in Scotland (about 100 million barrels), Estonia (possibly 100 million barrels), and Manchuria (more than 100 million barrels). It is estimated that by the end of 1961, 770 million tons of oil shale was mined producing about 400 million barrels of oil (4).

Most of the shale-retorting activities mentioned have succumbed sooner or later to the competition encountered from petroleum derived products. At the present time there is significant industry only in Estonia and Manchuria, while Brazil is attempting to establish an oil shale industry.

OIL SHALE ACTIVITIES IN THE UNITED STATES -- In the United States, activities in shale - oil development began about 1916, and over the past 55 years, many attempts have been made to mine and retort oil shale from deposits of the Piceance Creek Basin. (note Figure 1).

Since World War II, the major efforts have been devoted to one mining system, the room and pillar, and to three above ground retorting systems, those proposed by the U.S. Bureau of Mines, Union Oil Company of California, and The Oil Shale Corporation. Of late, the U.S. Bureau of Mines has extensively investigated in situ retorting of oil shale. In their above ground retorting process the U.S. Bureau of Mines (USBM) used



EXPLANATION


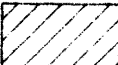
- |                                                                                                       |                                                                                                                  |
|-------------------------------------------------------------------------------------------------------|------------------------------------------------------------------------------------------------------------------|
|                    |                             |
| <p>Area underlain by the Green River Formation in which the oil shale is unappraised or low grade</p> | <p>Area underlain by oil shale more than 10 feet thick, which yields 25 gallons or more oil per ton of shale</p> |

FIGURE 1: DISTRIBUTION OF OIL SHALE IN THE GREEN RIVER FORMATION, COLORADO, UTAH, AND WYOMING (3)

Table I: Major Shale Oil Reserves (5)

	Oil in place, million bbl
Australia . . . . .	200
Brazil . . . . .	342,000
Bulgaria . . . . .	200
Burman and Thailand . . . . .	17,100
Canada . . . . .	34,200
China:	
Fushun, Manchuria . . . . .	2,000
Other deposits . . . . .	2,700
England . . . . .	1,400
Estonia . . . . .	17,300
France . . . . .	1,400
Germany (West) . . . . .	2,000
Israel . . . . .	20
Italy . . . . .	34,300
Malagasy Republic . . . . .	200
New Zealand . . . . .	200
Republic of the Congo (former Belgian Congo) . . . . .	103,000
Republic of South Africa . . . . .	30
Scotland . . . . .	600
Spain . . . . .	300
Sweden . . . . .	2,800
United States . . . . .	2,000,000
U.S.S.R. . . . .	6,800
Yugoslavia . . . . .	<u>1,400</u>
TOTAL . . . . .	2,570,050

a gas combustion retorting process. The gas combustion retorting process uses heat produced from the shale mass by combustion of a portion of the hydrocarbon vapors resulting from shale decomposition on heating. Crushed oil shale is charged intermittently to the top of a brick-lined steel shaft through a gas seal. By intermittent discharge of spent

shale from the bottom of the shaft, the raw shale gradually moves downward in the retort, first being preheated by contact with hot combustion products and hydrocarbon vapors. Coking, or carbon formation on the shale also occurs, and as the partially decomposed material moves lower, some of the remaining organic matter in the shale burns to CO and CO<sub>2</sub> in a rising stream of hot air. This provides some of the necessary heat for the retorting process, the balance and major fraction being produced by combustion of hydrocarbons in a portion of the separated retort gases recycled to the bottom of the shaft. Blowers furnish air at a controlled rate into the shale bed at a point about one-third of the distance to the top of the retort. Spent shale, ideally with very low carbon content, preheats the recycle gas as it moves through the lowest zone of the retort and finally is discharged through a gas seal at the base. The upflowing recycle gas burns to CO<sub>2</sub>, CO, and H<sub>2</sub>O in the combustion zone immediately above the air inlet ports.

In the Union Oil Company (UOC) process, crushed oil shale is retorted in a vertical bricklined shaft, the heat being furnished by burning the carbon remaining in the shale after the hydrocarbons have been vaporized. Upflow of solid shale is provided by charging it at the bottom through a hopper in which a large piston moves in and out of the retort. As the solid shale is forced slowly up through the shaft, it meets a descending stream of hot gases and hydrocarbon vapors. When its temperature reaches about 1000°F, decomposition and vaporization of hydrocarbons takes place. A suction fan in the vapor recovery system provides draft for moving the gases down through and out of the retort. Because the incoming shale is cold, oil vapors meeting it are largely condensed, and the liquid shale oil is drawn off at the bottom of the retort. Near the top of the shaft, the rising spent shale meets a descending stream of air which provides oxygen for combustion of carbon on the shale, generating the heat required for retorting in the zone immediately below. Burned shale, in a semi-fused or plastic state, is mechanically raked from the open top of the shaft and discarded.

In the Oil Shale Corporation (TOSCO II) process, crushed oil shale is preheated in a dilute-phase fluidized bed and then mixed with hot balls in a rotating drum. The balls and shale equilibrate at a temperature of above 900°F which is adequate to cause thermal decomposition and vaporization of the organic constituents of the shale. The vapors are condensed and fractionated into gas, naphtha, gas oil, and heavy residuum; concurrently, the balls are separated from the processed shale and recirculated to a ball heater. Heat is recovered from the processed shale. The processed shale is then moistened to obtain necessary compactive properties and to control dust (29).

In addition to the preceding approaches, a number of other methods have been discussed in the literature (7).

FUTURE PETROLEUM DEMANDS -- Present forecasts indicate that the domestic demand for petroleum in 1980 will be about 8 million barrels per day more than the domestic petroleum supply. This gap can be partially closed by North Slope crude, or synthetic crudes from coal, tar sands, and oil shale.

There are four principal alternatives for supplying this excess of demand over supply for petroleum in the United States (8). These alternatives are:

1. Increase the rate of discovery of petroleum,
2. Obtain a greater proportion of the oil from known reservoirs by new or improved methods,
3. Increase the proportion of demand supplied by imported oil,
4. Develop economical processes for producing liquid and gaseous fuel from alternative sources such as oil shale, coal, and tar sands.

A majority of the studies and forecasts made concerning the first three alternatives for meeting the greatly increased demand for liquid fuels agree that they probably will not yield enough oil to meet the entire increase. As a result, the use of shale oil to supplement crude oil resources becomes likely as a major future development.

As far as above-ground retorting is concerned, initial operations will probably occur in the southeastern Piceance Basin of Colorado. A commercial facility would process 50,000 to 100,000 tons of oil shale per day, and would produce 40,000 to 85,000 barrels per day of synthetic crude oil. A full-scale oil shale industry, including up to 10 such plants, might develop by 1985. A proposed initial plant site is located in Garfield County, Colorado, in the Parachute Creek escarpment area north of Grand Valley, Colorado (elevation 5,100 feet). Water reaching the Colorado River via Parachute Creek has dissolved solids concentrations as high as 800 mg/l during parts of the year (29).

The nearest U.S. Geological Survey water quality stations on the Colorado River above and below the oil shale area are, respectively, the stations near Glenwood Springs, Colorado (6.5 miles upstream from Roaring Fork River; drainage area 4,650 square miles) and near Cameo, Colorado (drainage area 8,050 square miles). While the flow of the Roaring Fork River is significant compared to that of the Colorado River, its salinity is consistently less. Examination of the records for the 5 year period of 1964 through 1968 reveals the fact that the salt load (in tons/day) of the Colorado River increases by a factor of 2.5 between Glenwood Springs and Cameo. In addition, the volume-weighted average concentration of dissolved solids (residue at 180°C) in the Colorado River increases from 327 mg/l at Glenwood Springs to 448 mg/l at Cameo (the time-weighted average concentration increases from 395 mg/l to 609 mg/l). The salt concentration of the Colorado River at Hoover Dam is 725 mg/l. Of this, 38% is contributed by natural diffuse sources (274 mg/l).

OIL SHALE RESIDUES -- In the event the industrial development of oil shale occurs, a considerable quantity of retorted oil shale residues will be produced. The minimum economic-sized shale oil plant will probably produce in excess of 50,000 tons of processed shale per day.

Some of the waste may be suitable for disposal as mine fill (a maximum of about 60%), railroad and highway road fill, or even land fill. It might even be possible to utilize some of the residue as raw materials for making concrete, cement blocks, and bricks (9). However, the demand for oil shale residue for these uses is small in relation to the amount of residue that will be produced. Often the kerogen (kerogen is the organic matter found in oil shale) content is less than 20 percent by weight of the discarded materials. This could leave millions of tons of unattractive barren piles of oil shale residue to mar the natural beauty of the land if the residue were merely dumped at the mining site. Dust from the dried out residue could contribute to air pollution and the runoff water could contaminate water supplies with salts and other materials.

EROSION OF SPENT SHALE PILES -- Erosion would be of particular concern on the steep slopes of unprotected residue piles. Storms could lead to the formation of deep gullies on the slopes and alter the pattern of drainage established from preceding runoffs. Continued erosion would also expose new surface areas to air and moisture which could lead to undesirable leaching and the creation of water quality problems. The effect of revegetation on these potential problem areas is unknown.

If unprotected, a large portion of the sediment from the spent shale piles might be deposited in stream channels near the disturbed area. However, sediment would also be carried into large streams, where it would settle out or move downstream. Thus, entire river basins could be adversely affected by the spent shale piles if no care was taken to prevent these potential problems.

Streams carrying heavy loads of sediment may require additional treatment to make them more suitable for domestic and industrial uses. Recreational use of streams could also be adversely affected by sediment, and fish habitat could be destroyed (10).

STABILIZATION OF SPENT SHALE PILES -- Erosion of spent shale piles may be lessened to some extent through physical, chemical, and vegetative methods of stabilization (11). Physical methods include covering the fine tailings with topsoil removed from underneath the shale residue piles. One possibility for a surface disposal site would be a canyon in the vicinity of a proposed commercial plant site. The processed shale could be placed in a series of horizontal layers 1 to 2 feet thick. The upper surface would be a temporary surface until the last layer is placed. Each layer could be started a little further back into the canyon, giving the front surface of the pile (permanent surface) a slope sufficiently less than the angle of repose to insure frictional stability.

Chemical stabilization involves reacting the residue with a reagent to form a water and air impermeable crust or layer.

Vegetative stabilization may pose some difficult problems. Wastes are usually deficient in plant nutrients or may contain material noxious to plant growth. Tailings and other fine wastes usually must be covered to a depth of four inches or more with soil and fertilized prior to seeding (12). However, Kentucky Blue Grass, fertilized at the rate of 150 pounds per acre twice per year and watered at the rate of 1 inch per week during the 10 week summer season has been grown on the TOSCO Process waste after conditioning with sawdust (29). The root zone of the Kentucky Blue Grass penetrated over 11 inches into the processed oil shale residue.

It is believed that the black color of the oil shale residue must not be directly exposed to the sun as the result of grass fires and/or over-grazing. Therefore, the surface color should be more nearly that of the native topsoil, which could be accomplished by covering with a relatively thin layer of native topsoil.

PURPOSE AND SCOPE OF REPORT -- The purpose of this report is to evaluate the potential water pollution of rainfall on spent oil shale residues in order that industry may be properly advised of the hazards before the fact and as a guide for the federal leasing program.

The spent oil shale residues investigated in this study were from three pilot plant operations. The processes were: (1) USBM, (2) UOC, and (3) TOSCO. The oil shale for all three pilot plants came from the Piceance Basin near Rifle, Colorado. The TOSCO residue was given considerably more attention because the Colony Development Operation (Atlantic Richfield Company Operator) is currently engaged in a \$17 million field program to investigate the feasibility of shale oil production on a commercial scale.

Given in Figures 2, 3, 4, and 5 are pictures of the raw shale and the residues from the various retorting processes covered in this report.

The project consisted of three phases of work: (1) Bench scale studies were used to determine (a) permeability, porosity, and particle size distribution, (b) the composition and maximum quantity of dissolved solids leachable by complete slurry treatment; and (c) the composition and quantity of dissolved solids leachable by simple downward percolation through residue columns. (2) Pilot studies were conducted on the TOSCO unweathered spent shale to define (a) the composition and concentration of dissolved solids in runoff from a spent shale pile; and (b) the properties of the residue within the pile before and after rainfall simulation. (3) Data was interpreted using statistical techniques to determine the quantitative relationships between the dependent and independent variables significant to spent oil shale residue leaching.

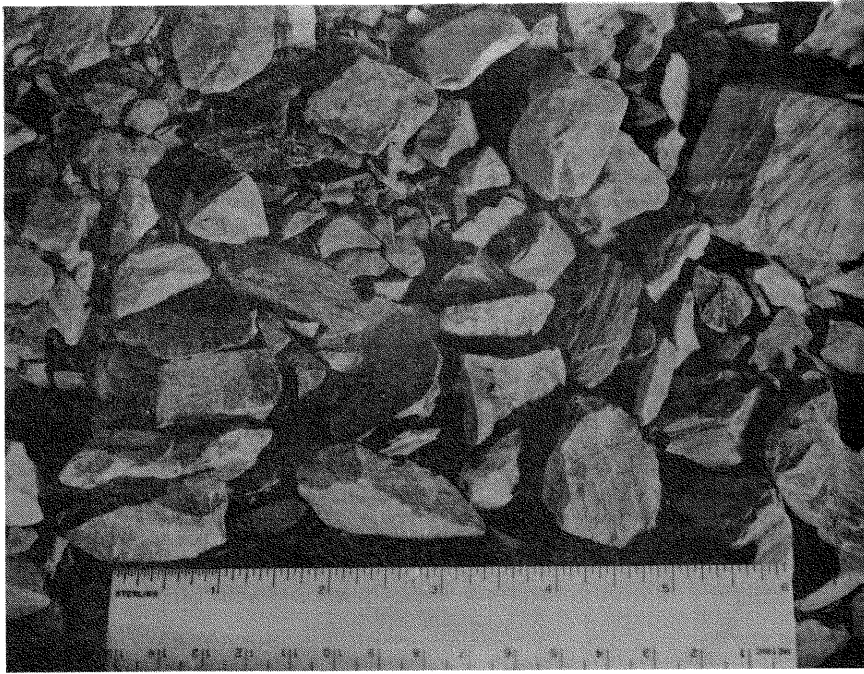


FIGURE 2: CRUSHED RAW SHALE

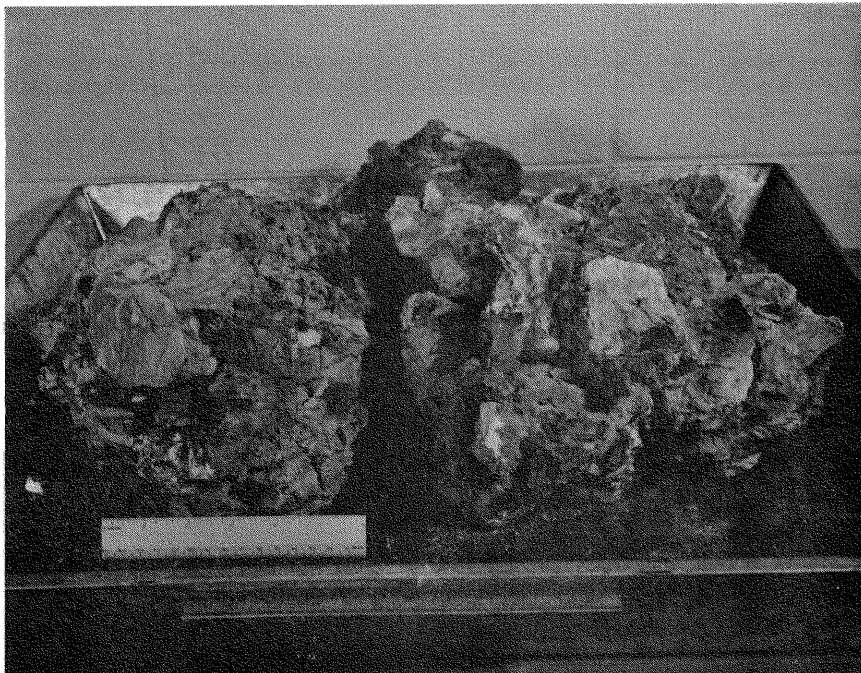


FIGURE 3: SPENT SHALE FROM UOC RETORTING PROCESS



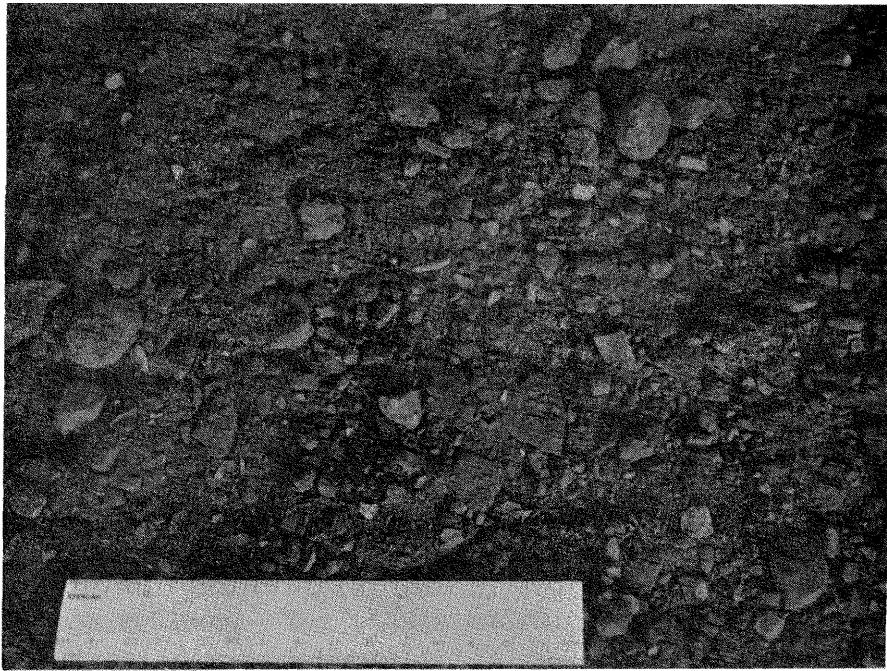


FIGURE 4: SPENT SHALE FROM USBOM RETORTING PROCESS

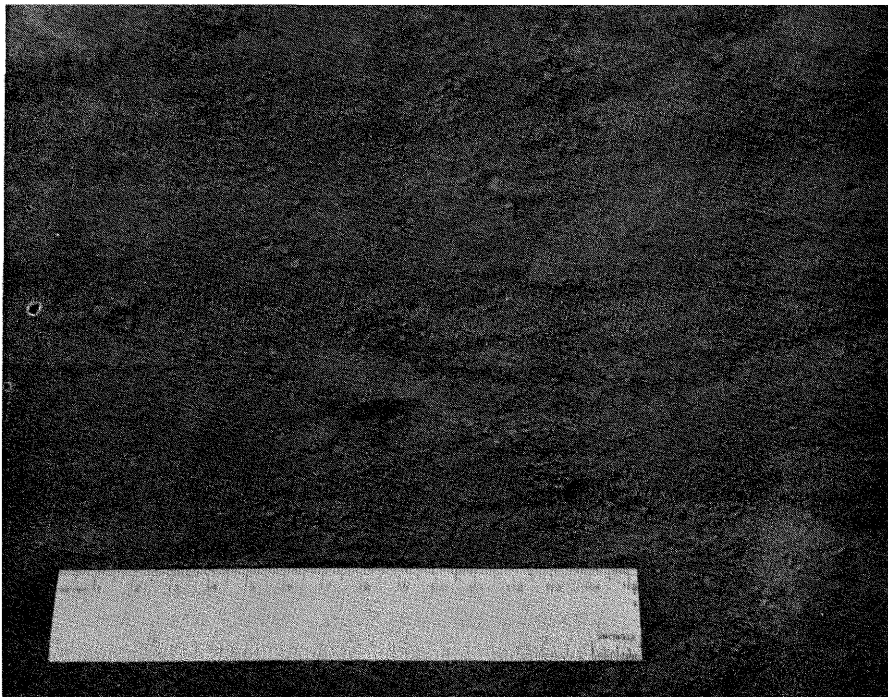


FIGURE 5: SPENT SHALE FROM TOSCO RETORTING PROCESS

## SECTION IV

### WATER POLLUTION CONSIDERATIONS

HYDROLOGIC ASPECTS -- Among other variables, the solids leached by the runoff water from a spent oil shale residue pile will be a function of the intensity of rainfall, length of overland flow, kinematic viscosity of the runoff water, and surface slope.

It would be advantageous to combine all of these parameters into one. By consideration of the overland flow hydrograph, such a parameter can be derived.

Using the model of laminar flow and the assumptions that (1) surface tension effects are negligible, (2) flow is two dimensional, and (3) there is no infiltration, the hydrograph for overland flow may be developed as follows. The change of velocity with respect to depth is given by:

$$\frac{dV}{dy} = \frac{g \text{ Sin}\theta (D-y)}{\nu} \quad (1)$$

where

$\frac{dV}{dy}$  = change of velocity with respect to depth, ft/(sec)(ft),

V = velocity at any depth, ft/sec,

y = any depth, ft,

$\nu$  = kinematic viscosity, ft<sup>2</sup>/sec,

D = total depth of flow at lower end, ft,

$\theta$  = slope angle (if slope angle is less than 6°, Sin $\theta$  may be replaced by the slope, s, with no loss of accuracy),

g = acceleration of gravity, 32.2 ft/sec<sup>2</sup>.

Applying the boundary conditions that V = 0 when y = 0, integration of equation 1 yields

$$V = \frac{g \text{ Sin}\theta (yD - y^2/2)}{\nu} \quad (2)$$

The mean velocity,  $\bar{V}$ , is defined as:

$$\bar{V} = \frac{\int_0^D V dy}{\int_0^D dy} \quad (3)$$

Substituting equation 2 for V into equation 3 gives

$$\bar{V} = \frac{\frac{g \sin\theta}{\nu} \int_0^D (yD - y^2/2) dy}{\int_0^D dy} \quad (4)$$

Completing the integration,  $\bar{V}$  may be expressed as

$$\bar{V} = \frac{g \sin\theta D^2}{3\nu} \quad (5)$$

The discharge per unit width,  $q$ , is  $\bar{V} D$  or

$$q = \frac{g \sin\theta D^3}{3\nu} \quad (6)$$

As with the mean velocity, the mean depth of flow may be defined as

$$\bar{D} = \frac{\int_0^L D_x dx}{\int_0^L dx} \quad (7)$$

where  $L$  is the total distance of overland flow (in feet), and  $x$  is in feet and is measured from the upstream end down. Clearly

$$q_x = \left(\frac{x}{L}\right) q \quad \text{and} \quad D_x = \left(\frac{3\nu q_x}{g \sin\theta}\right)^{1/3} = \left(\frac{3\nu x q}{Lg \sin\theta}\right)^{1/3}, \quad \text{and}$$

therefore,

$$\bar{D} = \frac{\left(\frac{3\nu q}{Lg \sin\theta}\right)^{1/3} \int_0^L x^{1/3} dx}{\int_0^L dx} \quad (8)$$

Integration of equation 8 gives

$$\bar{D} = \frac{3}{4} D \quad (9)$$

The equilibrium flow,  $q_e$ , is

$$q_e = \frac{iL}{43,200} \quad (10)$$

The constant 43,200 gives  $q_e$  in square feet per second when  $i$ , the intensity of rainfall, is in inches per hour. Substitution of equations

6 and 10 into equation 9 gives

$$\bar{D} = (9.70 \times 10^{-3}) \left( \frac{v \ iL}{\text{Sin}\theta} \right)^{1/3} \quad (11)$$

Therefore, from equation 11, it is seen that all the hydrologic parameters of concern are contained in the average depth of overland flow. At 20°C (68°F),

$$\bar{D} = (10^{-4}) \left( \frac{10 \ iL}{\text{Sin}\theta} \right)^{1/3} \quad (11A)$$

In order to use equation 11 a method of determining  $i$  must be used. Many studies have been directed to the development of empirical relations for estimating rainfall intensity as required in applying the rational formula and other similar equations (13). The resulting relations are usually of the form (14)

$$i = \frac{cT^m}{(t_d + d)^n} \quad (12)$$

where

$i$  = rainfall intensity in inches per hour,

$t_d$  = duration of the storm in minutes,

$T$  = frequency of occurrence in years,

$c, d, m,$  and  $n$  are regional coefficients and exponents.

(In North America,  $5 \leq c \leq 50$ ,  $0 \leq d \leq 30$ ,  $0.1 \leq m \leq 0.5$ , and  $0.4 \leq n \leq 1$ ).

The constants for equation 12 are obtained by a graphical or least squares fitting technique applied to original data. This has been done by Norton (15) for four Colorado and one Wyoming first order U.S. Weather Stations. These constants, shown in Table II, allow mathematical determination of the rainfall intensity for a given storm. Of particular interest in this study are the empirical constants for Grand Junction, Colorado.

To verify whether or not the assumption of laminar flow is met, the overland flow characteristics should be known. The Reynolds number,  $R$ , is used as an index of the occurrence of turbulence. The Reynolds number of overland flow at a section where the depth is  $D$  feet and the mean velocity is  $\bar{V}$  ft/sec, is

$$R = \frac{4\bar{V}D}{v} \quad (13)$$

Table II: Empirical Constants for Equation 12

Geographical Location of Station	Empirical Constants				Elevation of Station in feet above sea level
	c	m	d	n	
Pueblo, Colorado	29.9	0.232	8.9	0.872	4712
Grand Junction, Colorado	6.3	0.265	1.7	0.721	4845
Denver, Colorado	17.6	0.299	4.3	0.820	5331
Cheyenne, Wyoming	27.6	0.199	5.2	0.853	6156
Wagon Wheel Gap, Colorado	6.7	0.248	0.4	0.707	8390

Substituting equation 5 into equation 13 gives

$$R = \frac{4 g \sin\theta D^3}{3v^2} \quad (14)$$

Then, substituting equations 9 and 11 into equation 14 gives

$$R = 9.29 \times 10^{-5} \frac{iL}{v} \quad (15)$$

At 80°F,

$$R = 10.0 iL \quad (16)$$

Owen (16) states that overland flow becomes turbulent for R greater than 4,000. Therefore, to insure laminar flow

$$iL \leq 400 \quad (17)$$

**SURFACE RUNOFF WATER QUALITY** -- There are two major classifications of suspended solids in water, settleable suspended solids and nonsettleable suspended solids. The quantity of settleable solids are important in determining the size of sludge handling facilities and they can be determined from a standard Imhoff cone test (17).

The nonsettleable solids are either organic or inorganic. It is reasonable to assume that the concentration of the dissolved inorganic solids in the runoff water will be a function of the parameters described by equation 18,

$$C = f(i, \Delta\omega, t, v, s, L, \rho, k) \quad (18)$$

in which,

C = concentration (mg/l),

$\Delta\omega$  = decrease in surface moisture content since the last rain,  
dimensionless,

t = time since beginning of runoff, (hr),

$\rho$  = the gross density of the surface shale (g/cc),

k = permeability of the surface shale (cm<sup>2</sup>).

From equation 11,  $\bar{D} = f(i, v, L, s)$ . Therefore equation 18 becomes,

$$C = f(\bar{D}, \Delta\omega, t, \rho, k) . \quad (19)$$

Further refinement of equation 19 may be obtained by making the following assumptions.

1. The concentration of dissolved solids varies inversely with  $\bar{D}$  to some power, N,

$$C \propto \frac{1}{\bar{D}^N} . \quad (20)$$

2. The concentration of dissolved solids varies directly with the change in surface moisture. This effect of surface moisture is greatest at the beginning of a storm and diminishes with time. This suggests an exponential relationship of the form,

$$C \propto \exp\left(\frac{K\Delta\omega}{0.435}\right) \quad (21)$$

in which K is a constant. The reasoning for the above formulation of the relationship between C and  $\Delta\omega$  is explained in Appendix C.

3. The concentration of dissolved solids in the runoff decreases with time during a given storm. This implies an exponential relationship of the form,

$$C \propto \exp\left(\frac{-t^\gamma}{0.435}\right) \quad (22)$$

in which  $\gamma$  is a constant.

Combining equations 20, 21, and 22 with equation 19 yields

$$C = \frac{1}{\bar{D}^N} f(\rho, k) \exp\left(\frac{K\Delta\omega - t^\gamma}{0.435}\right) . \quad (23)$$

The coefficients, exponents, and  $f(\rho, k)$  now remain to be determined experimentally.

PERCOLATION WATER QUALITY -- One of the most important factors to be considered from a water quality standpoint is the increase in dissolved solids concentration of the percolation water as it percolates through the spent oil shale. This change takes place by the following mechanisms:

1. Ion exchange - Ion exchange is the reversible process by which cations and anions are exchanged between solid and liquid phases and between solid phases if in close enough contact with each other. Although ion exchange does not increase the total concentration in milliequivalents per liter of a solution, it can and does change the ionic composition of the percolating water.
2. Adsorption and Desorption of Ions - The solid components in the shale are capable of adsorbing or releasing (desorption) solutes from or to the soil solution. These processes differ from ion exchange in that an increase or decrease in concentration of solutes in the solution occurs.

The most important single factor in determining the composition of the water which percolates through the shale is the concentration and types of salts found in the shale. These may be divided into:

1. Soluble Salts - These salts are readily soluble in water and are leached rapidly from the shale.
2. Slightly Soluble Salts - These salts are only sparingly soluble in water and will leach slowly from the shale.

Previous studies (18) indicate the shale will contain  $\text{CaSO}_4$  as a slightly soluble salt and  $\text{MgSO}_4$  or  $\text{NaSO}_4$  as soluble salts.

All of the above factors govern the composition of the equilibrium solution, that is, the solution that would result if a solution were allowed to remain in contact with the shale until no further change in the resulting solution occurred.

To develop a theory that will enable the prediction of the quality of the percolating water, it is necessary to consider three phases. These phases are:

1. an exchange phase, consisting of  $\text{Ca}^{++}$ - $\text{Mg}^{++}$ - $\text{Na}^+$  shale,
2. a crystalline salt phase consisting of the slightly soluble salt,  $\text{CaSO}_4$ ,
3. a solution phase of  $\text{Ca}^{++}$ ,  $\text{Mg}^{++}$ , and  $\text{Na}^+$  salts.

EXCHANGE PHASE-SOLUTION PHASE RELATIONSHIPS -- The relationship between soluble and exchangeable ions in soils in equilibrium with a solution can be represented by relationships similar to those employed for chemical reactions in solutions.

For example, for the homovalent exchange of  $\text{Ca}^{++}$  and  $\text{Mg}^{++}$ , the exchange equation is (19)

$$\frac{[\text{Ca}_s^{++}]}{[\text{Mg}_s^{++}]} = K \frac{[\text{Ca}_a^{++}]}{[\text{Mg}_a^{++}]} \quad (24)$$

and for the monovalent-divalent exchange of  $\text{Ca}^{++}$ ,  $\text{Mg}^{++}$ , and  $\text{Na}^+$ , the exchange equation is

$$\frac{[\text{Na}_a^+]}{[\text{Ca}_a^{++}] + [\text{Mg}_a^{++}]} = K' \frac{[\text{Na}_s^+]}{\sqrt{[\text{Ca}_s^{++}] + [\text{Mg}_s^{++}]}} \quad (25)$$

In equations 24 and 25, the subscripts a and s refer to the adsorbed and solution ions respectively, square brackets denote concentration in moles per liter if in the solution phase, or moles per gram of soil if in the adsorbed phase. K and K' are equilibrium constants. K is dimensionless and K' is  $\sqrt{\text{moles/liter}}$ . If [X] and [Y] are the number of moles of  $\text{Na}^+$  and  $\text{Mg}^{++}$  per gram of soil leaving or entering the complex (entering the exchange complex will be considered positive) and B is the ratio of grams of oven dry soil to the liters of solution contained in the soil during percolation, equations 24 and 25 become

$$\begin{aligned} B(1 - K)Y^2 + [B(\text{Mg}_a + K\text{Ca}_a + 0.5 KX + 0.5 X) + \text{Ca}_s + K\text{Mg}_s]Y + \\ + \text{Ca}_s \text{Mg}_s - K\text{Mg}_s \text{Ca}_a + 0.5 X (B\text{Mg}_a + K\text{X}\text{Mg}_s) = 0 \end{aligned} \quad (26)$$

and

$$aX^4 + bX^3 + cX^2 + dX + e = 0 \quad (27)$$

where

$$a = 0.250 B^2 K'^2 \quad (28)$$

$$b = -K'^2 (B^2 \text{Ca}_a + B^2 \text{Mg}_a + 0.5 B \text{Na}_s) - 0.5 B \quad (29)$$

$$\begin{aligned} c = K'^2 (B^2 \text{Ca}_a^2 + 2 B \text{Na}_s \text{Ca}_a + 2 B^2 \text{Ca}_a \text{Mg}_a + 2 B \text{Na}_s \text{Mg}_a + B^2 \text{Mg}_a^2) \\ - \text{Ca}_s - \text{Mg}_s - B \text{Na}_a + 0.25 K'^2 \text{Na}_s^2 \end{aligned} \quad (30)$$

$$\begin{aligned} d = -2 K'^2 (B \text{Na}_s \text{Ca}_a^2 + 0.5 \text{Na}_s^2 \text{Ca}_a + 2 B \text{Na}_s \text{Ca}_a \text{Mg}_a + B \text{Na}_s \text{Mg}_a^2) \\ - 2 \text{Ca}_s \text{Na}_a - 2 \text{Mg}_s \text{Na}_a - 0.5 B \text{Na}_a^2 - \text{Mg}_a K'^2 \text{Na}_s^2 \end{aligned} \quad (31)$$

$$e = K'^2 \text{Na}_s^2 (\text{Ca}_a^2 + 2 \text{Ca}_a \text{Mg}_a + \text{Mg}_a^2) - \text{Na}_a^2 (\text{Ca}_s + \text{Mg}_s) \quad (32)$$



The concentrations of  $Mg_a$ ,  $Ca_a$ ,  $Ca_s$ ,  $Mg_s$ ,  $Na_s$ , and  $Na_a$  in equations 26-32 are all initial concentrations.

Solution of equations 26 and 27 will give the number of moles of  $Na^+$  and  $Mg^{++}$  per gram of soil leaving or entering the complex. Because the total equivalents of  $Ca^{++}$ ,  $Mg^{++}$ , and  $Na^+$  taking place in the exchange must sum to zero, the number of moles of  $Ca^{++}$  per gram of soil leaving or entering the exchange complex,  $[Z]$ , when a given solution is brought into contact may be computed from

$$Z = -(X/2 + Y) . \quad (33)$$

CRYSTALLINE SALT PHASE-SOLUTION PHASE RELATIONSHIPS -- The solubility of  $CaSO_4$  is described by the solubility product

$$f^2 [Ca_s][SO_{4s}] = K_{sp} = 2.4 \times 10^{-5} @ 25^\circ C. \quad (34)$$

$K_{sp}$  is the solubility product and  $f$  represents the activity coefficient  $a_s^{sp}$  calculated from the Debye-Huckel theory.

If  $w$  is the number of moles per liter of  $Ca^{++}$  and  $SO_4^{--}$  that dissolve or precipitate (positive  $w$  denotes dissolving), equation 34 may be written as

$$w^2 + (Ca_s + SO_{4s})w + Ca_s SO_{4s} - K_{sp}/f^2 = 0 . \quad (35)$$

$w$  may be obtained by using the quadratic formula. The concentration of  $Ca_s$  and  $SO_{4s}$  are initial concentrations.

Equations 26 and 27 give the relationship between the soil and solution, and equation 35 gives the relationship between the solution and  $CaSO_4$ . By alternately holding the soil phase and the gypsum ( $CaSO_4$ ) phase constant, the equilibrium solution for this three phase system may be calculated through an iterative procedure.

To calculate the quality of water percolating through the shale, the depth of shale is considered to be made up of  $n$  segments  $\Delta y$  in length. The total length of the column,  $y$ , is

$$y = \sum_{k=1}^{k=n} \Delta y_k \quad (36)$$

where  $k$  designates the particular segment. Assuming the amount of solution present in each segment,  $q_k$ , is the same in each segment, the final concentration of component  $j$ ,  $C_j^k$ , in the first aliquot will be

$$C'_j = C_j + \sum_{k=1}^{k=n} \Delta C_{kj} \quad (37)$$

where  $\Delta C_{kj}$  is the change in concentration of solute  $j$  when the aliquot  $q_1$  is passed through segment  $k$ . Using equations 26, 27, and 34, and making  $n$  in equation 37 finite, the average concentrations of the aliquots may be approximated and the quality of the water percolating through the shale predicted (19).

## SECTION V

### PROCEDURE AND EQUIPMENT

#### BENCH SCALE STUDIES:

1. Mechanical Sieve Analysis - A representative sample of the various oil shale residues was selected by proportioning. All samples were either air dried or oven dried until the moisture content was less than one percent. This moisture content was small enough not to interfere with the various analyses.

The 1 1/2", 1", 3/4", 1/2", 3/8", and Nos. 4, 8, 16, 30, 50, 120, and 200 U.S. standard size sieves were used for sieving. A portion of the sample was placed on the sieves and shaken for ten minutes on a mechanical shaker. At the end of that time the series of sieves were removed and the portion of sample retained on each sieve weighed and recorded. This procedure was followed until the total sample was sieved.

For that portion of the sample passing the No. 200 sieve, a hydrometer was used to determine the particle size distribution. Fifty grams of the fraction passing the No. 200 sieve were placed in a beaker with 250 ml of distilled water and stirred mechanically for one hour. After stirring, the mixture was transferred to a graduated glass cylinder and distilled water added until a total volume of 1000 ml was obtained. The cylinder was then transferred to a constant temperature bath. After the soil suspension reached a constant temperature, the cylinder was removed, thoroughly shaken, and returned to the bath. Hydrometer readings were then taken at the end of 2, 3, 5, 15, 30, 60, and 360 minutes.

2. Porosity - The porosity of the USBM and TOSCO spent shales was determined by placing 2000 grams of the respective shale in a plastic cylinder. The walls of the container were tapped with a wooden mallet until the volume of the sample remained constant.

The sample was then placed under a vacuum for 3 hours, to remove any trapped air. A known quantity of water was then applied to the shale through a valve located at the bottom of the cylinder. The porosity,  $\epsilon$ , was then calculated from the equation

$$\epsilon = \frac{V_v}{V_t} \quad (38)$$

where

$V_v$  = the volume of water to fill the voids of the sample, and

$V_t$  = the total volume of the sample.

Because of its size and irregularity, the porosity of the clinkers from the UOC burned shale was determined using a different procedure. A container was filled with Ottawa sand, weighed, and the apparent weight density of the sand determined. The volume of the oil shale residue sample was determined by calculating the volume displaced by the sample when it was buried in the container filled with sand. The voids of the UOC sample were determined as previously described and the porosity calculated from equation 38.

3. Density - The density of the spent shales was determined from a 50 gram portion of the sample which had passed a No. 40 sieve. A 250 ml flask was used for a pycometer, and the procedure as outlined in reference (20) was used to determine density.

4. Permeability - The permeability of the spent shales was determined using a series of three samples. Each sample weighed 500 grams, and was placed in a constant head permeameter, and compacted to the same bulk density as in the porosity determinations. In order to prevent clogging of the inlet and outlet of the permeameter, 1 centimeter of fine gravel was placed at both ends of the sample. The head loss through the gravel was assumed zero because its permeability was many orders of magnitude greater than that of the spent shale. The samples were vacuum saturated and placed under a constant head of 100 cm of water.

Darcy's law which is valid for the linear laminar flow regime in porous media, is

$$\frac{dp}{dy} = \frac{\mu v}{k} \quad (39)$$

To calculate permeability, equation 39 may be written as

$$k = \frac{\mu v}{\Delta p / \Delta y} \quad (40)$$

where

k is the permeability of the porous medium in cm<sup>2</sup>,

v is the macroscopic velocity in cm/sec,

μ is the absolute viscosity of the fluid in poises, and

$\frac{dp}{dy}$  is the pressure drop per unit length due to friction, in dynes per cm<sup>2</sup> per cm.

5. Blender, Shaker, and Column Experiments - In order to determine the composition and concentration of dissolved solids leachable from the spent shales, three experiments were devised. The first experiment was the blender experiment which consisted of taking a 100 gram sample of the shale (which passed the No. 40 sieve) and then mixing it with 250 ml of distilled water in a blender for 5 minutes. The mixture was then

removed from the blender, 750 ml of distilled water was added, and the suspension was filtered using a vacuum system with a Büchner funnel and No. 40 Whatman filter paper. The filtrate was then refiltered and the resulting solution placed in a plastic bottle for storage until the conductance could be measured and a chemical analysis completed.

The second experiment was the shaker experiment which consisted of taking a 100 gram sample of shale (which passed the No. 40 sieve) and placing it in a one gallon container. One liter of distilled water was added and then the container was shaken manually for 5 minutes. The mixture was filtered and the solution stored as described above.

To determine the quantities of dissolved solids leachable by simple percolation, a column experiment was conducted on the TOSCO shale. The apparatus for the experiment consisted of a plastic column 120 cm in length and 10 cm in diameter. Taps were inserted into the column at 10, 40, 70, 100, and 120 centimeters from the top of the column so that percolation water could be removed at these levels. The column was filled with 12,500 grams of the TOSCO spent shale and compacted to the bulk density used in the porosity determination. A constant head of 2 cm of tap water was maintained on the top of the shale. Concentrations in the tap water were subtracted from observed concentrations.

Figure 6 shows a picture of a segment of the column and a portion of the spent shale as removed from the column after percolation.

#### PILOT STUDIES:

The most important phase of the study was a pilot study program, using TOSCO unweathered spent shale, conducted on the Colorado State University rainfall-runoff facility. The pilot study objectives were:

1. To determine the quality and quantity of total runoff from spent shale piles using natural and simulated rainfall.
2. To determine the properties of the residue within the piles before and after rainfall simulation.

Model Characteristics - The model used for the study had the following characteristics:

1. Approximately 68 tons of TOSCO unweathered spent shale were placed in a pile 80 feet long, 8 feet wide at the bottom, and 12 feet wide at the top, with a depth of 2 feet. The surface of the shale had a 0.75 percent slope. This is roughly the maximum permissible slope if excessive erosion is to be prevented.
2. A four-inch layer of sand was placed below the shale to serve as a drain for any percolation water.
3. An impermeable plastic barrier was placed below the sand filter and along the sides of the facility to insure that no percolation losses occurred.
4. A three-inch perforated plastic pipe was placed in the sand filter to collect any percolation water and divert it to a 50-gallon drum for storage.

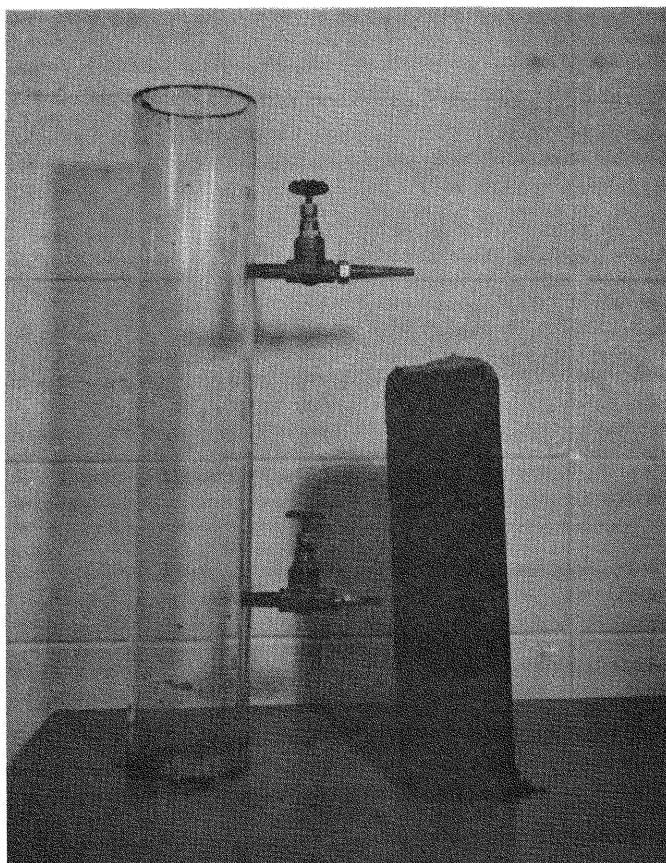


FIGURE 6: SEGMENT OF COLUMN AND PORTION OF TOSCO SPENT SHALE USED IN COLUMN STUDY

5. Artificial rainfall was generated by a system of nozzles spraying into the air over the facility. The system had the capability of producing rainfall intensities from about 1/2 inch per hour to over 2.5 inches per hour.
6. Cumulative rainfall mass curves were obtained from a recording-type raingage. The surface runoff was measured by an H-flume with a standard float gage. After passing through the flume, the runoff water was diverted to a small settling basin where it evaporated and seeped into the soil.
7. Three access tubes for use of a neutron moisture probe were installed in the middle of the shale at 20, 40, and 60 feet from the upstream end of the facility.
8. Four thermistors were installed 60 feet downstream for the upstream end to monitor the temperature of (a) the air, (b) the surface of the shale, and (c) the shale at depths of one and two feet below the surface.
9. A trailer was located at the downstream end of the facility to serve as an onsite laboratory.

Shown in Figures 7 thru 15 are pictures taken during the various stages of construction of the facility.

CHEMICAL ANALYSES -- The procedure used to determine the concentrations of the various constituents is found in the 1965 edition of Standard Methods for the Examination of Water and Wastewater, (17), except for the following ions:  $H^+$ ,  $Na^+$ ,  $Ca^{++}$ ,  $Pb^{++}$ ,  $Cl^-$ ,  $F^-$ ,  $I^-$ ,  $NO_3^-$ , and  $Br^-$ . The concentrations of these ions were determined with the use of the respective specific ion activity electrodes.

Briefly, measurement of ion activity is accomplished with the electrodes by determining the potential that is developed between the test sample and the special filling solution inside the electrode. The Nernst equation predicts that at 25°C the potential for a monovalent sensing electrode will change approximately 59 millivolts for each decade change in ion activity, while for a divalent sensing electrode the change is 29.5 millivolts, etc. By determining the activity coefficient,  $f$ , the concentration,  $c$ , of a particular ion is given by

$$c = \frac{a}{f} \quad (41)$$

where

$a$  = the activity of a particular ion in moles per liter.

The complete procedure for determining  $f$  and  $c$  is given in Appendix A.

Figure 16 is a picture of the Orion specific ion activity electrode equipment used for ionic analysis.

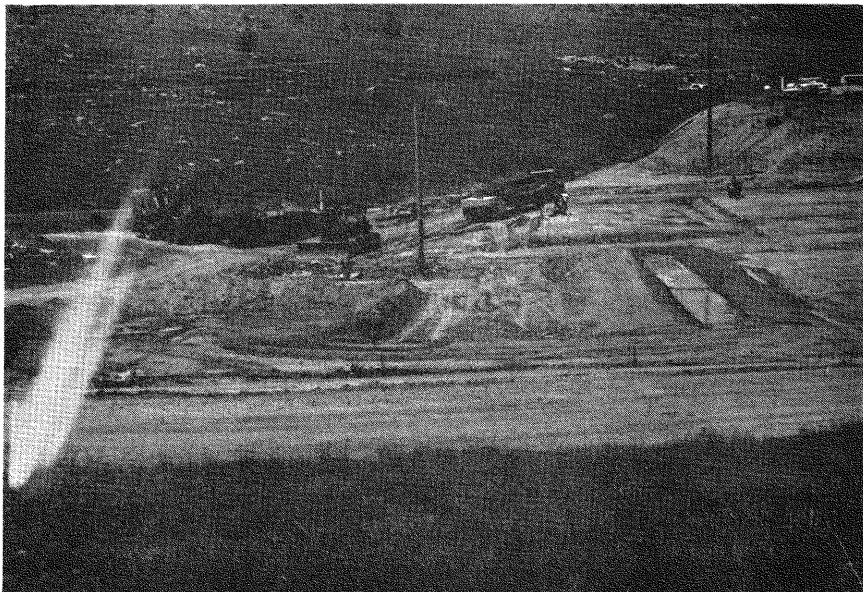


FIGURE 7: OVERALL LAYOUT OF RAINFALL FACILITY: Excavation for oil shale on right and holding pond for runoff water on left. Large tower in center used to mount floodlights for night work.





FIGURE 8: CLOSE-UP OF EXCAVATION: Approximately 3 feet deep x 8 feet wide x 80 feet long.

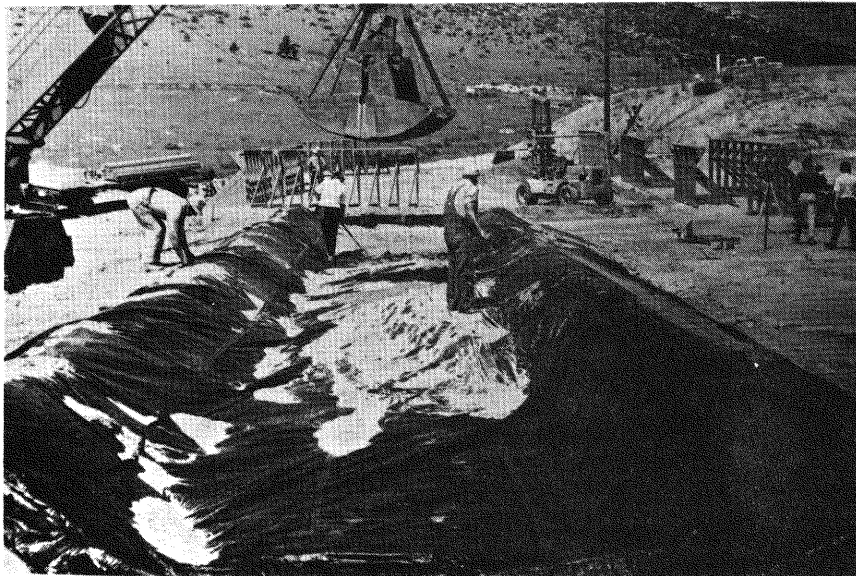


FIGURE 9: INSTALLATION OF PLASTIC LINER

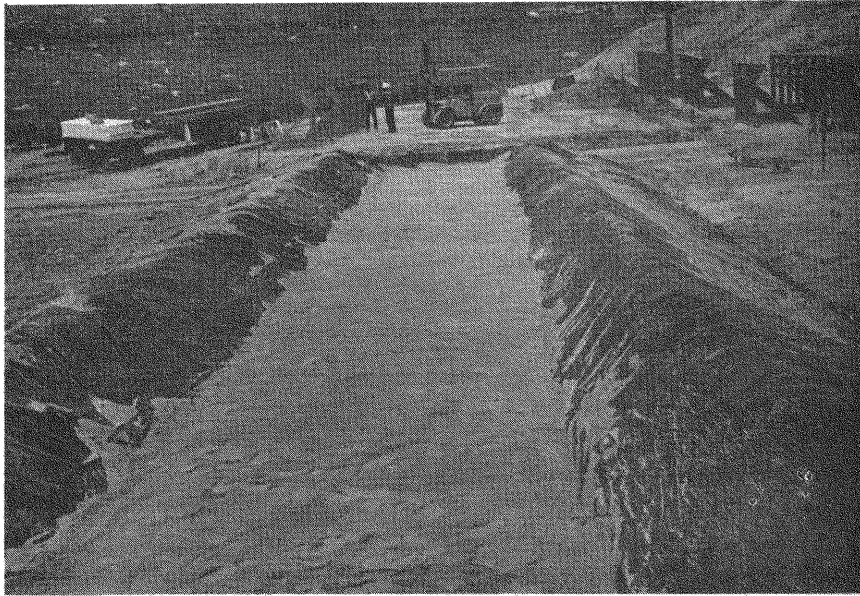


FIGURE 10: SAND DRAIN UNDERLYING SPENT SHALE: Four inch layer of sand underlying spent shale to serve as a drain of percolation water.

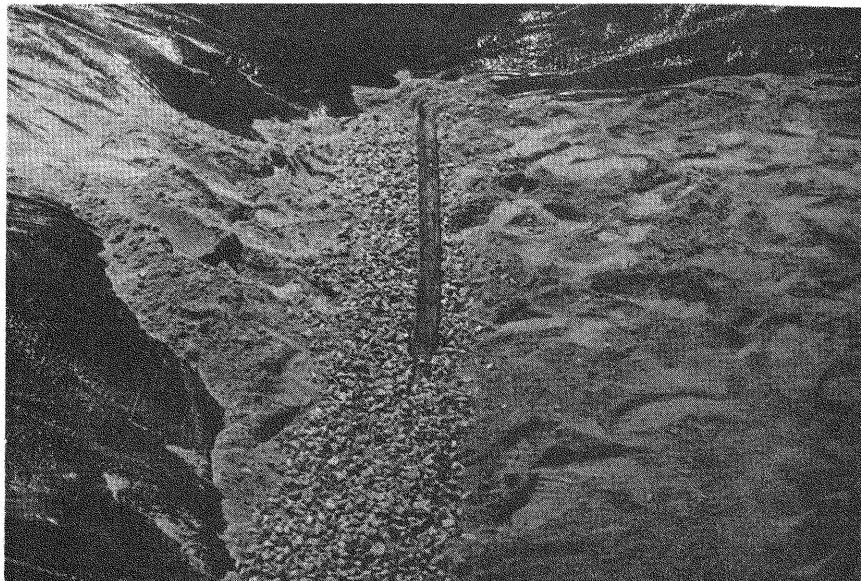


FIGURE 11: COLLECTION LINE FOR PERCOLATION WATER: A 3-inch perforated pipe in a gravel trench collects infiltration water and transports it to a 50-gallon drum for storage.

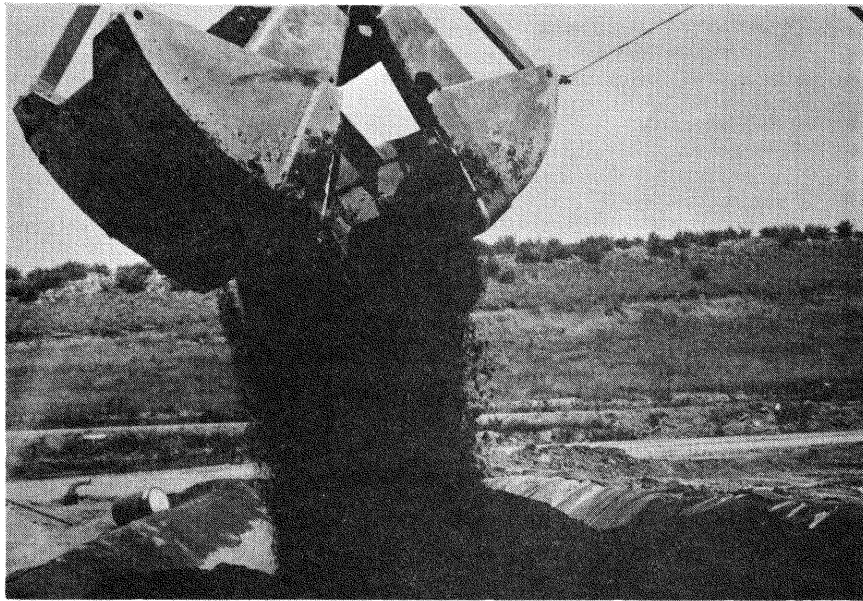


FIGURE 12: BACKFILLING OF FACILITY WITH 68 TONS OF FRESH TOSCO OIL SHALE RETORTING RESIDUE

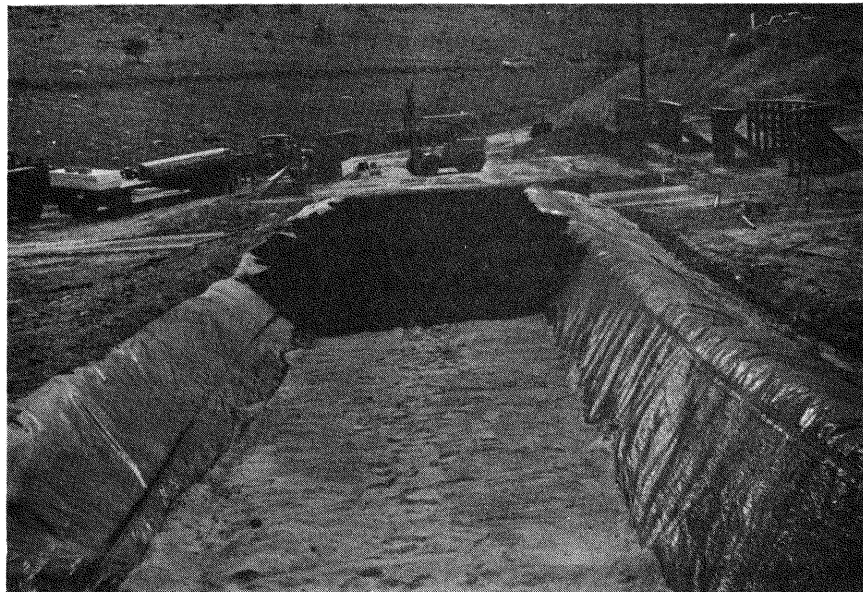


FIGURE 13: PARTIALLY BACKFILLED FACILITY

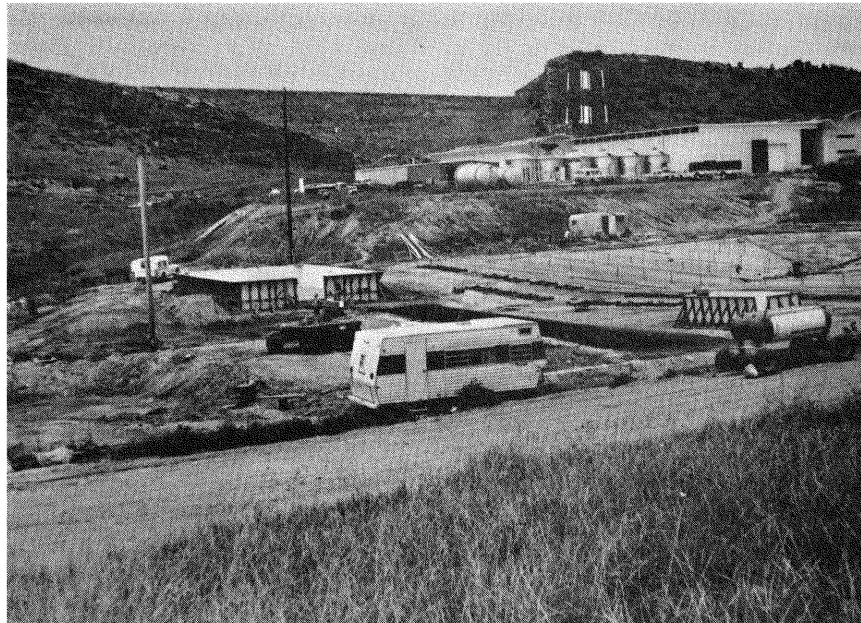


FIGURE 14: COMPLETED FACILITY: Trailer was used as a field laboratory.

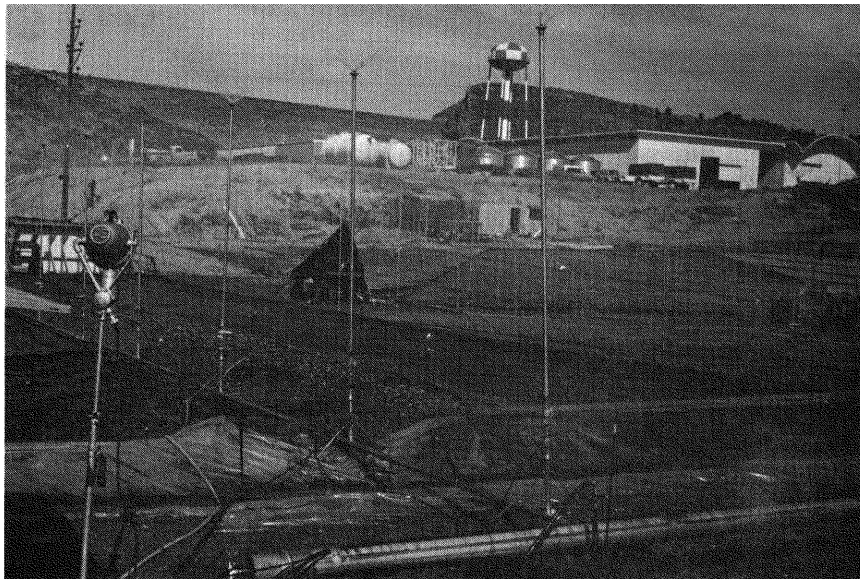


FIGURE 15: COMPLETED FACILITY WITH SIMULATED 1-1/2" RAIN OCCURRING: Note vertical pipes in center of shale for insertion of nuclear moisture probe and rain gage partially hidden by floodlight.

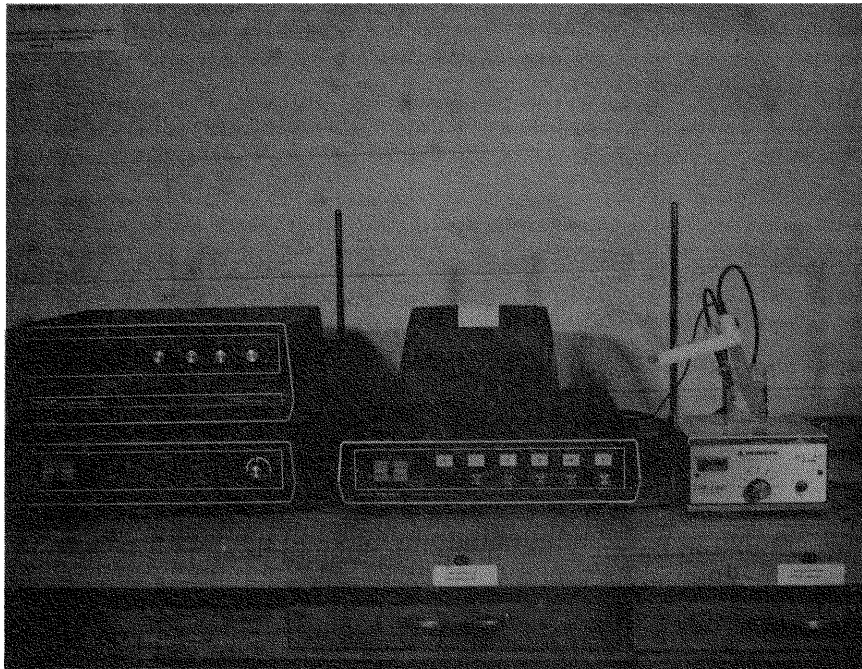


FIGURE 16: ORION SPECIFIC ION EQUIPMENT USED FOR CHEMICAL ANALYSES

## SECTION VI

### EXPERIMENTAL DATA AND RESULTS

#### BENCH SCALE STUDIES

Physical Properties - The results of the mechanical sieve analysis for the USBM and TOSCO spent shales are given in Tables III and IV. A mechanical sieve analysis of the UOC burned shale was not possible because most of the burned shale is in the form of large clinkers as shown in Figure 3.

The observed data were plotted on logarithmic probability paper as shown in Figures 17 and 18. In general, 68.2 percent of the plotted points will fall between the two dashed lines if the data are distributed in accordance with a geometrically normal frequency distribution. The method involved in determining the position of the two dashed lines is described by Ward (21). Both graphs indicate that the size distribution of the particles may be approximated by a geometric distribution, especially in the lower ranges of particle sizes (< 0.10 cm). The smaller particles are of the most concern since they will have the greatest effect on the other physical parameters such as porosity, surface area per unit volume, and permeability.

If the particle size distribution is geometrically (or log normal) distributed, then the geometric mean of the particle size distribution,  $M_g$ , in cm, can be calculated from the results of the sieve analysis using the following equation:

$$\log M_g = \sum p \log X \quad (42)$$

where  $p$  is the decimal fraction of the total sieve sample retained between 2 sieves whose geometric mean size is  $X$  cm. If  $X_1$  represents the size of the upper sieve and  $X_2$  represents the size of the lower sieve, then  $X = \sqrt{X_1 X_2}$ . The geometric standard deviation of the particle size distribution,  $\sigma_g$ , dimensionless, is calculated using the equation

$$\log \sigma_g = (\sum p \log^2 x_g)^{1/2} \quad (43)$$

where

$$x_g = X/M_g \quad .$$

Knowing the permeability, geometric mean size, geometric standard deviation, and porosity, the shape factor,  $\phi$  (dimensionless), of the

Table III: Sieve Analysis of Bureau of Mines Spent Oil Shale Residue

Sieve U.S. standard	Opening (mm)	Weight retained in grams	Percent retained	Cumulative percent finer
1.50 in.	38.10	0	0.00	100.00
1.00 in.	25.40	398	2.09	97.91
0.75 in.	19.05	1,834	9.63	88.28
0.50 in.	12.70	2,567	13.48	74.80
0.345 in.	9.52	1,715	9.01	65.79
No. 4	4.76	2,441	12.82	52.97
No. 8	2.38	1,807	9.49	43.48
No. 16	1.19	1,422	7.47	36.01
No. 30	0.595	1,181	6.20	29.81
No. 50	0.297	1,061	5.57	24.24
No. 120	0.125	1,660	8.72	15.52
No. 200	0.074	1,546	8.12	7.40
Hydrometer	0.0346	533	2.80	4.60
	0.0336	381	2.00	2.60
	0.0268	446	2.34	0.26
	0.0157	38	0.20	0.06
	0.0077	12	0.06	0.00
Summation		19,042	100.00	

media may be calculated from the following equation (23):

$$\phi^2 = \frac{(k)(36 KT)(1 - \epsilon)^2 \sigma \frac{1 \text{ n}\sigma \text{ g}}{\text{g}}}{\epsilon^3 \frac{\text{M}^2}{\text{g}}} \quad (44)$$

where

36 is a pure number,  $0 \leq \phi \leq 1$  ( $\phi = 1$  for spheres),  
 T = tortuosity. The theoretical value of T for fully saturated unconsolidated porous media that are isotropic is 2 (24),

Table IV: Sieve Analysis of TOSCO Spent Oil Shale Residue

Sieve U.S. Standard	Opening (mm)	Weight retained in grams	Percent retained	Cummulative percent finer
No. 8	2.38	0	0.00	100.00
No. 16	1.19	567	5.14	94.86
No. 30	0.595	390	3.53	91.33
No. 50	0.297	588	15.33	86.00
No. 120	0.125	1,170	10.60	75.40
No. 200	0.074	784	7.10	68.30
Hydrometer	0.0461	1,134	10.28	58.02
	0.0346	1,125	10.20	47.82
	0.0336	2,043	18.50	29.32
	0.0268	2,882	26.10	3.22
	0.0157	287	2.60	0.62
	0.0077	68	0.62	0.00
Summation		11,038	100.00	

K = a dimensionless constant that depends on the shape of the cross-section of flow and theoretically,  $2 < K < 3$ . Ward (25) has determined experimentally that K has a value of  $2.36 \pm 0.11$  for unconsolidated porous media. K is exactly 3 for a cross-section formed by closely spaced parallel plates and is exactly 2 for a circular cross section.

The permeability experiments were run over a period of one week, with readings taken at various time intervals. The observed data were plotted as shown in Figure 19. As the graph indicates, the permeability of the spent oil shale residues appears to decrease with time and this decrease may be approximated by

$$k \text{ (cm}^2\text{)} = \frac{0.585}{t_{1/2}} \times 10^{-9} + 2.17 \times 10^{-9} \text{ (USBM)} \quad (45)$$



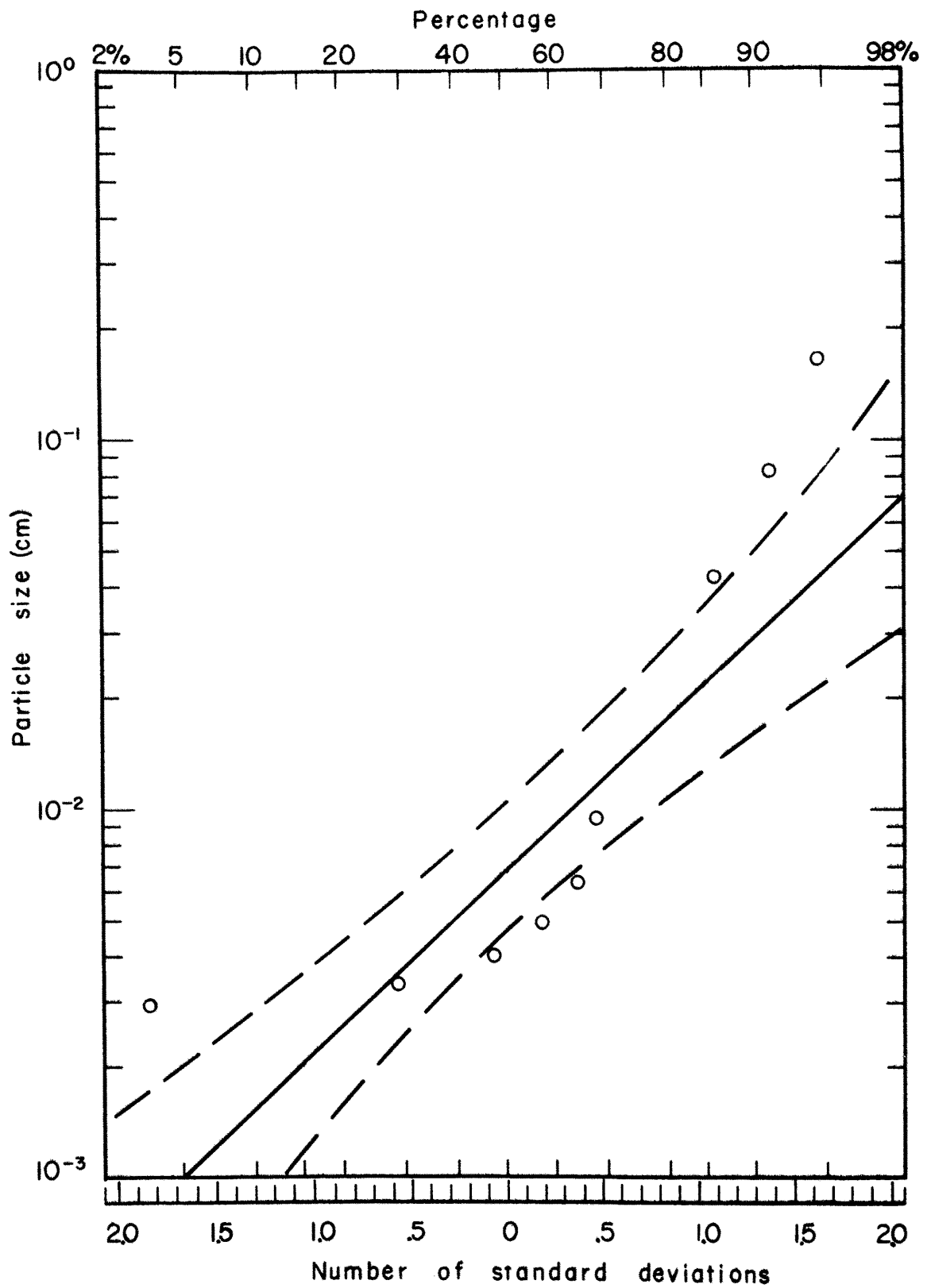


FIGURE 17: LOGARITHMIC PROBABILITY PLOT OF SIZE DISTRIBUTION OF TOSCO SPENT OIL SHALE

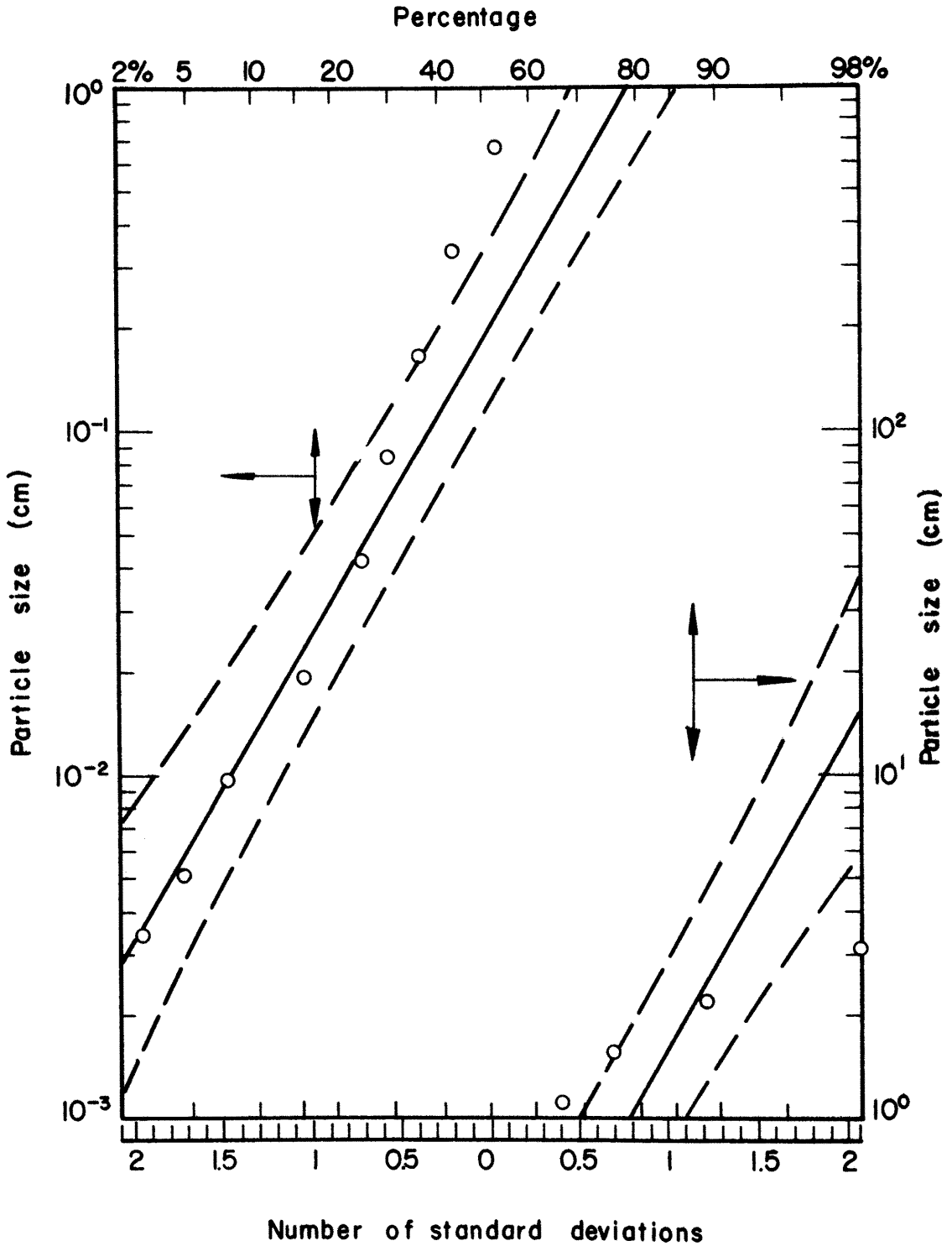


FIGURE 18: LOGARITHMIC PROBABILITY PLOT OF SIZE DISTRIBUTION OF USBM SPENT OIL SHALE

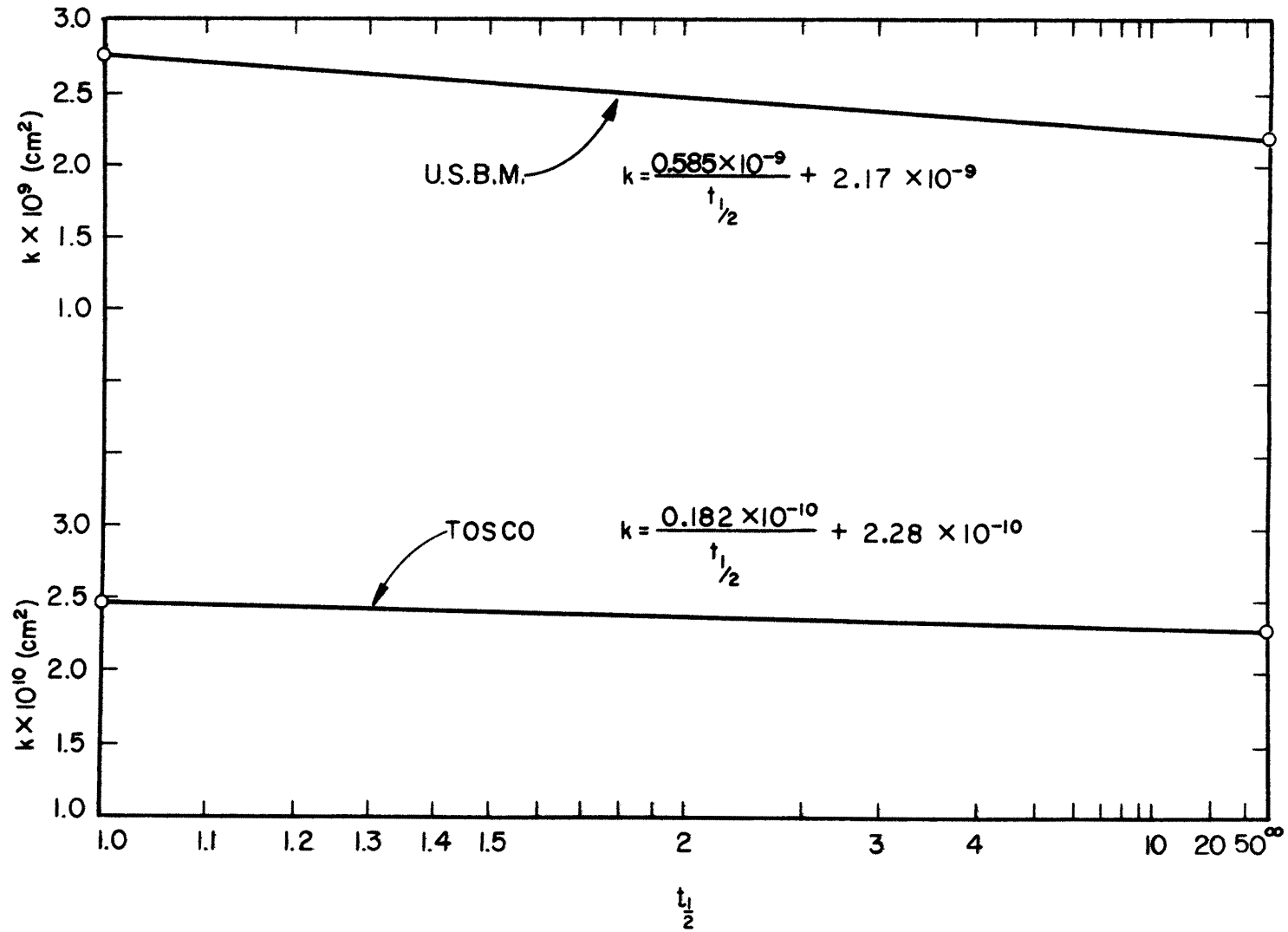


FIGURE 19: VARIATION OF THE PERMEABILITY OF TOSCO AND USBM SPENT SHALES WITH TIME

and

$$k \text{ (cm}^2\text{)} = \frac{0.182}{t_{1/2}} \times 10^{-10} + 2.28 \times 10^{-10} \text{ (TOSCO)} \quad (46)$$

in which

$t_{1/2}$  = the number of half days from the start of the permeability test.

Equations 45 and 46 are valid only for  $1 < t_{1/2} < \infty$ . The initial permeability, at  $t_{1/2} = 0$ , was determined by averaging the permeability of three respective samples immediately after saturation.

A summary of the physical properties of the various oil shale residues is given in Table V.

Table V: Physical Properties of the Various Oil Shale Residues

Oil Shale Residue	USBM	TOSCO	UOC	RAW
geometric mean size, cm	0.205	0.007		
geometric standard deviation	8.05	3.27		
particle shape factor	0.0526	0.097		
bulk density, g/cc	1.44	1.30	1.80	
solids density, g/cc	2.46	2.49	2.71	2.34
porosity	0.41	0.47	0.33	
permeability, cm <sup>2</sup>	$3.46 \times 10^{-9}$	$2.5 \times 10^{-10}$		
maximum size, cm	<3.81	<0.476		
minimum size, cm	>0.00077	>0.00077		

It is interesting to note that the eventual permeabilities of the USBM and TOSCO residues are 63 and 91% respectively of their initial permeabilities.

Additional permeability experiments were conducted on the TOSCO spent shale because it was to be used in the pilot study. In particular, the permeability of the TOSCO spent shale and its relationship to the degree of saturation was determined.

To determine this relationship, it is first more convenient to express relative permeability as a function of the capillary pressure,  $p_c$ , and

then using certain approximations obtain the desired relationship. For  $p_c > p_b$ , this relationship is described by

$$K_{rw} = \left( \frac{p_b}{p_c} \right)^{\zeta} \quad (47)$$

in which

$p_c$  is in dynes/cm<sup>2</sup>,

$p_b$  is a parameter called the bubbling pressure and is the approximate capillary pressure at which the nonwetting phase becomes continuous throughout the media, dynes/cm<sup>2</sup>,

$K_{rw}$  is the relative permeability (dimensionless) and is the ratio of the effective permeability for the wetting phase at some particular saturation to the permeability at saturation,  $k$ .

A plot of the data from the capillary pressure - permeability experiment is given in Figure 20. In Figure 20,  $\gamma$  is the weight density of the fluid in dynes/cm<sup>3</sup>. The equation of the line for  $p_c < p_b$  is

$$K_{rw} = \left( \frac{205}{p_c} \right)^{19.5} \quad (48)$$

From Figure 20, the saturation value of  $p_c/\gamma$  is 135 cm.

Using the relationships developed by Corey (26) and assuming the residual saturation for this type of media is zero, equation 48 becomes

$$K_{rw} \approx S^{3.34} \quad (49)$$

in which  $S$  = the degree of saturation, dimensionless. The saturation moisture content of the TOSCO oil shale residue is 38% by weight (47% by volume).  $S = 1$  and  $K_{rw} = 1$  when the moisture content is 38% by weight. The value of the exponent in equation 49 (3.34) indicates that the pore size distribution is almost uniform [a value of 3 indicates a completely uniform pore size distribution (26)].

Blender and Shaker Experiment - The chemical analyses of the blender and shaker experiments are given in Tables VI and VII respectively. The data given in each table represents the average of three samples.

The results indicate that the concentration of dissolved solids in the filtrate from the blender experiment is slightly higher than that from the shaker. However, allowing for differences in composition due to sampling, it could be concluded that the blender and shaker experiments yield a filtrate of approximately the same concentration and composition.

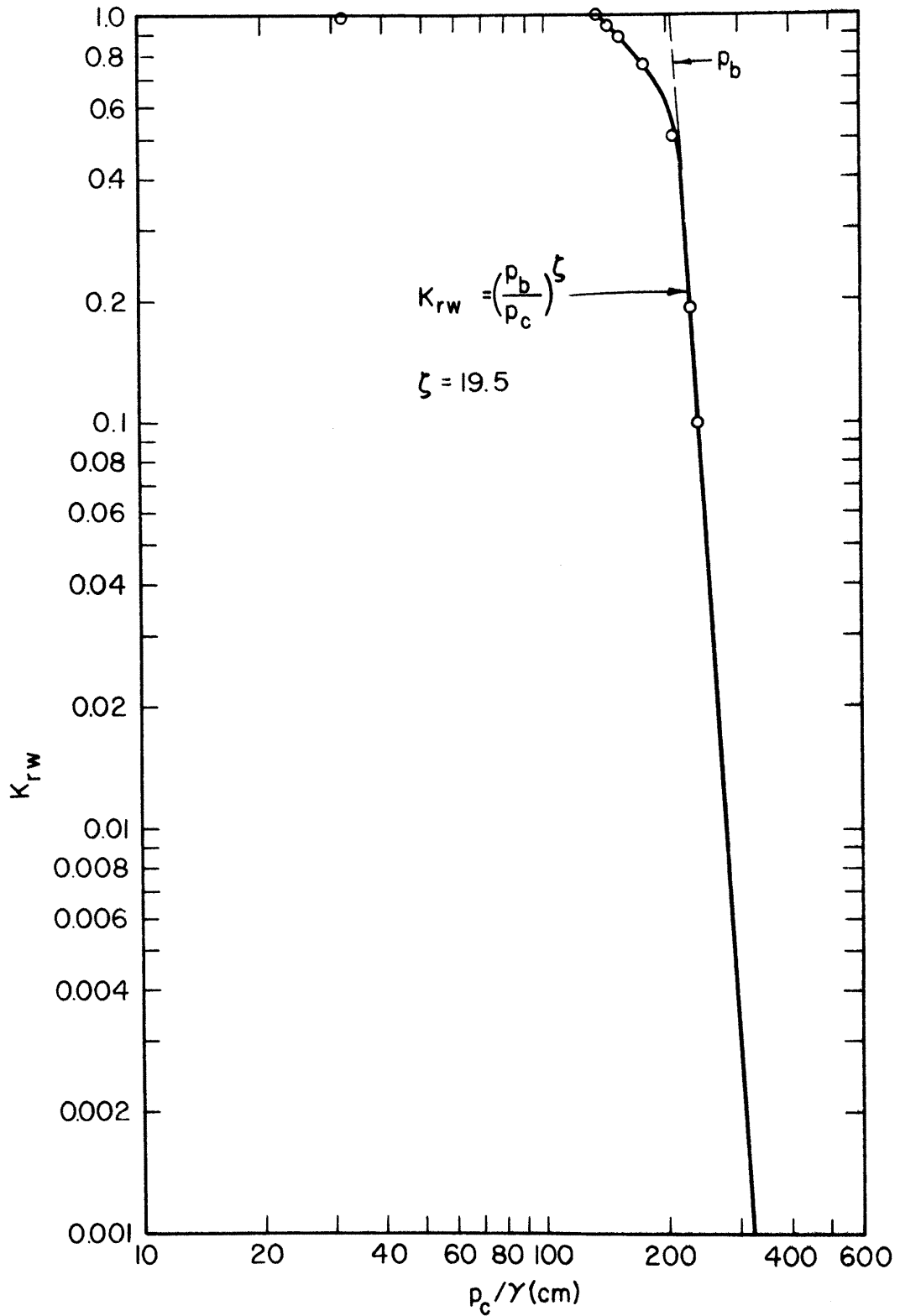


FIGURE 20: CAPILLARY PRESSURE VERSUS RELATIVE PERMEABILITY FOR TOSCO SPENT OIL SHALE

Table VI: Results of the Blender Experiment

Sample	pH	Conductance μmhos/cm @ 25°C	TDS (mg/l)			Concentrations (mg/l)						
			103°C	180°C	600°C	K <sup>+</sup>	Na <sup>+</sup>	Ca <sup>++</sup>	Mg <sup>++</sup>	HCO <sub>3</sub> <sup>-</sup>	Cl <sup>-</sup>	SO <sub>4</sub> <sup>=</sup>
Raw	8.15	310	277	146	134	24	48	10	1.0	75	2.2	79
USBM	7.78	1,495	1,091	1,001	892	72	225	42	3.5	38	13	600
UOC	9.94	11,050	10,011	9,702	9,680	625	2,100	327	91	28	33	6,230
TOSCO*	8.40	1,750	1,262	1,115	1,058	32	165	114	27	20	7.6	730

46

Table VII: Results of the Shaker Experiment

Sample	pH	Conductance μmhos/cm @ 25°C	TDS (mg/l) @ 103°C	Concentrations (mg/l)							
				K <sup>+</sup>	Na <sup>+</sup>	Ca <sup>++</sup>	Mg <sup>++</sup>	HCO <sub>3</sub> <sup>-</sup>	Cl <sup>-</sup>	SO <sub>4</sub> <sup>=</sup>	
Raw	8.41	300	270	---	---	---	---	---	---	---	---
USBM	7.82	1,320	970	---	---	---	---	---	---	---	---
TOSCO*	8.43	1,640	1,121	10	206	102	31	20	5.8	775	

\* NO<sub>3</sub><sup>-</sup> concentrations for the blender and shaker were 5.6 and 5.1 mg/l respectively.

Column Study - The first leachate from the column of TOSCO spent shale took 2 weeks to move through the column after the water was first applied. For the following 28 days, volumes of leachate were collected at various time intervals until a total of 4.6 liters had been percolated and collected. All samples were collected at the bottom of the column because it was impossible to obtain a sample from the various taps that had been installed in the column. (see Figure 6).

The volume and conductance of each leachate sample collected was determined. The major constituents and their concentrations for the first eight samples were determined. These results are given in Table VIII.

A computer program was developed to calculate the concentration and composition of the percolation water by the procedure described in Section III. A simplified flow chart of the entire program is shown in Figure 21, and Table IX gives the definitions of the terms used in the program. An entire listing of the program as written for a CDC 6400 computer may be found in Appendix D.

The quantities required for the calculation are:

1. The initial concentration in moles per liter of the ions in the solution which is to be percolated through the shale.
2. The concentrations of the exchangeable ions in the shale complex in moles per gram of shale.
3. The concentrations of the soluble ions in moles per liter at a water content of B, where B is the ratio of grams of oven dry shale residue to liters of solution contained in the soil during percolation.
4. One half the summation of the product of the concentration of the solution anions, excluding  $\text{SO}_4^{=}$ , in moles per liter times the valence squared, and the values of the exchange constants K and K' as found in equations 24 and 25.

The following assumptions were made:

1.  $\text{K}^+$  was present in negligible amounts (see Tables VI and VII),
2.  $\text{Cl}^-$  did not enter into the reactions,
3.  $\text{CaSO}_4$  was the only moderately soluble salt present,
4. Uniform physical and chemical properties of the shale,
5. The chemical reactions are adequately described by equations 24 and 25.

The experimental values and theoretical values versus volume leached are shown in Figures 22 and 23. Although some segments of the calculated curves deviate considerably from measured values, the overall agreement, and in particular, the equilibrium values, is quite good.

The bottom row of figures in Table VIII are the expected eventual final steady state concentrations that would be expected after a very large quantity of water had passed through the spent oil shale residue. In other words, one would not expect concentrations less than these, regardless of how much prior leaching had occurred. It is clear that



Table VIII: Experimental Results of the Percolation Experiment  
 Conducted on TOSCO Spent Oil Shale Retorting Residue

Volume of leachate sample (cc)	Total volume of leachate (cc)	Conductance of sample ( $\mu\text{mhos/cm @ } 25^\circ\text{C}$ )	Concentration (mg/l) of sample				
			Na <sup>+</sup>	Ca <sup>++</sup>	Mg <sup>++</sup>	SO <sub>4</sub> <sup>=</sup>	Cl <sup>-</sup>
254	254	78,100	35,200	3,150	4,720	90,000	3,080
340	594	61,600	26,700	2,145	3,725	70,000	1,900
316	910	43,800	14,900	1,560	2,650	42,500	913
150	1,060	25,100	6,900	900	1,450	21,500	370
260	1,320	13,550	2,530	560	500	8,200	205
125	1,445	9,200	1,210	569	579	5,900	138
155	1,600	7,350	735	585	468	4,520	138
250	1,850	6,825	502	609	536	4,450	80
650	2,500	5,700	-	-	-	-	-
650	3,150	4,800	-	-	-	-	-
650	3,800	4,250	-	-	-	-	-
760	4,560	3,850	-	-	-	-	-
	∞*	1,800	86	64	118	740	11

\* These are extrapolated values and obviously were not actually observed. These extrapolated values are probably accurate to within  $\pm 6\%$ .

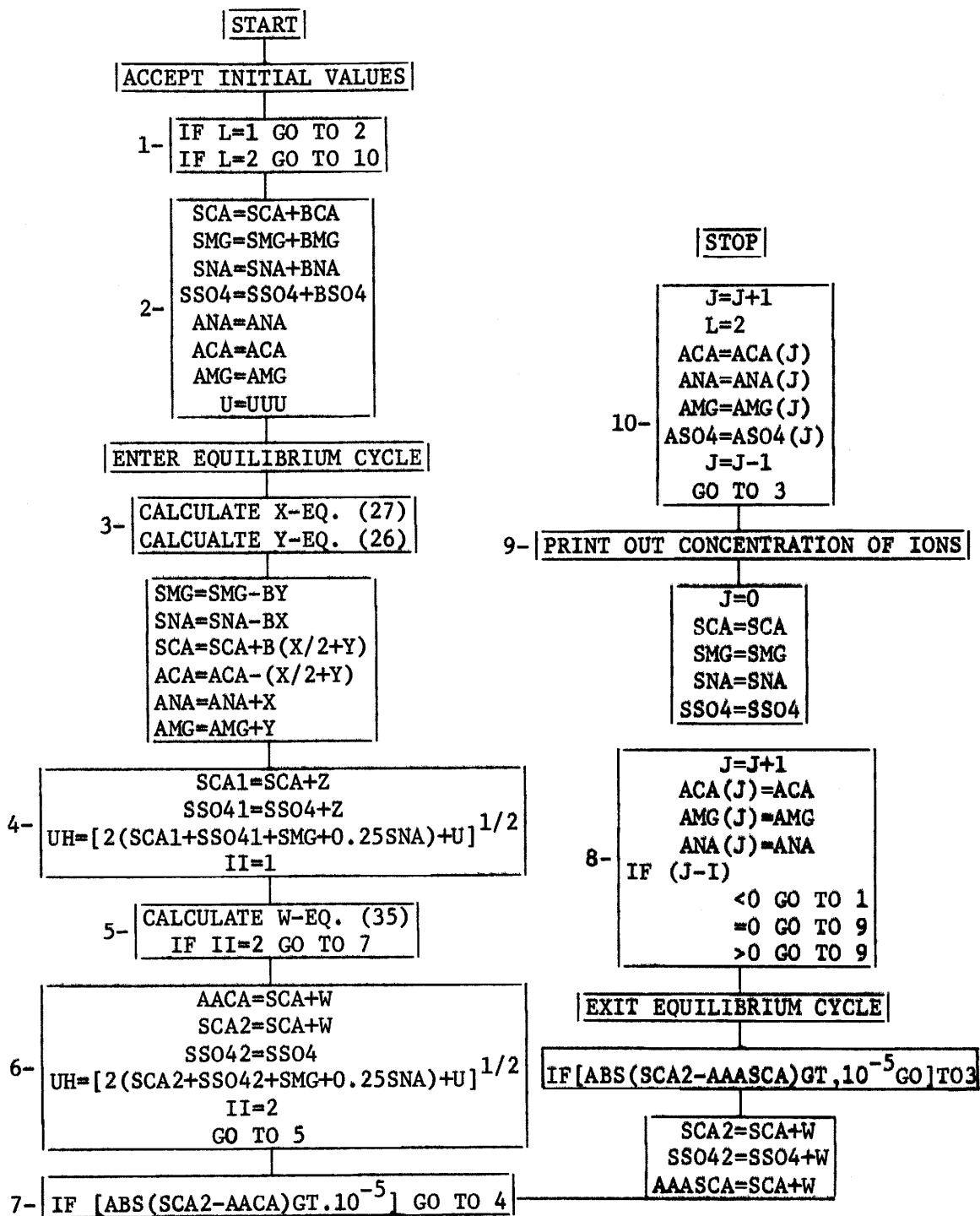


Figure 21: Flow chart for computer program.

Table IX: Definition of Terms Used in Computer Program for Predicting the Quality of Spent Oil Shale Percolation Water

Computer Symbol	Definition
SCA	Concentration in moles/liter of $\text{Ca}^{++}$ in the applied water
SNA	Concentration in moles/liter of $\text{Na}^+$ in the applied water
SMG	Concentration in moles/liter of $\text{Mg}^{++}$ in the applied water
SCL	Concentration in moles/liter of $\text{Cl}^-$ in the applied water
SSO4	Concentration in moles/liter of $\text{SO}_4^{==}$ in the applied water
ANA	Concentration in moles/gram of soil of exchangeable $\text{Na}^+$ on the shale
ACA	Concentration in moles/gram of soil of exchangeable $\text{Ca}^{++}$ on the shale
AMG	Concentration in moles/gram of soil of exchangeable $\text{Mg}^{++}$ on the shale
CK1	Exchange constant in equation 25, $K'$
CK2	Exchange constant in equation 24, $K$
CKS	Solubility product of gypsum
BETA	The moisture content of the shale during percolation
BMG	The concentration in moles/liter of soluble $\text{Mg}^{++}$
BNA	The concentration in moles/liter of soluble $\text{Na}^+$
BCA	The concentration in moles/liter of soluble $\text{Ca}^{++}$
BSO4	The concentration in moles/liter of soluble $\text{SO}_4^{==}$
UU	One half the summation of the product of the concentration of the solution anions, excluding $\text{SO}_4^{==}$ , in moles/liter times the valence squared
L, II, J	Parameters to direct program

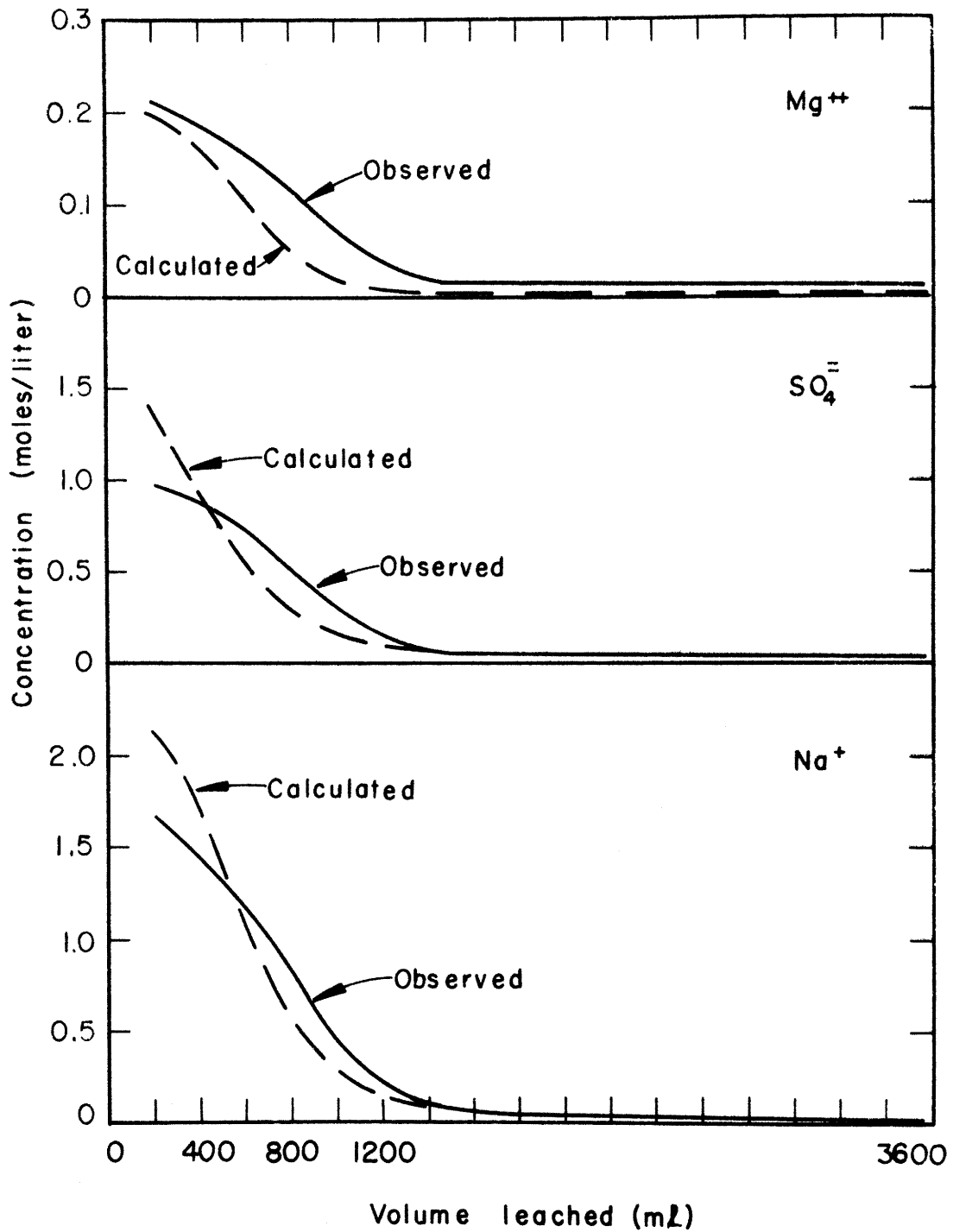


FIGURE 22: CALCULATED AND OBSERVED VALUES OF Na<sup>+</sup>, SO<sub>4</sub><sup>=</sup> AND Mg<sup>++</sup> VERSUS VOLUME OF WATER LEACHED

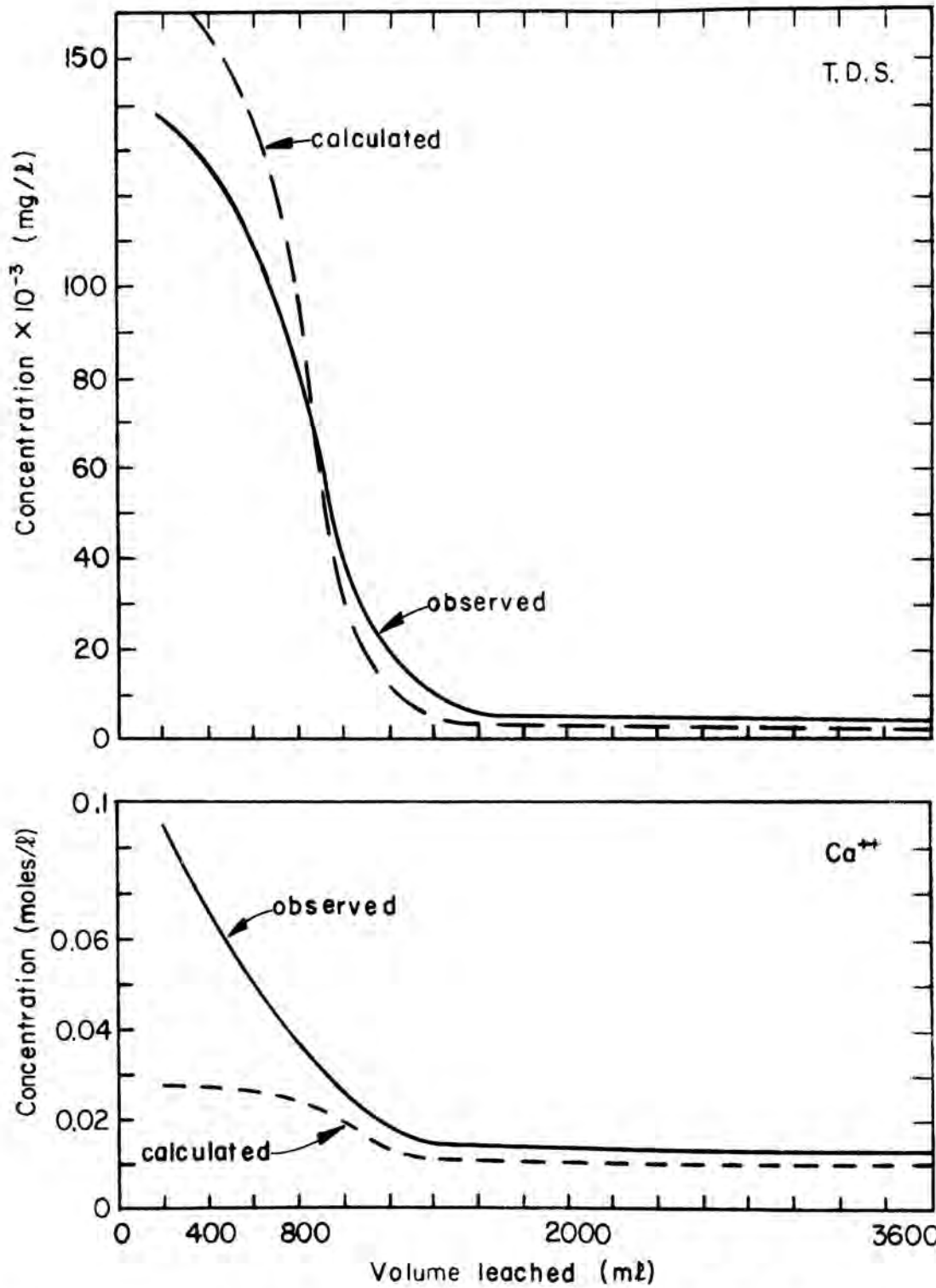


FIGURE 23: CALCULATED AND OBSERVED VALUES OF Ca<sup>++</sup> AND TDS VERSUS VOLUME OF WATER LEACHED

even these minimum possible values would be in excess of the maximum permissible allowed for drinking water, namely 250 mg/l for  $SO_4^{=}$  and a total dissolved solids (T.D.S.) concentration of 500 mg/l. On the other hand, the concentrations naturally occurring in the ground water in this area are unknown. It is worth noting in this connection that 10% of the salinity of the Colorado River at Hoover Dam is contributed by natural point sources with an average salinity of 3,220 mg/l. Therefore, it is not inconceivable that the natural ground water salinity in the oil shale area may have a salinity as great as the percolation water from oil shale residue. Examination of the records for the Colorado River near Cameo, Colorado, for the water years (a water year begins October 1 the previous year and ends September 30 of the water year) 1964 through 1968 showed that the maximum annual dissolved solids concentration observed occurred at the minimum annual flow rate observed, in general. Low flows are usually composed primarily of ground water inflow, and therefore low flow quality generally is representative of groundwater quality. The values observed are as follows:

Date	Mean Discharge (cfs)	Dissolved Solids Concentration in mg/l (residue at 180°C)
September 1-30, 1966	1,700	691
January 1-17, 1968	1,398	875
March 1-23, 1965	1,350	876
December 13-26, 1966	1,234	956
December 1-31, 1963	1,153	970
	0*	1,600*

\* extrapolated value (not observed)

Apparently the ground water salinity in the Colorado River Basin above Cameo is somewhere between 970 and 1,600 mg/l typically. Comparison of these latter 2 figures with those on the bottom row of Table VIII indicate that the ultimate effect on ground water salinity may not be significant. On the other hand, the data in Table VIII show that the initial effect of oil shale development (by surface retorting) on ground water salinity may be substantial.

#### RAINFALL PILOT STUDIES

A total of 13 experiments were conducted on the rainfall-runoff facility. Of these, 10 of the storms were simulated and 3 were natural. The total water applied amounted to over 44 inches in a 130 day period or about three years of precipitation for the oil shale area.

The inplace density of the surface of the shale (top 3 inches) for the first 9 experiments was 86 lbs/ft<sup>3</sup>. For the last 4 experiments the

shale was mechanically compacted to a surface density of 101 lbs/ft<sup>3</sup>. The overall inplace density in both instances was about 55 lbs/ft<sup>3</sup>.

As developed in Section IV, the concentration of dissolved solids in the runoff water may be described by equation 23. The values of the exponents, constants, and various relationships were determined as follows.

First, plots of total dissolved solids versus time for each simulated run were made. The values of concentration at time equal zero were extrapolated from each graph and plotted on semilog paper against  $\Delta\omega$ , the change in moisture content from the saturated value that occurred as the result of solar drying prior to the rainfall event. By selecting the value of concentration in this manner, all independent parameters except  $\Delta\omega$  were constant. The data yielded the following relationship:

$$C \propto \exp \left( \frac{4.5\Delta\omega}{0.435} \right) \quad (50)$$

Secondly, the values of concentration were extrapolated to time  $\infty$  on a reciprocal time plot and these values plotted against  $\bar{D}$  on log-log paper. The plot gave a straight line of the form

$$C \propto \frac{1}{\bar{D}^2} \quad (51)$$

Next values of concentration observed after runoff equilibrium had been reached (when runoff rate equals rainfall rate) were plotted versus time on semi-log paper. A straight line was obtained when

$$C \propto \exp \left( \frac{-t^{1/3}}{0.435} \right) \quad (52)$$

Various relationships involving  $\rho$ ,  $k$ , and concentration were tried and it was found that  $C$  could best be related to  $\rho$  and  $k$  by

$$C \propto \frac{\rho}{k} \quad (53)$$

Combining equations 50, 51, 52, and 53 yields

$$C \propto \frac{\rho}{k\bar{D}^2} \exp \left( \frac{4.5\Delta\omega - t^{1/3}}{0.435} \right) \quad (54)$$

Data from all simulated runs were then plotted as shown in Figure 24, and a least squares analysis performed to give the relationship:

$$C = \frac{10^{-9} \rho}{k\bar{D}^2} \exp \left( \frac{4.5\Delta\omega - t^{1/3}}{0.435} \right) \quad (55)$$

in which C is expressed in mg/ℓ of inorganic dissolved solids. In Figure 24, r is the coefficient of correlation. In general,  $0 \leq |r| \leq 1$ . When r = 0, there is no correlation, and when  $|r| = 1$  there is perfect correlation. The value of r = 0.968, means that 96.8% of the observed variance is explained by equation 55. In equation 55,

k is expressed in cm<sup>2</sup>,  
 $\bar{D}^2$  is expressed in cm<sup>2</sup>,  
 ρ is expressed in grams/cc, and  
 t is expressed in hours.

The permeability for the different compactions was calculated from equation 44 using in-place values of porosity.

As with the bench top studies, the major constituents in the surface runoff from the spent shale pile were Ca<sup>++</sup>, Mg<sup>++</sup>, Na<sup>+</sup>, SO<sub>4</sub><sup>=</sup>, and HCO<sub>3</sub><sup>-</sup>. The composition of the runoff water also varies with time. In general, at the beginning of a run, Na<sup>+</sup> constituted the greatest portion of the cations while near the end of the run, the runoff water was essentially Ca<sup>++</sup> in cation concentration. The SO<sub>4</sub><sup>=</sup> ion constituted the major part of the anion concentration, with HCO<sub>3</sub><sup>-</sup> concentration essentially constant at 0.3 to 0.4 me/ℓ.

Moisture content also affected composition. Drying of the shale surface causes movement of water from the interior to the surface by capillary action. On reaching the surface, the water evaporates leaving behind a white deposit that is clearly visible on the black surface. This deposit is dissolved during the rainfall with the result that both concentration and composition of dissolved solids in the runoff water vary with time and depend on the amount of drying prior to the rain. Figure 25 is a picture of this deposit. From equation 55, it would appear that compaction increases the concentration of dissolved solids in the runoff because compaction increases ρ and decreases k. The rate at which the deposit is formed therefore is clearly dependent on the rate at which capillary action can carry the very concentrated solution from the pores within the shale residue to the surface, because the material can be evaporated more rapidly than it can be transported to the surface by capillary action. If the reverse were true, compaction would have no effect on runoff concentrations, because evaporation would be the rate determining step. The maximum rate of capillary movement can therefore be estimated from evaporation rates. In the area where these experiments took place, the maximum evaporation rate from a fresh water surface is about 9 inches per month (in July). The interstitial or microscopic velocity in the pores corresponding to this rate is  $\sqrt{T/\epsilon}$  times the



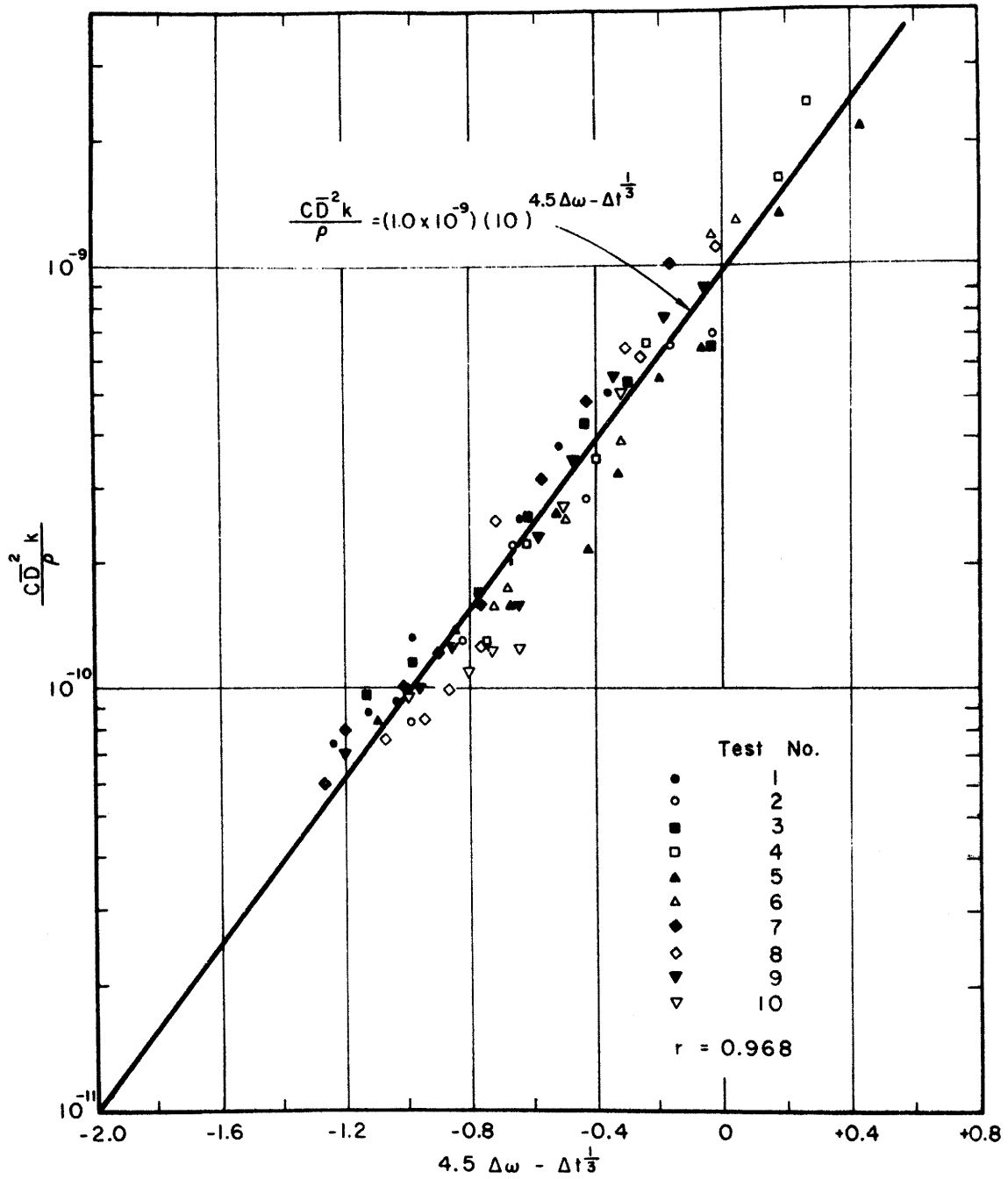


FIGURE 24: RELATIONSHIP OF TDS IN SPENT SHALE RUNOFF WATER TO INDEPENDENT PARAMETERS

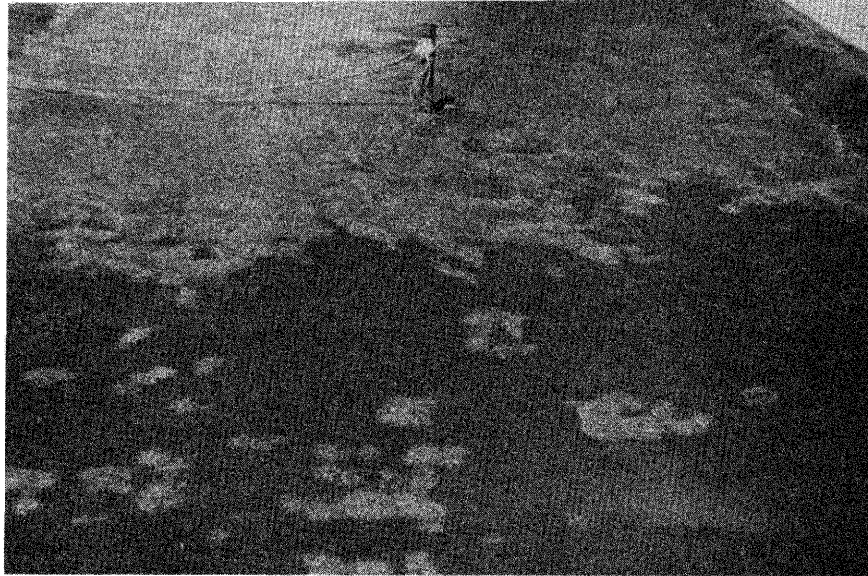


FIGURE 25: SURFACE DEPOSIT ON TOSCO SPENT OIL SHALE

aforementioned evaporation velocity, or  $\left( \frac{9 \times \sqrt{2}}{0.345} = \right)$  37 inches per month or about 1 inch per day for fully saturated oil shale retorting residual.

It should also be noted that the parameter  $t$  in equation 55 is the time from the beginning of runoff from a given storm. While equation 55 indicates that if a storm were of infinite duration, the runoff concentration would approach that of rainfall (all simulated and natural rainfall concentrations were subtracted from observed runoff concentrations), it does not mean that eventually, after several rainfalls, very little would be leached. In fact, there was no observable decrease in the leaching characteristics of the outdoor oil shale residue from the first to the last experimental run, as Figure 24 clearly indicates. Of course all the rainfall tests were conducted during one summer, and many years of weathering might show an eventual decrease in leaching characteristics.

If one substitutes equation 11 into equation 55, one obtains

$$C = \frac{1.14 \times 10^{-8} \rho(\text{Sin}\theta)^{2/3}}{k (\nu iL)^{2/3}} \exp \left( \frac{4.5\Delta\omega - t^{1/3}}{0.435} \right) \quad (55A)$$

or at 60°F,

$$C = \frac{10^{-4} \rho(\text{Sin}\theta)^{2/3}}{k (10 iL)^{2/3}} \exp \left( \frac{4.5\Delta\omega - t^{1/3}}{0.435} \right) \quad (55B)$$

From equation 55A, it would appear that the maximum concentrations in the runoff will be found when compaction is greatest, slopes are steep, drying has been extensive, runoff has just begun, the shale residue has a low permeability, runoff water temperature is high, rainfall intensity is low, and length of overland flow is short. However, it should be noted that equation 55A is based on data from only one slope and only 2 different compactions. Further work should be done on the effect of compaction and slope angle. The quantities having the greatest effect on runoff dissolved solids concentrations are the extent of drying before rainfall and time since runoff began. Next in effect are the bulk density and permeability of the residue. Least effective (but still very important) are slope of residue surface, runoff water viscosity, rainfall intensity, and length of overland flow.

In order to get a feel for runoff concentrations, perhaps an example calculation is in order. Assume: runoff water temperature = 60°F, 1 year storm frequency, 60 minute storm duration, Grand Junction (Colorado) data applies,  $\rho = 1.63 \text{ g/cm}^3$ , slope = 0.1,  $\Delta\omega = 0.202$ , runoff has just started,  $k = 6.11 \times 10^{-11} \text{ cm}^2$ , and  $iL = 400 \text{ inch-feet per hour}$ .

From equation 12,  $i = 6.3 T^{0.265} / (t + 1.7)^{0.721} = 6.3 / (61.7)^{0.721} = 0.321$  inches per hour, so that the length of overland flow is 1,247 feet. Substituting these values into equation 55B, one obtains

$$C = \frac{(10^{-4})(1.63)(0.1)^{2/3}}{(6.11 \times 10^{-11})[(10)(400)]^{2/3}} \exp \left[ \frac{(4.5)(0.202)}{0.435} \right]$$

$$= 18,300 \text{ mg/l.}$$

Using equation 16, equations 11A and 55B can be put in terms of the Reynolds number, R:

$$\bar{D} \approx (10^{-4}) \left( \frac{R}{\sin\theta} \right)^{1/3} \text{ feet} \quad (11B)$$

and

$$C \approx \frac{10^{-4} \rho (\sin\theta)^{2/3}}{k R^{2/3}} \exp \left( \frac{4.5\Delta\omega - t^{1/3}}{0.435} \right) \quad (55C)$$

Ostensibly, the maximum value of R for which equations 11B and 55C are valid is 4,000. Substituting this value into equations 11B and 55C, one obtains

$$\bar{D} \approx \frac{1.59 \times 10^{-3}}{(\sin\theta)^{1/3}} \text{ feet} \quad (11C)$$

and

$$C \approx \frac{3.95 \times 10^{-7} \rho (\sin\theta)^{2/3}}{k} \exp \left( \frac{4.5\Delta\omega - t^{1/3}}{0.435} \right) \quad (55D)$$

Figure 26 shows the variance of composition. To determine the percentage of any of the major cations present in the runoff water, only the change in moisture from saturation,  $\Delta\omega$ , and t, the time since beginning of runoff need to be known. For the previous example,  $4.5\Delta\omega - t^{1/3} \approx 0.9$ , so the composition is 9%  $\text{Ca}^{++}$ , 78%  $\text{Na}^+$ , and 13%  $\text{Mg}^{++}$ . From Figure 31, 18,300 mg/l is equivalent to 260 me/l of cations. Therefore, the concentrations are 23 me/l  $\text{Ca}^{++}$ , 203 me/l  $\text{Na}^+$ , and 34 me/l  $\text{Mg}^{++}$ . The concentration of  $\text{SO}_4$  then would be roughly 260 me/l.

To determine the composition of the deposit left on the shale surface a sample of this white deposit was dissolved in a liter of water and an

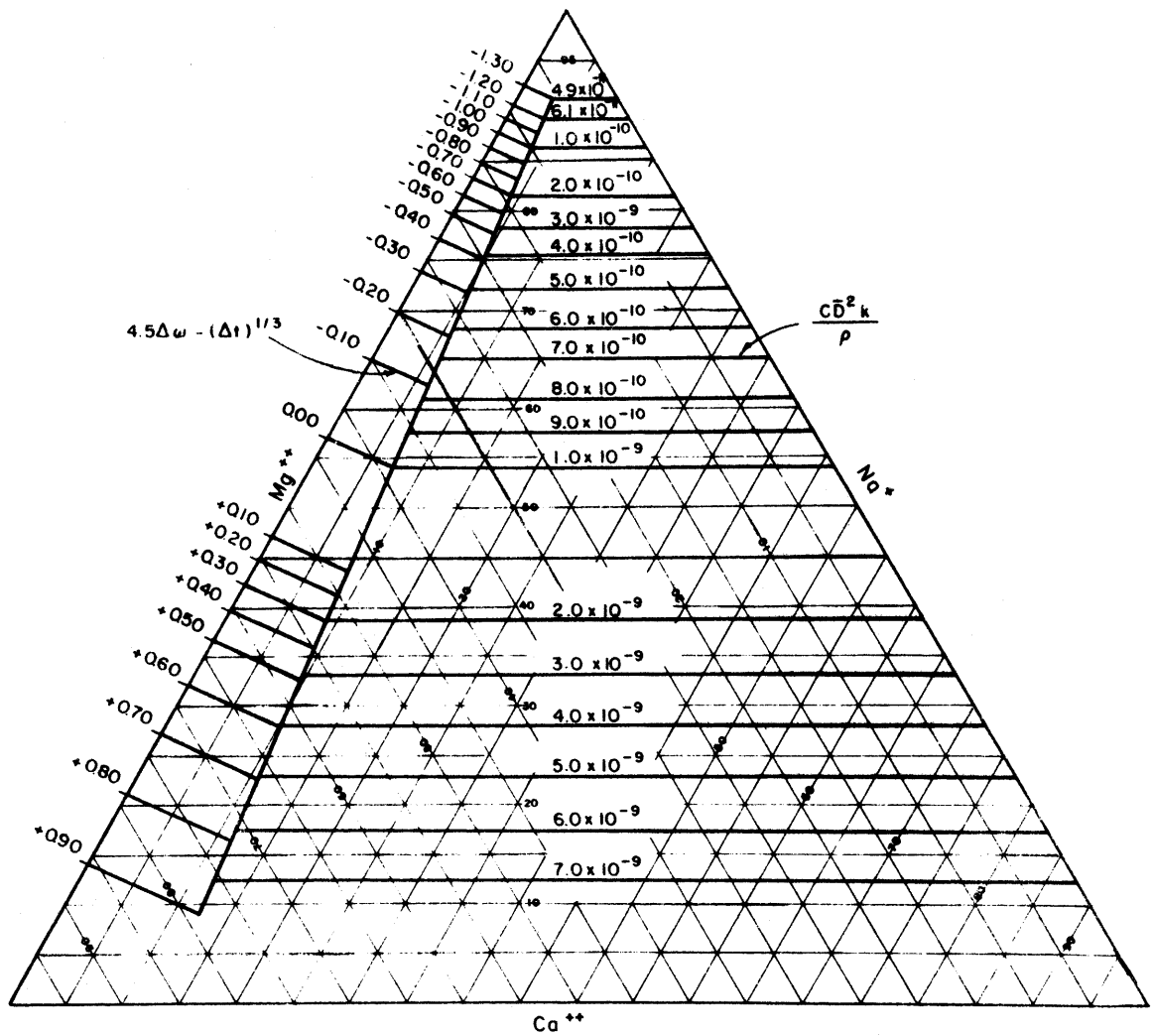


FIGURE 26: PERCENTAGE COMPOSITION OF CATIONS IN SURFACE RUNOFF FROM SPENT SHALE AS RELATED TO INDEPENDENT PARAMETERS

analysis made for the major constituents. The results are presented in Table X:

Table X: Chemical Analysis of Surface Salt Evaporation Deposit

Conductance $\mu\text{mhos/cm}$ @ 25°C	Concentration (me/l)			
	$\text{Na}^+$	$\text{Mg}^{++}$	$\text{Ca}^{++}$	$\text{SO}_4^{\#}$
28,500	580	80	10	740

As seen from Table X, the resulting solution was composed basically of  $\text{Na}^+$  and  $\text{SO}_4^{\#}$  with  $\text{Mg}^{++}$  and  $\text{Ca}^{++}$  present in smaller quantities. Therefore, it seems reasonable to assume that the initial runoff will be composed primarily of  $\text{Na}^+$  and  $\text{SO}_4^{\#}$ , with  $\text{Mg}^{++}$  present in greater concentrations than  $\text{Ca}^{++}$ .

Sediment - The yield of sediment from the spent shale piles is a complex process responding to all variations that exist in precipitation, vegetation, runoff, and topography. This study is aimed only toward a discernment of gross sediment yields from such piles.

An Imhoff cone test was used to determine the amount of sediment transported by the runoff water from the shale. Table XI gives the amount of sediment transported in a three hour period by each storm.

Table XI: Calculated Sediment Yield in Three Hour Period from Simulated Storms

Storm	Sediment, lb	Accumulated sediment (lb)	Sediment Yield $\text{lb}/(\text{ft}^2)(\text{hr})$
1	45.0	45.0	0.0150
2	20.0	65.0	0.0067
3	50.5	115.5	0.0143
4	73.8	189.3	0.033
5	153	342.3	0.083
6	170	512.3	0.0484
7	20.0	532.3	0.0062
8	74.6	606.9	0.028
9	136	742.9	0.0454
10	121	863.9	0.0643

To obtain an insight into how sediment yield might vary with the various parameters, a modification was made of the extensively used equation developed by Musgrave (28). This equation states

$$E' \propto i_{30}^{1.75} s^{1.35} L^{0.35} \quad (56)$$

where

$E'$  = rate of erosion (tons/acre),  
 $i_{30}$  = maximum 30 minute rainfall intensity of 2 year frequency  
 $= \frac{c2^m}{(30 + d)^n}$ ,

$s$  = slope, and  
 $L$  = length of slope (ft).

Assuming sediment yield varies inversely with relative moisture content,  $\omega_r (\omega_r = \omega/\omega_s)$ , equation 56 becomes

$$E \propto \frac{i^{1.75} s^{1.35} L^{0.35}}{\omega_r} \quad (57)$$

in which  $E$  = sediment yield (lb/hr-ft<sup>2</sup>).

A plot of this relationship is given in Figure 27. Such a plot may be used to give gross estimates of sediment yield from a particular storm. In the aforementioned example,  $\omega_r = \frac{0.115}{0.317} = 0.363$ , and

$$i^{1.75} s^{1.35} L^{0.35} / \omega_r = \frac{(0.321)^{1.75} (0.1)^{1.35} (1,247)^{0.35}}{0.363} = 2.06 \times 10^{-1}.$$

Extrapolating Figure 27, one obtains a sediment yield of 0.1 lb/(hr)(ft<sup>2</sup>). The equation of the straight line in Figure 27 is

$$E = 0.243 i^{0.99} s^{0.764} L^{0.198} / \omega_r^{0.566} \quad (57A)$$

To obtain an idea of the size distribution of the sediment, a sample of the sediment in the settling basin was analyzed. The results are listed in Table XII.

The size distribution of the sediment in the runoff is arithmetically normal with a mean size of 0.0317 millimeters and a standard deviation of 0.0109 millimeters. Comparing this information and the data in Table XII with the data in Table V, it appears that particles larger than the geometric mean size of the oil shale retorting residue are not

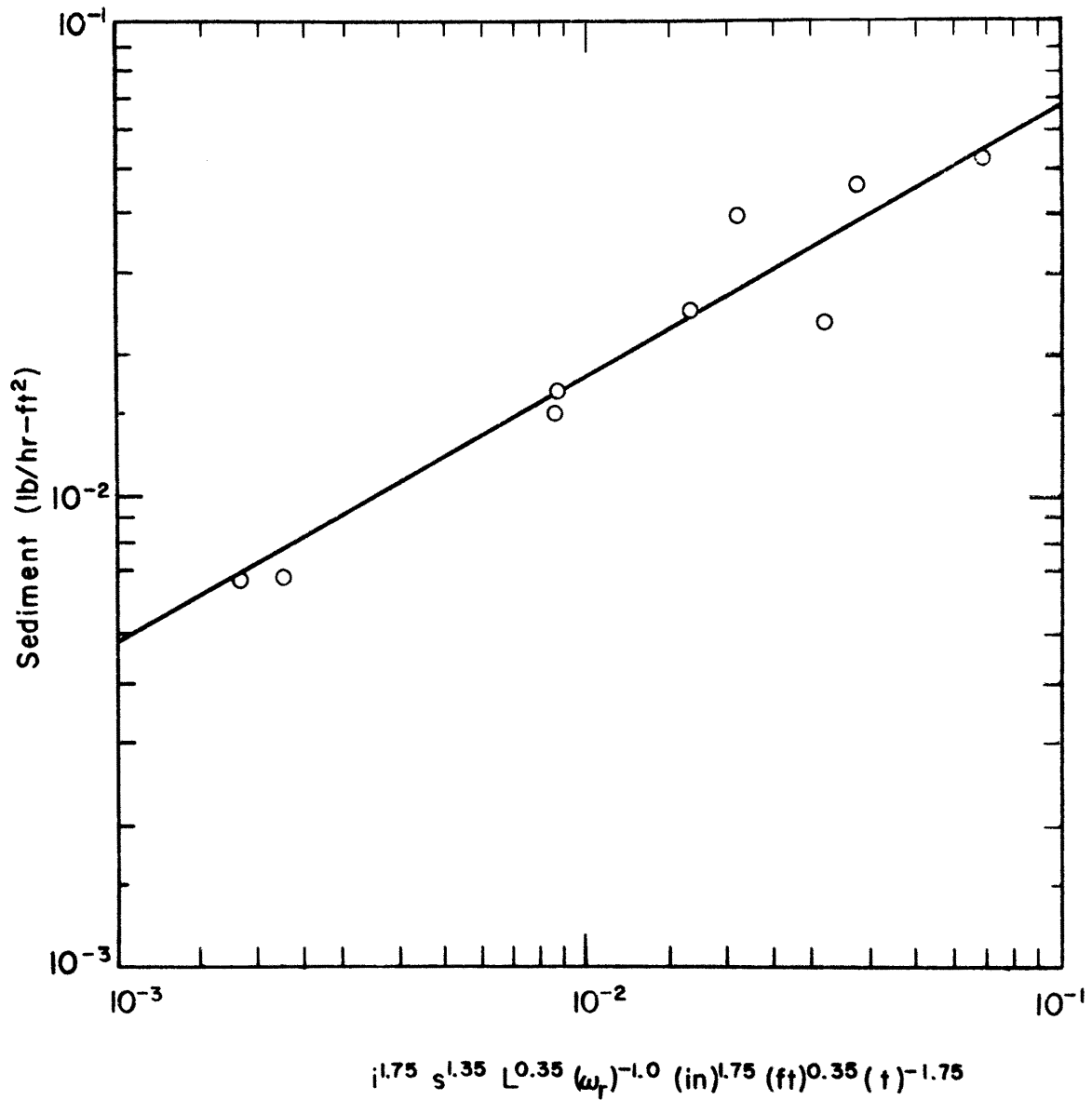


FIGURE 27: SEDIMENT YIELD FROM SPENT SHALE FOR 3-HOUR PERIOD OF SIMULATED RAINFALL



Table XII: Size Distribution of Sediment in Runoff

Size (mm)	% Finer
0.074	100
0.037	68
0.026	30
0.015	6
0.0074	2
0.0015	1

subject to erosion by rainfall, at least under the conditions of the test runs. On the other hand, approximately 1/2 of the residue (by weight) would appear to be subject to erosion by runoff from rainfall. The settling velocity of the mean size particles appears to be roughly 0.05 cm/sec (Stokes' law range) at 10°C. Stokes law is

$$v_s = (g/18)[(s_s - 1)/\nu]d^2 \quad (58)$$

where any consistent set of units can be used. In the cgs system,  $v_s$  is the settling velocity in cm/sec,  $g$  is the acceleration (the acceleration due to gravity is 981 cm/sec<sup>2</sup>),  $s_s$  is the specific gravity,  $\nu$  is the kinematic viscosity in cm<sup>2</sup>/sec, and  $d$  is the particle diameter in cm. At 85°F, the settling velocity of the TOSCO runoff sediment is

$$v_s = 10^4 d^2 \quad (59)$$

Therefore, in order to remove 99% of the sediment from the runoff, without the aid of chemical coagulants, the overflow rate of the settling basin must be less than about 10<sup>-4</sup> cm/sec. On the other hand, if the overflow rate is 10<sup>-2</sup> cm/sec, about 97% of the sediment will be removed without the aid of chemical coagulants. In a basin of 12 feet deep, with this latter overflow rate, approximately 10 hours retention time will be necessary to remove 97% of the sediment in the runoff.

To determine whether or not this settling time can be reduced by the use of a coagulant, a standard jar test was run on the sediment and Al<sub>2</sub>(SO<sub>4</sub>)<sub>3</sub> · 14H<sub>2</sub>O used as a coagulant. The results of this test are presented in Table XIII. These results indicate that Al<sub>2</sub>(SO<sub>4</sub>)<sub>3</sub> · 14H<sub>2</sub>O would make a good coagulant when applied in a concentration of 2.5 mg/l and at a pH of 8.3. Under these conditions, the apparent settling velocity of the suspension is roughly 10<sup>-2</sup> cm/sec.

To account for the water, a water balance was made on each run. These results are given in Table XIV.

The volume of water applied is the average rainfall intensity multiplied by the time of application times the area of application. The volume of runoff water was determined from the hydrograph recorded by the stage recorder. If no allowance is made for evaporation, the volume of water stored may be calculated by subtracting the amount of runoff water from the amount of water applied. The observed volume of water stored was obtained by multiplying the area of application by the average rainfall intensity times the observed time for the surface of the shale to become saturated. (At best, this observed time would be within  $\pm 10\%$ ).

As indicated by the data, the volume of water stored is small (2.0%). This is also indicated by the change in moisture within the shale as determined by use of a neutron moisture probe. The moisture content of the shale as monitored for the first 43 days of the experiment is given in Figures 28 and 29.

Thermistors located 60 feet downstream indicated temperatures within the shale remained relatively constant between 20-24°C throughout the duration of the experiments. However, the dark color of the spent shale caused temperatures as high as 77°C to be measured on the surface. Temperatures this high could be lethal to germinating seeds.

Minor Constituents - Chemical analyses for minor constituents were performed on various samples. The maximum concentrations of these constituents and the sources are given in Table XV.

Organic Analyses - Several samples were selected and analyzed for total nitrogen and carbon. These results are given in Table XVI. The samples were prepared by taking a 100 ml portion of the respective sample, evaporating it at 80°C, and then analyzing the residue.

Table XIII: Jar Test Data for Sediment in Runoff from Oil Shale Residue

Sample	Alum mg/l	pH	First Floc (min)	Description of water after given time						
				3 min.	5 min.	10 min.	30 min.	1 hr.	8hr.	36 hr.
1	0.5	8.92	none	dense	dense	dense	dense	dense	dense	fair
2	1.0	8.53	none	dense	dense	dense	dense	dense	smoky	excellent
3	1.5	8.32	10	smoky	smoky	smoky	fair	good	fair	excellent
4	2.0	8.37	2	smoky	smoky	fair	good	excellent	excellent	excellent
5	2.5	8.26	1.5	fair	good	excellent	excellent	excellent	excellent	excellent
6	3.0	8.18	1.5	fair	good	excellent	excellent	excellent	excellent	excellent

66

Table XIV: Water Balance Data for Simulated Rainfall

Run	Volume of water applied (ft <sup>3</sup> )	Volume of water runoff (ft <sup>3</sup> )	Volume of water stored (ft <sup>3</sup> )	
			Calculated	Observed
1	179	173	+ 6	+ 9
2	160	148	+12	+14
3	350	350	0	+10
4	480	500	-20	+20
5	780	755	+25	+19
6	333	320	+13	+18
7	117	120	- 3	+ 9
8	377	352	+25	+31
9	666	658	+ 8	+16
10	288	279	+ 9	+ 7
Total	3,730	3,655	+75	+153

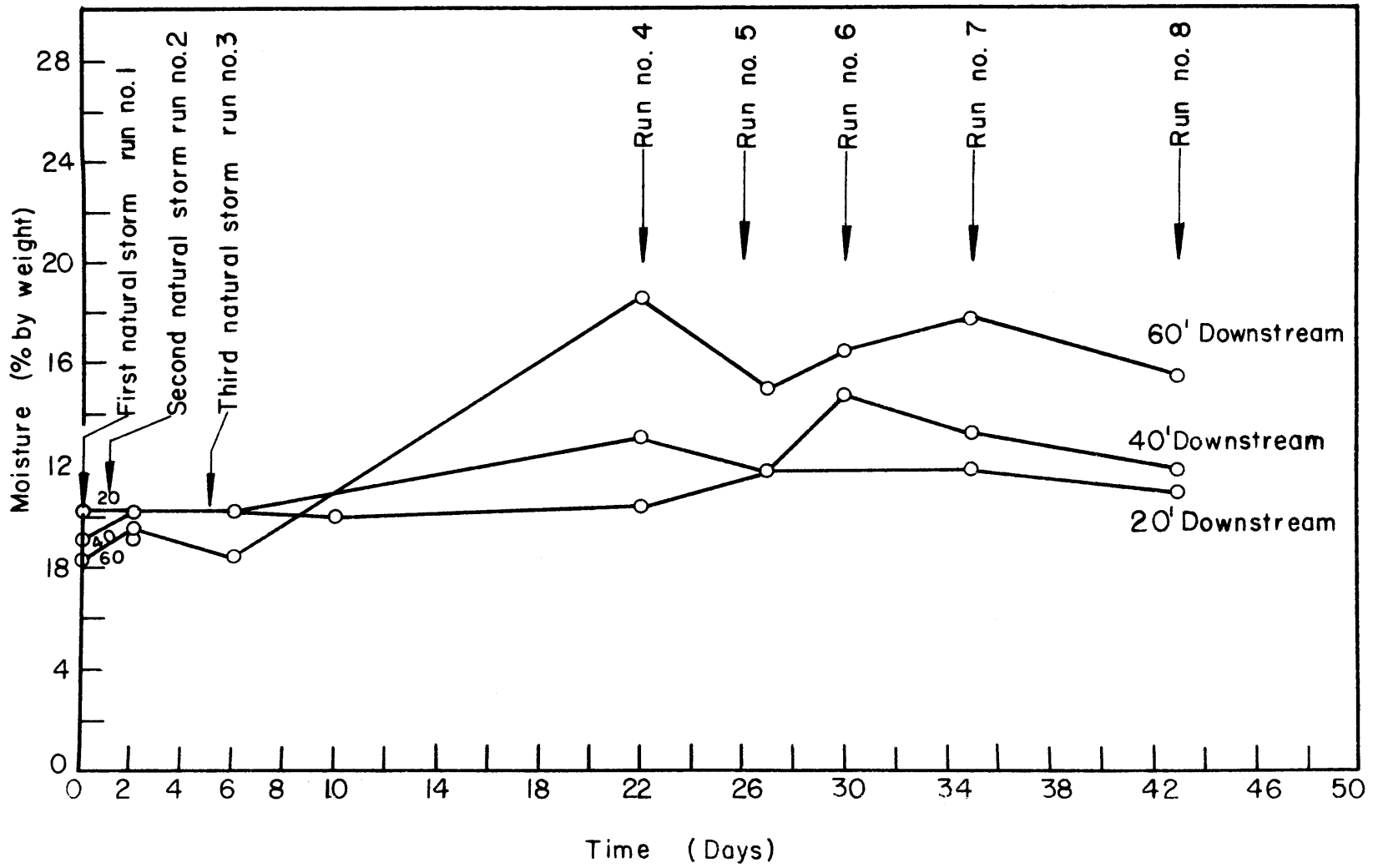


FIGURE 28: MOISTURE CONTENT OF SPENT SHALE VERSUS TIME AT 1-FOOT DEPTH

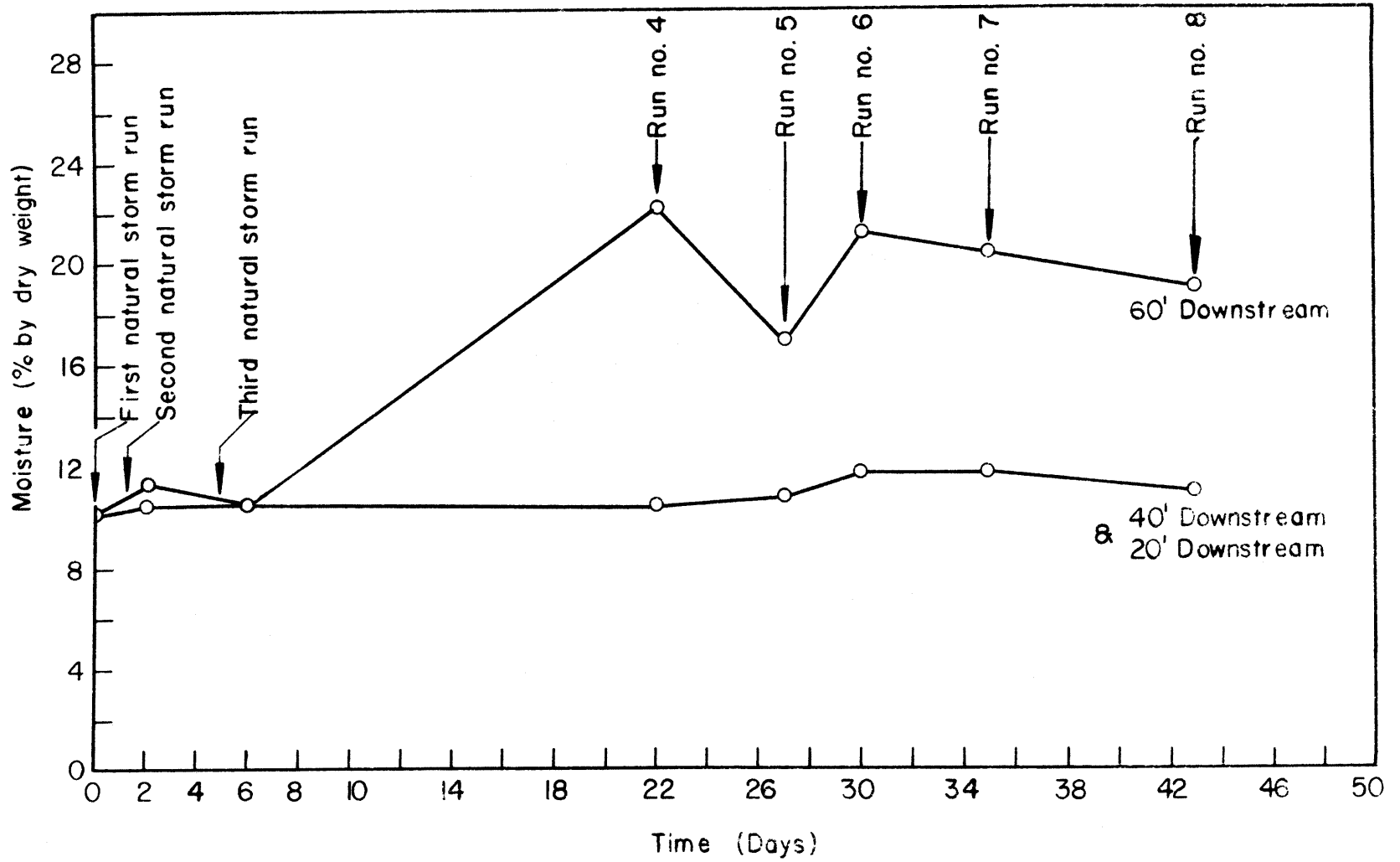


FIGURE 29: MOISTURE CONTENT OF SPENT SHALE VERSUS TIME AT 1-FOOT,  
6-INCH DEPTH

Table XV: Concentrations of Minor Constituents

Ion	Maximum concentration observed (mg/l) *	Source	Test
Al <sup>+++</sup>	2.5	TOSCO	column (first leachate)
Ba <sup>++</sup>	4.0	RAW	blender
Br <sup>-</sup>	<0.1	---	---
Cl <sup>-</sup>	3,000	TOSCO	column (first leachate)
CO <sub>3</sub> <sup>=</sup>	21	UOC	blender
Cu <sup>++</sup>	<0.1	---	---
Cr <sup>+6</sup>	<0.1	---	---
F <sup>-</sup>	3.4	UOC	blender
Fe <sup>+++</sup>	1.7	TOSCO	column (first leachate)
I <sup>-</sup>	0.16	---	---
K <sup>+</sup>	1,100	TOSCO	column (first leachate)
Mn <sup>++</sup>	<0.1	---	---
NO <sub>3</sub> <sup>-</sup>	186	TOSCO	column (first leachate)
Pb <sup>++</sup>	<0.1	TOSCO	column (first leachate)
PO <sub>4</sub> <sup>=</sup>	35	TOSCO	column (first leachate)
Zn <sup>++</sup>	2.5	TOSCO	column (first leachate)

\* Maximum concentrations in actual runoff would be expected to be less than 4% of these values. Therefore, none of the ions listed in this Table XV would be present in runoff in concentrations greater than allowable for human drinking water. In other words, the total maximum concentration of all these ions in actual runoff would be less than 174 mg/l.

Table XVI: Carbon and Nitrogen Content of Selected Samples

Sample	Values found, % by weight		Total residue, mg/l
	Carbon	Nitrogen	
TOSCO Spent Shale	10.2	0.38	-
BOM Spent Shale	8.2	0.28	-
Raw Shale	14.7	0.39	-
Sample from column after 1,320 ml of water had been leached through spent shale*	0.72	0	11,900
Sample from column after 3,150 ml of water had been leached through spent shale*	1.12	0	4,907
Sample taken 1/2 hour after simulated 1" rainfall began on first compaction*	1.79	0.79	1,219
Sample taken 1/2 hour after simulated 1" rainfall began on second compaction*	0.76	0.44	2,458

\*TOSCO spent shale

## SECTION VII

### DISCUSSION OF RESULTS

#### PHYSICAL TESTS

As shown in Figure 19, the permeability of both the TOSCO and USBM residues decreased with time. The reason for the decrease in permeability might be attributed to one or more of three phenomena:

1. movement of fines
2. swelling
3. precipitation of  $\text{CaCO}_3$  or some other cementing compound.

To determine if the movement of fines might be the cause of the decrease in permeability, each sample, on which the test was run, was divided in half and a sieve analysis run on each section. The sieve analysis showed an almost completely homogeneous sample with respect to size distribution. Therefore, it was concluded that there was no significant movement of fines in the samples. However, it is conceivable that a short migration of the fines might block interstices and cause a reduction in permeability. This latter possibility might not show up in the 2 sieve analyses made.

These same samples were also closely examined under a microscope for any noticeable deposition of a cementing compound. None was observed.

Therefore, the most likely reason for the decrease in permeability is swelling of the shale. Because the chemical analyses of all experiments indicate the presence of  $\text{Na}^+$ , the swelling could be due to the hydration effects of the sodium ion.

In order to put the results of the shaker, blender, and column experiments on a comparative basis, the mass of the various ions leached per 100 grams of TOSCO spent shale were determined. These results are given in Table XVII. As indicated by the data, the amounts of the various ionic species leached per 100 grams of shale residue are very similar.

Table XVII: Mass of Various Ions (mg) Leached  
per 100 Grams of TOSCO Spent Shale

Ion	Shaker	Blender	Percolation
$\text{Ca}^{++}$	102	114	64
$\text{Mg}^{++}$	31	27	40
$\text{Na}^+$	206	165	258
$\text{SO}_4^-$	775	728	675
$\text{Cl}^-$	5	8	18
Total	1,119	1,042	1,055



Also, for comparison with the bench-scale study results, blender experiments were conducted on six surface soil samples, and chemical analyses made of the major constituents found in 3 samples of surface soil obtained in Parachute Canyon near Grand Valley, Colorado. These results are given in Table XVIII. Figure B3 shows the approximate locations of the surface soil samples. These soil and talus slope samples were obtained April 3, 1970, and are as follows:

1. Surface soil east slope
2. from cut below #1, 10 feet of colluvial material (colluvial soils are soils that contain sharp angular fragments of the rock from which they originated)
3. nearly level surface soil
4. from cut on road, colluvial material about 10 feet below the surface
5. about 10 feet below surface colluvial material exposed in gravel pit
6. surface soil in pasture.

The data indicate a great deal of variation in the concentration and composition of each ion found in the surface soil. However, the total concentration of the ions is of the same order of magnitude as the total concentrations determined in the blender experiments on the TOSCO and USBM spent oil shale retorting residues. The composition of the surface soil samples is shown in Figure B1.

Table XVIII: Chemical Analyses of Filtrate from Blender Experiments Conducted on Surface Soil Samples

Sample Number	Conductance μmhos/cm @ 25°C	Concentration (me/l)							
		Ca <sup>++</sup>	Mg <sup>++</sup>	Na <sup>+</sup>	K <sup>+</sup>	SO <sub>4</sub> <sup>=</sup>	HCO <sub>3</sub> <sup>-</sup>	Cl <sup>-</sup>	Total
1	865	--	--	--	--	--	--	--	---
2	1,610	9.70	3.08	1.33	0.12	12.80	0.72	0.24	+0.47
3	87	--	--	--	--	--	--	--	---
4	700	0.72	0.25	5.55	0.10	3.87	0.86	2.06	-0.17
5	1,870	--	--	--	--	--	--	--	---
6	148	0.85	<0.01	0.41	0.13	0.29	0.92	0.19	<-0.01

This seems reasonable because the local surface soil, for the most part, is "weathered" shale. The weathered oil shale, because of surface exposure over a long period of time, has lost most of its organic content; consequently it is similar to the spent shales. However, a direct comparison between surface soil and oil shale residue would only have meaning if surface soil tests were performed on the runoff facility. The results in Table XVIII can be compared with those listed in Table VI.

## PILOT STUDY

As described in the preceding section, the concentration of TDS in the runoff is given by equation 55, and the cationic composition in the runoff is given in Figure 26.

To verify these results, equation 55 and Figure 26 were used to predict the concentration of  $\text{Ca}^{++}$ ,  $\text{Mg}^{++}$ , and  $\text{Na}^+$  in the runoff water from the three natural rainfall events (the first 3 tests) that occurred during the course of this study. This was done as follows.

First a plot of conductance vs TDS was constructed for the assimilated data, as shown in Figure 30. Thus, from the simple measurement of conductance, an estimate of the TDS of a sample can be determined.

Next, a graph of TDS versus total me/l of cations was constructed as given in Figure 31. Therefore, knowing the TDS as determined from Figure 30, the me/l of cations can be estimated.

Using the value of intensity as determined by the recording rain gage, an estimate of  $\bar{D}$  was made from equation 11. Using this value of  $\bar{D}$ , the quantity  $\frac{\overline{CD}^2}{\rho} k$  was calculated and the percentage composition of the cations in the surface runoff determined from Figure 26. Because the  $\text{HCO}_3^-$  concentration is relatively constant (about 0.35 me/l), the  $\text{SO}_4^{=}$  concentration was calculated from anion-cation balance.

The results of the measured concentrations versus the predicted values are given in Figure 32. The figure indicates the described procedure may be used to give a reasonable prediction of runoff quality by knowing only the conductance of the runoff water and the intensity of rainfall.

The results of the column study indicated that the soluble salts would be leached by percolation through the spent shale. This result could not be verified in the pilot study because no percolation occurred during the rainfall simulation.

In general, only minor fluctuations were observed in the moisture content of the shale below the 9 inch depth. The greatest moisture change occurred at the station located at the downstream end of the facility. This should be expected because a greater portion of the runoff passes this point.

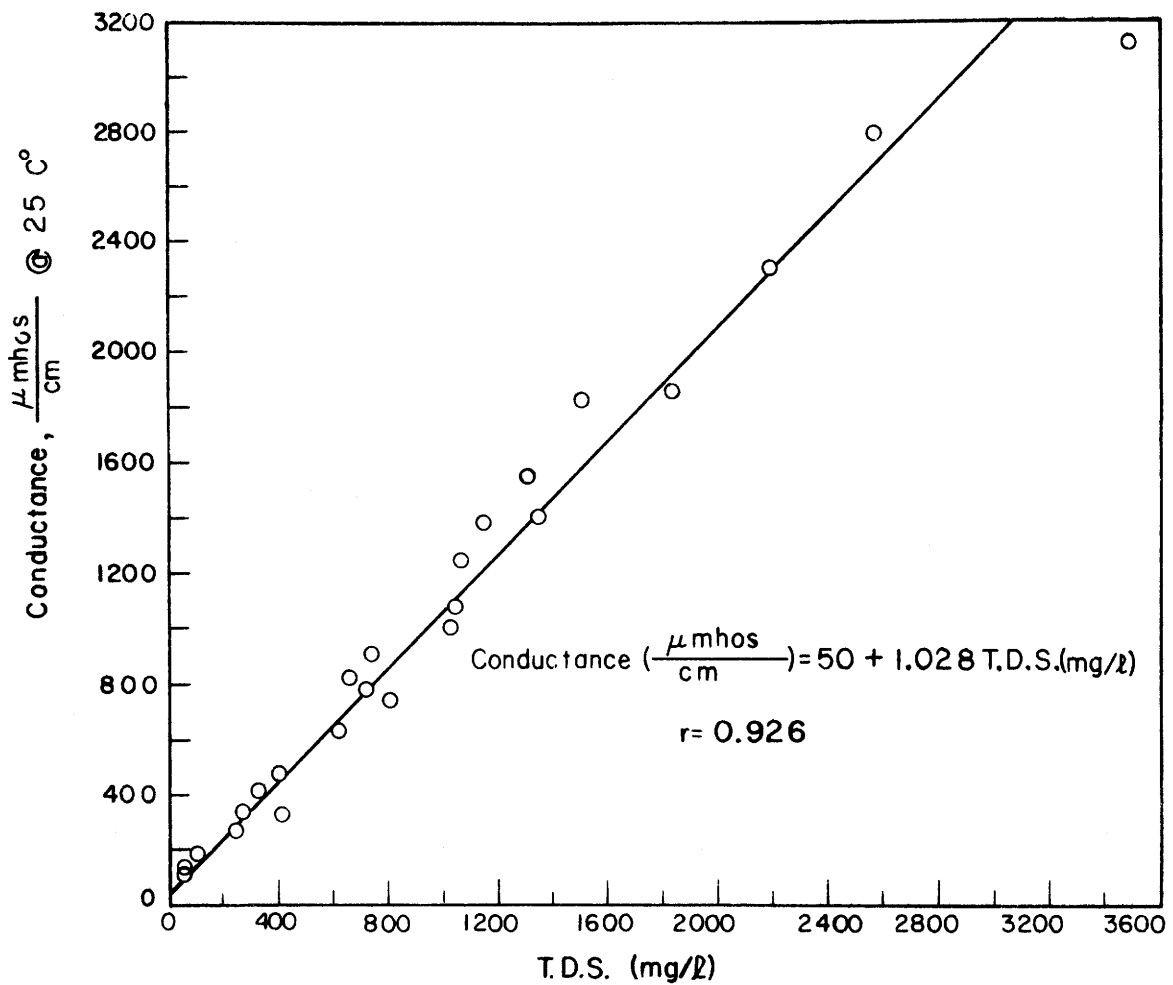


FIGURE 30: TDS VERSUS CONDUCTANCE FOR SPENT SHALE SURFACE RUNOFF

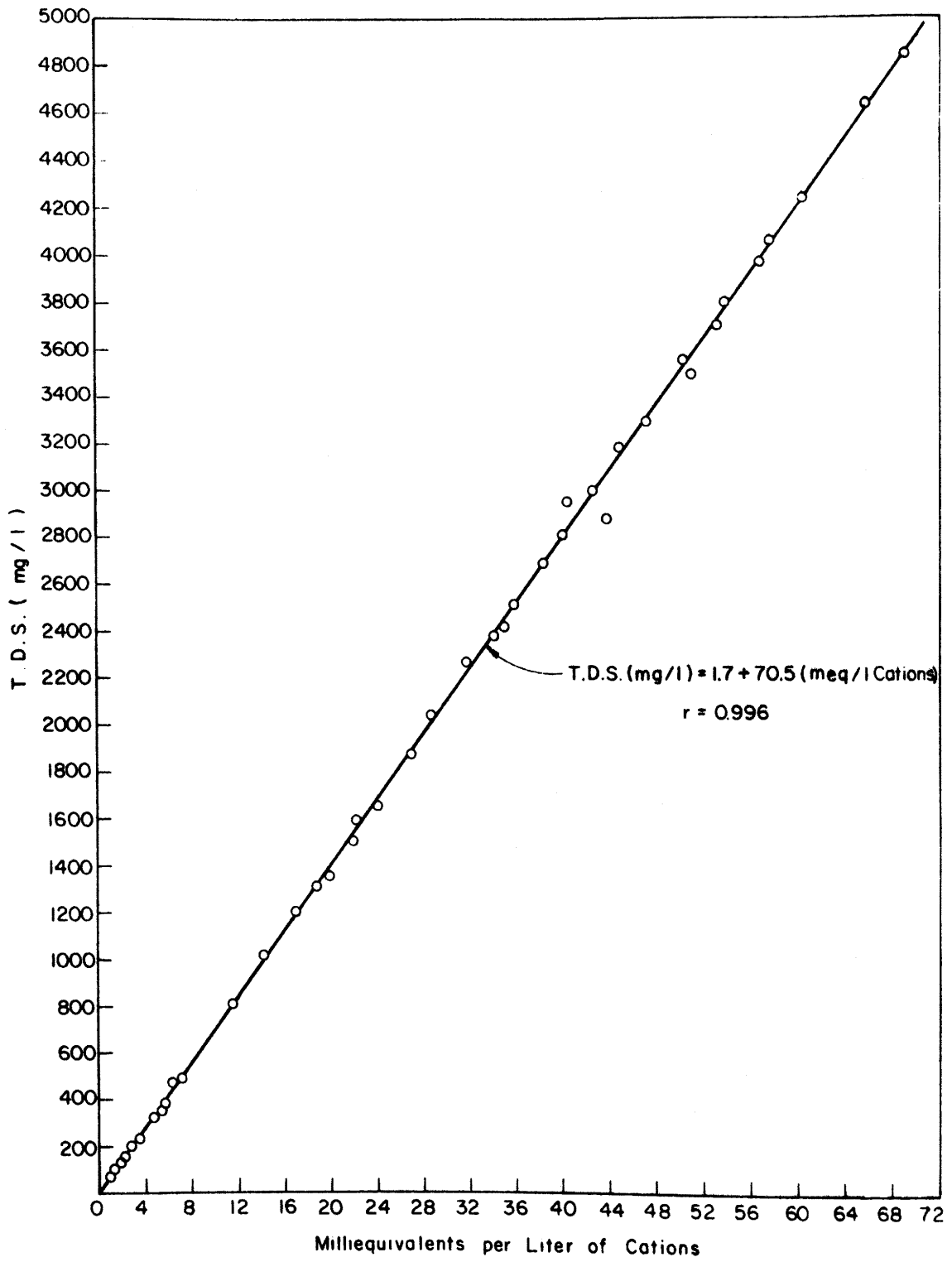


FIGURE 31: TDS VERSUS MEQ/L OF CATIONS FOR SPENT SHALE RUNOFF

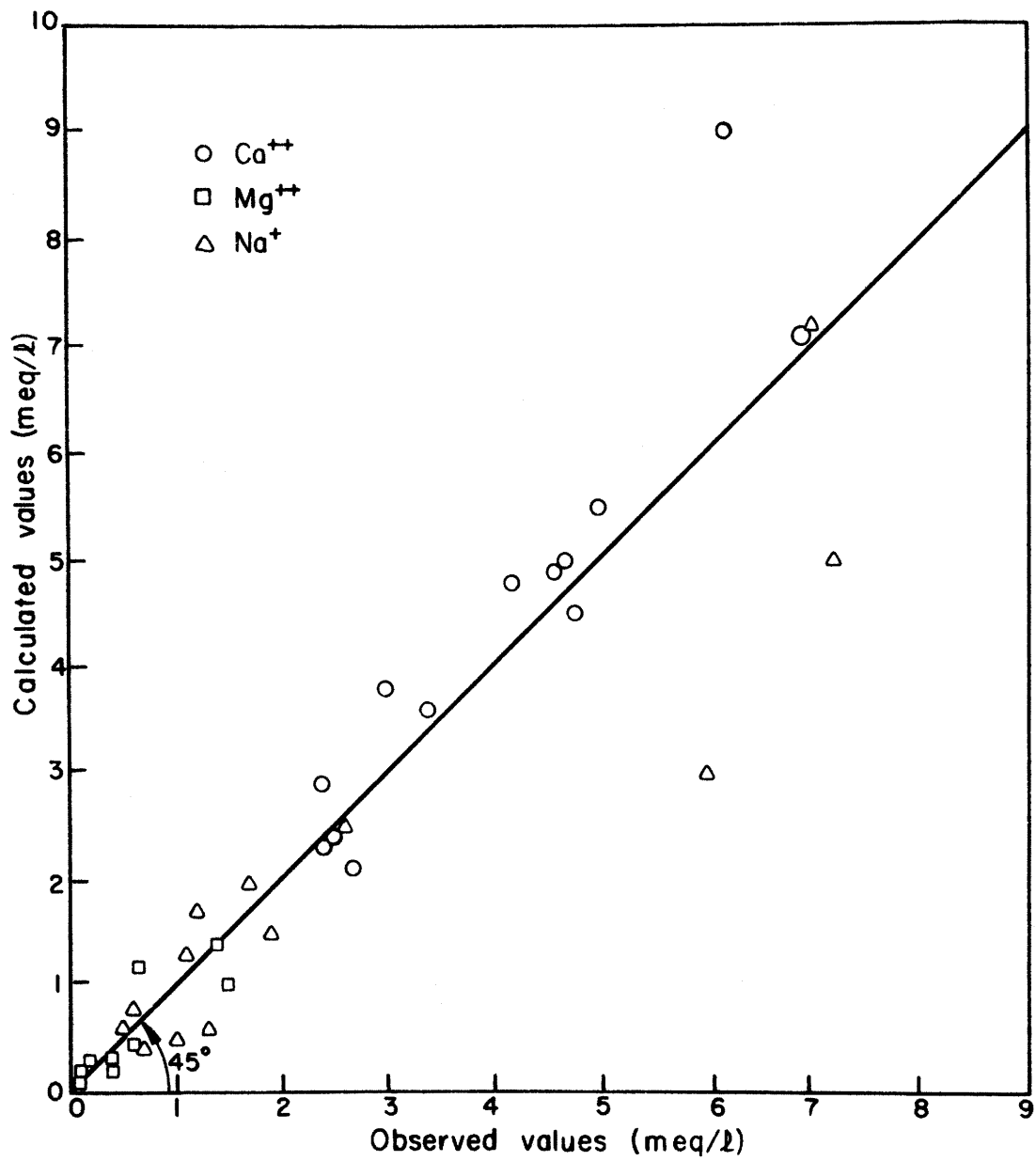


FIGURE 32: MEASURED CONCENTRATION VERSUS CALCULATED CONCENTRATION OF CATIONS IN SURFACE RUNOFF FROM SPENT SHALE

## SECTION VIII

### ACKNOWLEDGEMENTS

This paper is based on research supported by the Water Quality Office of the Environmental Protection Agency. Five percent of the total project cost was provided by Colorado State University. The extensive cooperation of the Union Oil Company, the U.S. Bureau of Mines, and the TOSCO organization was indispensable in making this study possible.

The help provided by Mr. Fred Pfeffer, the Grant Project Officer is acknowledged with sincere thanks.

The authors of this report are Dr. John C. Ward, Gary A. Margheim, and Dr. George O. G. Löf. Doctors Ward and Löf are Professors of Civil Engineering at Colorado State University. Mr. Margheim was a graduate research assistant in the Sanitary Engineering Program of the Department of Civil Engineering at Colorado State University during the course of this project.

The first draft of the final report was sent to the following people for review:

Don K. McSparran  
Colony Development Operation (TOSCO)  
Atlantic Richfield Company Operator

Harold E. Carver, Project Manager  
Oil Shale Department  
Union Oil Company of California

Gerald U. Dinneen, Research Director  
Laramie Energy Research Center  
Bureau of Mines

Fred M. Pfeffer, Project Officer  
Treatment and Control Research Program  
Robert S. Kerr Water Research Center  
Environmental Protection Agency

The authors wish to thank these gentlemen for their review and many valuable comments and suggestions.

## SECTION IX

### REFERENCES

1. U.S. Bureau of Mines, Mineral Facts and Problems, Bulletin 585, (1960), pp. 573-580.
2. Colorado State Board of Immigration, Mineral, Oil and Shale Resources (1924), p. 13.
3. Duncan, Donald C., and Vernon E. Swanson, "Organic Rich Shale of The United States and World Land Areas," Geological Survey Circular 523, (1965), p. 12.
4. Ibid (3), p. 5.
5. Throne, H. M., K. E. Stanfield, G. U. Dinneen, W. R. Murphy, "Oil Shale Technology: A Review," Bureau of Mines Information Circular 8216, (1964), p. 24.
6. Project BRONCO, A Joint Government-Industry Study of Nuclear Fracturing and In-Situ Retorting of Oil Shale, Clearinghouse for Federal Scientific and Technical Information, National Bureau of Standards, U.S. Department of Commerce, Springfield, Virginia, October 13, 1967, p. 4.
7. Prien, Charles H., "Oil Shale and Shale Oil," Paper presented at Second Oil Shale and Cannel Coal Conference, Royal Technical College, Glasgow, Scotland, July 3-7, 1950.
8. Ibid (6), p. 2.
9. Gambs, G. C., "Power Plant Ash - A Neglected Asset," Mining Engineering, Vol. 19, (1967), pp. 42-44.
10. Bocardy, J. A., and W. M. Spaulding, "Effects of Surface Mining on Fish and Wildlife in Appalachia," Resource Publication 65, Bureau of Sport Fisheries and Wildlife, Washington, D. C., Government Printing Office, (1968), p. 4.
11. Dean, K. C., H. Dolezal, and R. Havens, "New Approaches to Solid Mineral Wastes," Mining Engineering, Vol. 22, (1968), pp. 59-62.
12. Schmehl, W. R., and B. D. McCaslin, "Some Properties of Spent Oil-Shale Significant to Plant Growth," Research Report to Colony Development Company, Denver, Colorado, (1969), p. 11.
13. Linsley, R. K., Jr., M. A. Kohler, and J. L. Paulhus, Hydrology for Engineers, McGraw-Hill Book Company, Inc., 1958, pp. 267.

14. Fair, G. M., J. C. Geyer, and D. A. Okum, Water and Wastewater Engineering, Vol. 1 - Water and Wastewater Removal, John Wiley and Sons, Inc., 1966, Chapters 7 and 15.
15. Norton, Thomas N., "Cattle Feedlot Water Quality Hydrology," Masters Thesis, Colorado State University, March, 1969, p. 37.
16. Owen, W. M., "Laminar to Turbulent Flow in Wide Open Channels," Proceedings ASCE, 9 separate No. 188, April, 1953.
17. American Public Health Association, Inc., Standard Methods for the Examination of Water and Wastewater, Twelfth Edition, New York, 1965.
18. Ibid (12), p. 18.
19. Margheim, G. A., "Predicting Quality of Irrigation Return Flows," Masters Thesis, Department of Civil Engineering, Colorado State University, Fort Collins, Colorado, December, 1967.
20. The Asphalt Institute, "Soils Manual for Design of Asphalt Pavement Structures," Manual Series No. 10 (MS-10), 2 edition, April, 1963, p. 217.
21. Ward, J. C., "Stream Flow Quantity and Quality Correlations and Statistical Analyses," Research Report No. 3, University of Arkansas, Engineering Experiment Station, 1963, pp. 19-32.
22. Fair, G. M., J. C. Geyer, Water Supply and Wastewater Disposal, John Wiley and Sons, Inc., New York, Seventh Printing, October, 1966, pp. 111-113.
23. Ward, J. C., "Turbulent Flow in Porous Media," Closure, Journal of Hydraulics Division, ASCE, Volume 92, No. HY4, Proc. Paper 4859, July, 1966, pp. 110-121.
24. Corey, A.T., Fluid Mechanics of Porous Solids, Colorado State University, Fort Collins, Colorado, 1965, p. 48.
25. Ibid (23), pp. 110-121.
26. Ibid (24), pp. 50-57.
27. Margheim, Gary A., Dissertation, Colorado State University, Department of Civil Engineering.
28. Musgrave, G. W., "Quantitative Evaluation of Factors in Water Erosion - First Approximation," Journal Soil and Water Conservation, Volume 2, No. 3, (1947), pp. 133-138.



29. "The Environmental Aspects of a Commercial Oil Shale Operation,"  
by J. S. Hutchins, W. W. Krech, and M. W. Legatski, AIME  
Environmental Quality Conference, June 7-9, 1971, pages 59-68.

## SECTION X

## SYMBOLS AND ABBREVIATIONS

a	= subscript referring to absorbed phase, also ionic activity
B	= ratio of grams of oven dry soil to liters of solution contained in the shale during percolation, grams/liter
C	= concentration, mg/l
c	= coefficient in equation 12, also concentration in moles/liter
$C_j$	= initial concentration of component j, moles/liter
$C'_j$	= final concentration of component j, moles/liter
$C_{kj}$	= concentration of component j in segment k, moles/liter
$\underline{D}$	= depth of flow at lower end of watershed, ft
$\bar{D}$	= mean depth of flow, ft
$D_x$	= depth of flow at a distance x downstream, ft
d	= parameter in equation 12
E	= sediment yield in equation 57, lb/(hr)(ft <sup>2</sup> )
E'	= rate of erosion, tons/acre
e	= 2.71828... (base of Napierian logarithms)
f	= activity coefficient, dimensionless
g	= acceleration of gravity, 32.2 ft/sec <sup>2</sup> or 981 cm/sec <sup>2</sup>
i	= intensity of rainfall, in/hr
$2i_{30}$	= maximum 30 minute rainfall of 2 year frequency, in/hr
j	= subscript referring to jth component
K	= constant used in equation 21 (4.5), equilibrium constant in equation 24, and constant characteristic of the cross-section of flow through porous media (2.36) in equation 44, dimensionless in all 3 cases
K'	= equilibrium constant in equation 25, $\sqrt{\text{moles/liter}}$
$K_{rw}$	= relative permeability (ratio of the permeability at a given saturation to the permeability at 100% saturation), dimensionless
$K_{sp}$	= solubility product for CaSO <sub>4</sub> = $2.4 \times 10^{-5}$ (moles/liter) <sup>2</sup> at 25°C
k	= permeability, cm <sup>2</sup> or subscript indicating particular segment
L	= total length of overland flow, ft
$M_g$	= geometric mean size of the particle size distribution, cm
m	= exponent in equation 12
N	= exponent in equation 20 = 2
n	= exponent in equation 12
p	= pressure, dynes/cm <sup>2</sup> , and fraction by weight of sample retained between adjacent sieves, dimensionless
$p_b$	= bubbling pressure, dynes/cm <sup>2</sup>
$p_c$	= capillary pressure, dynes/cm <sup>2</sup>
q	= discharge per unit width, ft <sup>2</sup> /sec
$q_e$	= equilibrium discharge per unit width, ft <sup>2</sup> /sec
$q_k$	= volume of solution present in kth segment, liters

$q_x$  = discharge per unit width at a distance  $x$  downstream,  $\text{ft}^2/\text{sec}$   
 $R$  = Reynolds number, dimensionless  
 $S$  = degree of saturation, dimensionless  
 $s$  = slope (dimensionless) or subscript denoting solution phase  
 $T$  = tortuosity of porous media (2), dimensionless, and frequency of occurrence, years  
 $t$  = time since beginning of runoff in hours (equation 18)  
 $t_d$  = duration of storm in minutes (equation 12)  
 $t_{1/2}$  = time in half days, days/2  
 $v$  = macroscopic velocity in porous media,  $\text{cm}/\text{sec}$   
 $V$  = velocity of overland flow,  $\text{ft}/\text{sec}$   
 $V_t$  = bulk volume of shale,  $\text{cm}^3$   
 $V_v$  = void volume of shale,  $\text{cm}^3$   
 $w$  = moles per liter of  $\text{Ca}^{++}$  or  $\text{SO}_4^{=}$  that precipitate  
 $X$  = moles of  $\text{Na}^+$  per gram of shale entering exchange complex, moles/gram, and the geometric mean size of the sieve openings between adjacent sieves,  $\text{cm}$   
 $x$  = a horizontal coordinate, feet  
 $x_g$  = geometric deviation, dimensionless  
 $Y$  = moles of  $\text{Mg}^{++}$  per gram of shale entering exchange complex, moles/gram  
 $y$  = total depth of shale and a vertical coordinate, feet  
 $Z$  = moles of  $\text{Ca}^{++}$  per gram of shale entering exchange complex, moles/gram  
 $\epsilon$  = porosity, dimensionless  
 $\theta$  = slope angle, degrees or radians  
 $\mu$  = viscosity, poises =  $\text{gram}/(\text{cm})(\text{sec})$   
 $\nu$  = kinematic viscosity,  $\text{ft}^2/\text{sec}$  and  $\text{cm}^2/\text{sec}$  = stokes  
 $\zeta$  = exponent in equation 47  
 $\rho$  = density,  $\text{grams}/\text{cc}$   
 $\sigma_g$  = geometric standard deviation, dimensionless  
 $\phi$  = shape factor, dimensionless  
 $\omega$  = moisture content by weight, dimensionless  
 $\omega_r$  = relative moisture content (ratio of moisture content to moisture content at saturation), dimensionless  
 $\omega_s$  = saturation moisture content by weight, dimensionless  
 $\bar{D}$  the bar over a symbol indicates the mean value  
 $\propto$  proportional to  
 $>$  greater than  
 $<$  less than  
 $\Sigma$  summation  
 $\Delta$  finite difference

$\infty$  infinity  
d derivative  
 $\int$  integral  
 $^{\circ}\text{C}$  centigrade degrees  
cc cubic centimeter  
cm centimeter  
ft foot  
g gram  
hr hour  
in. inch  
 $\ell$  liter  
lb pound  
 $\ln$  base e logarithm  
 $\log$  base 10 logarithm  
me milliequivalent  
mg milligram  
ml milliliter  
mm millimeter  
No. number  
sec second  
TDS total dissolved solids  
TOSCO The Oil Shale Corporation  
UOC Union Oil Company  
USBM United States Bureau of Mines

SECTION XI

APPENDICES

	<u>Page No.</u>
A. Chemical Analysis with Specific Ion Activity	
Electrodes . . . . .	89
Figure A1: Conductance Versus Calculated Ionic Strength . . . . .	91
Figure A2: Ionic Strength Versus Activity Coefficients . . . . .	94
B. Soil Data . . . . .	95
Figure B1: % Composition of Cations and Anions in Filtrate from Blender Experiments Conducted on Surface Soil Samples . . . . .	95
Figure B2: Moisture Calibration Curve . . . . .	96
Figure B3: Approximate Location of Surface Soil Samples . . . . .	97
C. Experimental Data . . . . .	99
Table C1: Experimental Test Conditions . . . . .	99
D. Computer Program . . . . .	111

## APPENDIX A

### CHEMICAL ANALYSIS WITH SPECIFIC ION ACTIVITY ELECTRODES

Direct potentiometric measurement of ion activity is based on the fact that definite energy levels exist between two different states of the same matter; and that these differences are proportional to the relative populations of the atoms or ions involved. In electrolyte solutions, these energy level differences are measured as an electrical potential. The Nernst equation of classical thermodynamics expresses this potential for a given activity of an ion relative to a standard state as follows:

$$E = E_0 - [RT/(zF)] \ln a \quad (A1)$$

where

E = potential observed for any given activity of a particular ion, volts

E<sub>0</sub> = potential of the standard state (a = 1 mole/liter), volts

R = universal gas constant = 8.314 joules/(°K)(mole)

T = absolute temperature in degrees Kelvin

z = number of electrons transferred in the reversible reaction  
= equivalents per mole (for specific ion measurements, z takes the sign of the ion and is simply the valence of the ion)

F = Faraday constant = 96,500 coulombs per equivalent

and

a = the activity of the particular ion to be determined, moles per liter.

Measurement of ion activity is accomplished with the electrodes by determining the potential that is developed between the test sample and the special filling solution inside the electrode. The Nernst equation predicts that at 25°Centigrade the potential for a monovalent sensing electrode will change approximately 59 millivolts for each decade change in ion activity, while for a divalent sensing electrode the change is 29.5 millivolts per decade change in ion activity, etc.

In order to determine the concentration of a particular ion it is first necessary to prepare a working curve on semi-logarithmic graph paper by plotting the electrode potentials given by a standardizing solution on the linear axis. The log axis represents the activity of the particular ion in solution.

The following procedure was developed to measure the concentration of a particular ion in a solution. The concentration of a particular ion is given by

$$a = fc \quad (A2)$$

where

a = the activity of a particular ion, moles/liter  
c = the concentration of a particular ion, moles/liter and  
f = the activity coefficient, dimensionless.

Because the electrode measures activity, it is necessary to determine the activity coefficient in order that the concentration may be obtained. Because the activity depends upon the total ionic strength, it is necessary to relate the ionic strength to some easily measured parameter.

During the course of this project, an empirical relationship between ionic strength  $\mu$  and conductance of aqueous solutions contacted with oil shale retorting residues was determined. For  $\mu$  in moles/liter, the relationship is

$$\mu = (2.5 \times 10^{-7}) (\text{conductivity})^{1.57} \quad (\text{A3})$$

where the conductivity is in  $\mu\text{mhos/cm}$  at  $25^\circ\text{C}$ . A plot of equation A3 along with the experimental data from which it was determined is shown in Figure A1.

The activity coefficient may be calculated from the Debye-Huckel formula,

$$\log_{10} f = - \frac{0.5 z^2 \sqrt{\mu}}{1 + \sqrt{\mu}} \quad (\text{A4})$$

in which  $z$  denotes the valence of the ion. Equation A4 is valid for  $\mu \leq 0.1$  moles/liter.

Knowing the above relationships, it is a simple matter to estimate the activity coefficient by simply measuring the conductance of a given solution. When the analysis is complete, the true ionic strength may be calculated from

$$\mu = \frac{1}{2} \sum_{i=1}^{i=n} c_i z_i^2 \quad (\text{A5})$$

where  $c_i$  is the concentration of the  $i$ th type of ion,  $z_i$  is its valence, and the summation is carried out for all types of ions, both positive and negative, in the solution ( $n$  is the number of different ions in solution).

If the agreement between the assumed ionic strength and the calculated ionic strength is good, no adjustment in the activity coefficient is necessary. If there is a large difference between the assumed and calculated ionic strength, the activity coefficient must be adjusted until the agreement is tolerable.

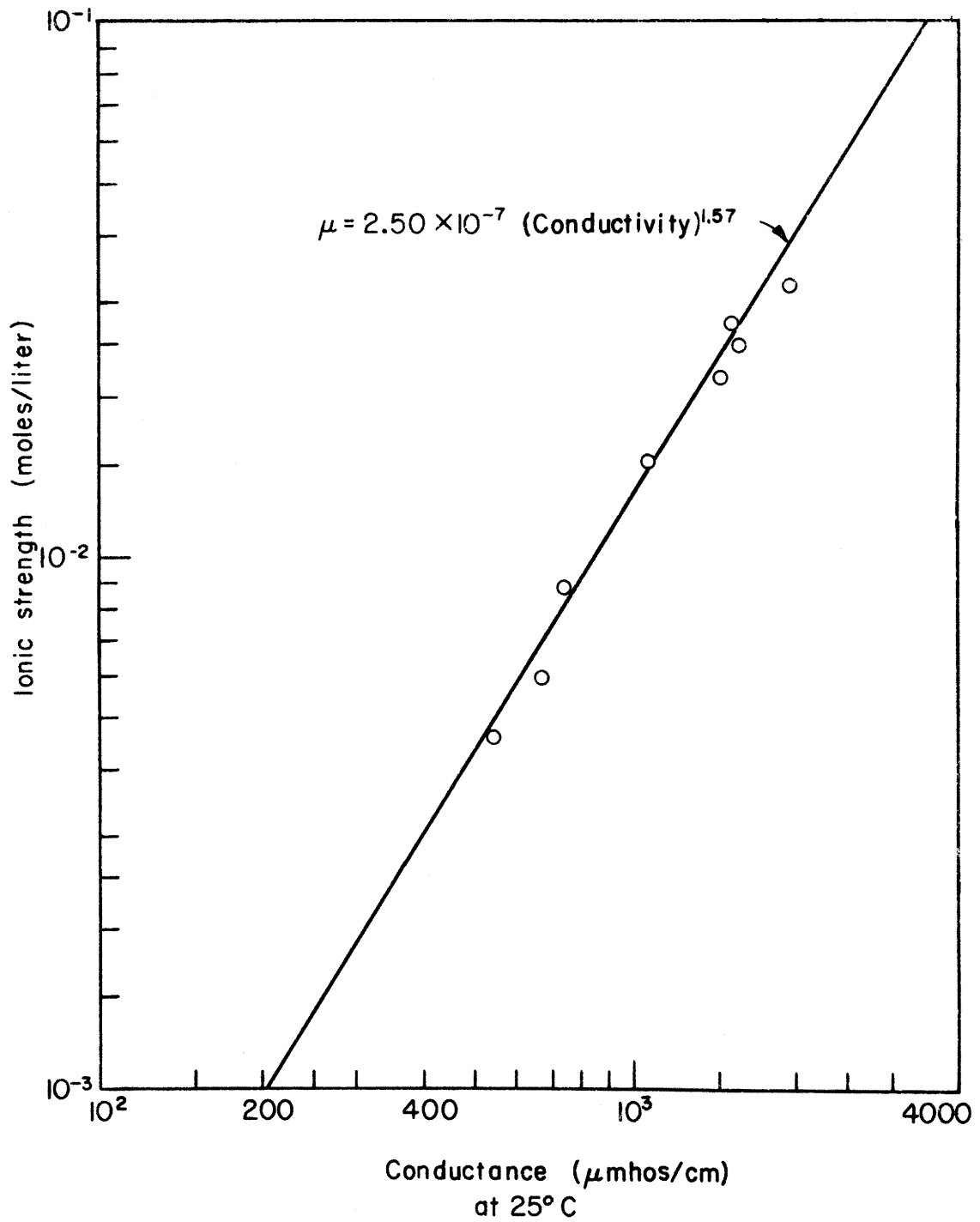


FIGURE A1: CONDUCTANCE VERSUS CALCULATED IONIC STRENGTH



Using the subscripts 1, 2, and 3 to denote, respectively, singly, doubly, and triply charged ions, one can rewrite equations A4 and A5 respectively as follows:

$$-\log f_1 = \frac{0.5 \sqrt{\mu}}{1 + \sqrt{\mu}} \quad (\text{A6})$$

and

$$\mu_c = \frac{1}{2} [\Sigma c_1 + 4 \Sigma c_2 + 9 \Sigma c_3] . \quad (\text{A7})$$

Using equation A2, equation A7 may be rewritten as

$$\mu = \frac{1}{2} \left[ \frac{1}{f_1} \Sigma a_1 + \frac{4}{f_2} \Sigma a_2 + \frac{9}{f_3} \Sigma a_3 \right] . \quad (\text{A8})$$

Clearly  $f_1 = f_2^{1/4} = f_3^{1/9}$ , so equation A8 may be rewritten

$$\mu_a = \frac{1}{2} \left[ \frac{\Sigma a_1}{f_1} + \frac{4 \Sigma a_2}{f_1^4} + \frac{9 \Sigma a_3}{f_1^9} \right] \quad (\text{A9})$$

Simultaneous solution of equations A9 and A6 gives the true value of the ionic strength  $\mu$  providing that the activities of all the ions in solution have been determined. Short of a complete chemical analysis, equation A3 is most useful. The usual case, however, is that some of the activities are known and some of the concentrations are known. In this latter case, equations A7 and A9 may be combined to give

$$\mu = \mu_c + \mu_a \quad (\text{A10})$$

where  $\mu_c$  is a constant for a given solution and  $\mu_a$  is a function only of  $f_1$  for a given solution. Consequently, simultaneous solution of equations A10 and A6 gives the true value of the ionic strength  $\mu$ . The range of plotting values of  $f_1$  for which equation A6 is valid is 0.76 to 1.

A suggested systematic procedure for obtaining the true value of  $\mu$  with as little effort as possible is as follows:

- (1) use equation A3 to estimate  $\mu$ ,
- (2) use equation A6 to calculate  $f_1$ ,
- (3) calculate  $\mu_c$  using equation A7,
- (4) estimate  $\mu_c$  using equation A9,
- (5) estimate  $\mu_a$  using equation A10,
- (6) if the  $\mu$  obtained in step 5 is the same as the  $\mu$  obtained in step 1, no further work is necessary,

- (7) if the condition in step 6 does not hold, then the  $\mu$  obtained in step 5 should be used to calculate a new value of  $f_1$  using equation A6, and steps 4 through 7 repeated until equations A10 and A6 are both satisfied by the same values of  $f_1$  and  $\mu$ .

An alternate graphical procedure would be to plot equation A10 on a graph on which equation A6 is already plotted. Because the plot of equation A6 is the same for all solutions, a master graph could be made using 3 cycle semi-log graph paper with  $\log \mu$  plotted versus  $f_1$ . At any rate the correct values of  $\mu$  and  $f_1$  are those where equations A6 and A10 intersect on the graph. A master graph such as that mentioned above is Figure A2. Also plotted on the same graph are values of

$$f_1^4 = f_2 \text{ and } f_1^9 = f_3 .$$

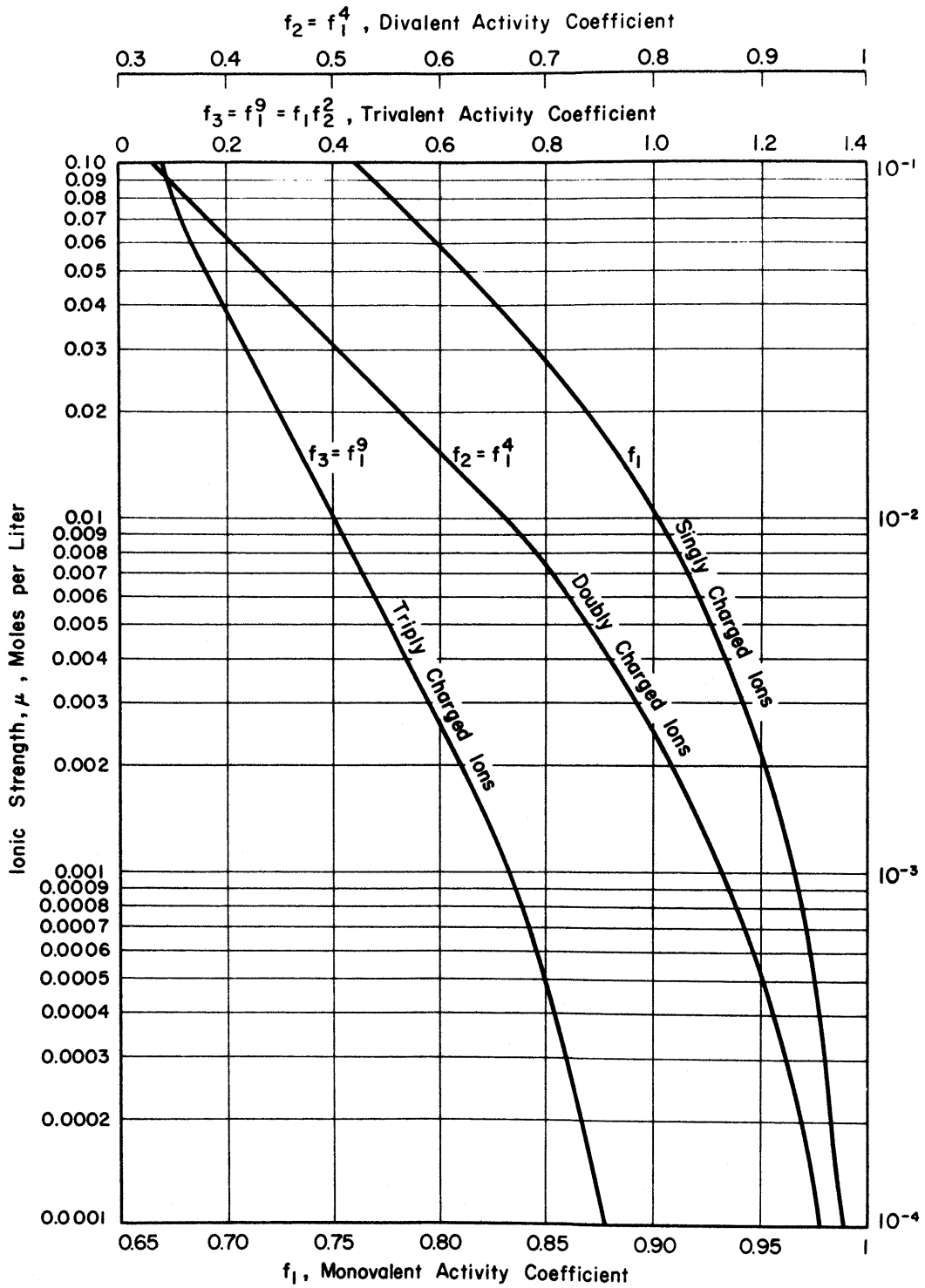


Figure A2: Activity Coefficients as a Function of Ionic Strength. (Equation A4)

APPENDIX B

SOIL DATA

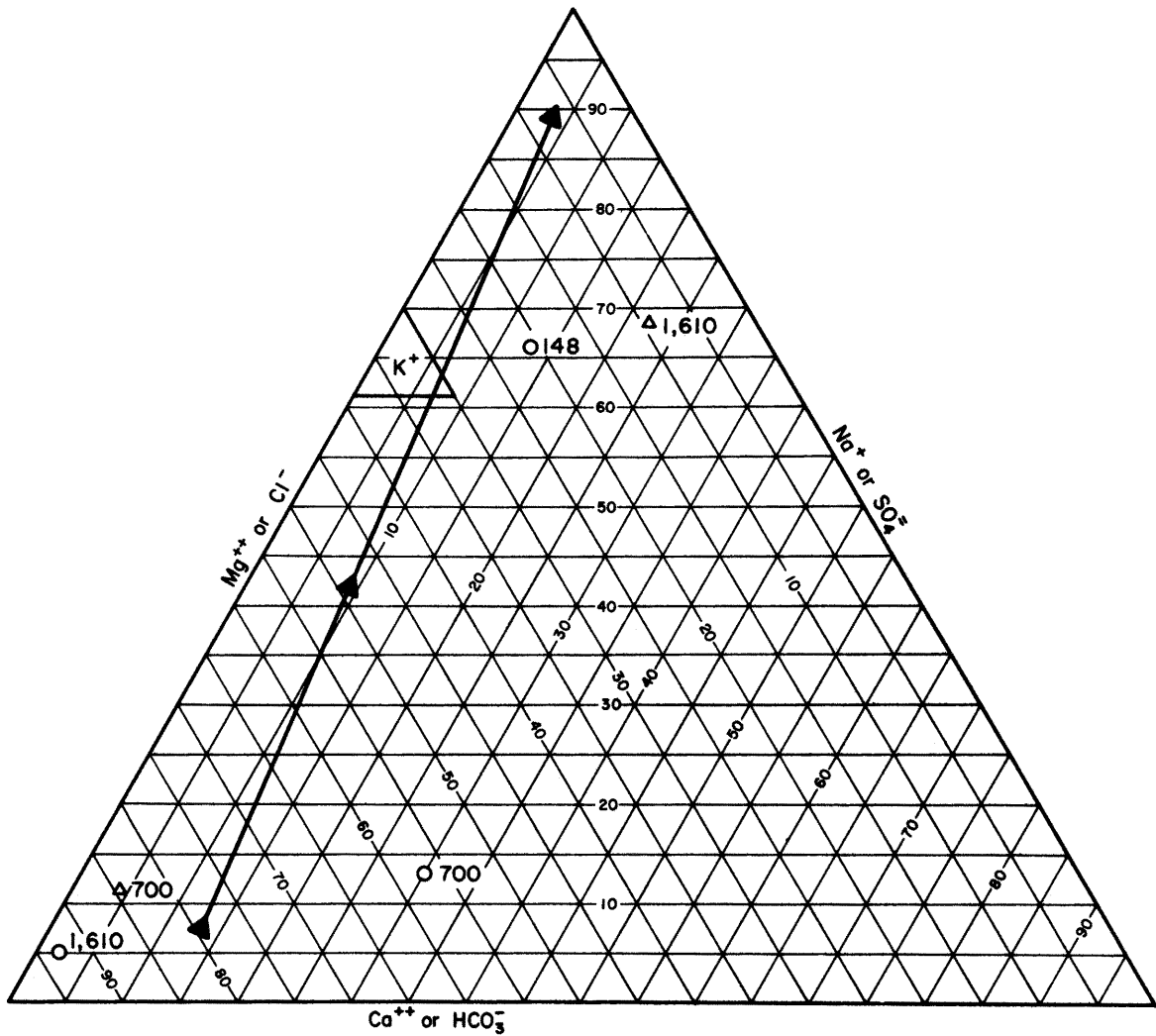


Figure B1: % Composition of Cations and Anions in Filtrate from Blender Experiments Conducted on Surface Soil Samples.

Triangles are cation composition (height of triangle indicates % $\text{K}^+$ ), and circles are anion composition. Numbers are sample conductance in  $\mu\text{mhos/cm}$  at  $25^\circ\text{C}$ . Straight line is composition of runoff from oil shale retorting residue. Arrows indicate the direction in which composition changes during a given rainfall.

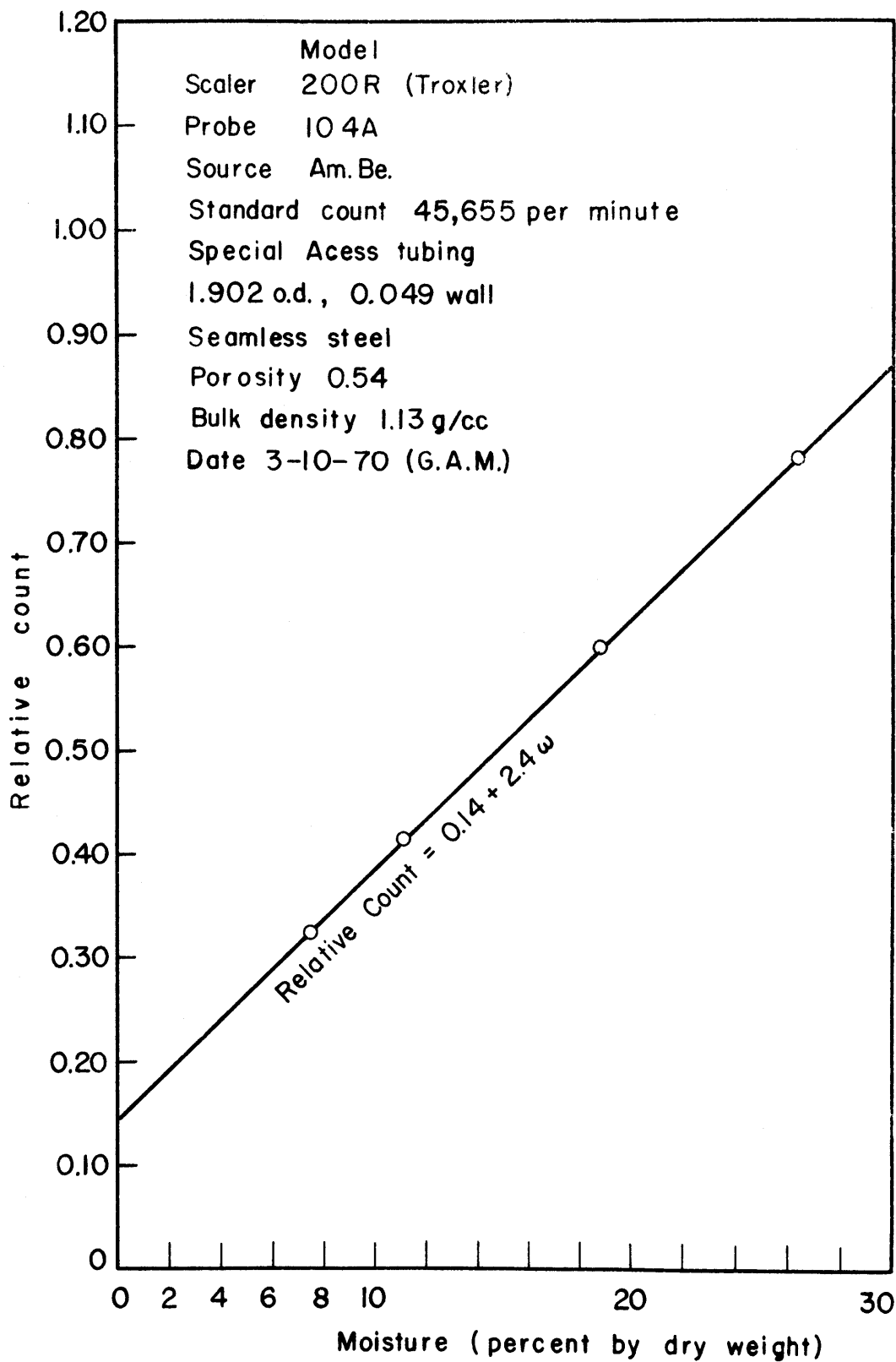


FIGURE B2: MOISTURE CALIBRATION CURVE

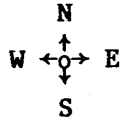


Figure B3: Approximate Location of Surface Soil Samples (Garfield County, Colorado).

Explanation on following page.

Each N x E square is 36 square miles (1 inch = 4.5 miles).



The oil shale mines at N = 8.1, E = 6.6 (8,000 feet) and at N = 8.6, E = 4.9 (7,300 feet) should be noted. The Bureau of Mines Experiment Station (N = 7.8, E = 6.8) appears to be at an elevation of about 5,700 feet. The coordinates of the TOSCO offices and experimental plant are roughly N = 9.2, E = 4.8 and N = 9.1, E = 5 respectively. The coordinates at which the 6 samples were taken were approximately as follows:

Sample Number	Coordinates	
	N	E
1	9.4	4.9
2	9.4	4.9
3	8.8	4.9
4	8.9	4.8
5	8.4	4.8
6	7.4	4.9

APPENDIX C

EXPERIMENTAL DATA

The experimental data for the experiments on the CSU rainfall-runoff facility are summarized below. It is of interest to note that the dissolved solids removed during a given test, F, in lb/(hr)(10<sup>3</sup>ft<sup>2</sup>) was directly related to Δω by the following empirical equation:

$$\log_{10} F = - 1 + 3.7\Delta\omega \quad (C1)$$

However, equation C1 is strictly limited to the CSU rainfall-runoff facility and can not be applied elsewhere. Therefore, it is simply a qualitative expression that shows that F is directly related to Δω, and is in fact the basis for the formulation of equation 21.

The test conditions are summarized in Table C1.

Table C1: Experimental Test Conditions

Tests	$\rho_s$ , g/cm <sup>3</sup>	$\epsilon$	$\omega_s$	$k \times 10^{10}$ , cm <sup>2</sup>	$\omega$	$i$ , in./hr
1-6	1.39	0.442	0.317	1.42	0.115-0.256	0.46-2.25
7-10	1.63	0.345	0.212	0.611	0.11 -0.165	0.40-2.12
Table V	1.30	0.47	0.38	2.5		

$\rho_s$  is the residue bulk density,  $\epsilon$  is the residue porosity by volume,  $\omega_s$  is the saturation moisture content by weight,  $k$  is the residue permeability,  $\omega$  is the observed moisture content by weight ( $\Delta\omega = \omega_s - \omega$ ), and  $i$  is the rainfall intensity.

In the following tables, the total me/l = me/l cations - me/l anions. Also the total mg/l = mg/l Na<sup>+</sup> + mg/l Ca<sup>++</sup> + mg/l Mg<sup>++</sup> + mg/l SO<sub>4</sub><sup>-</sup> + mg/l HCO<sub>3</sub><sup>-</sup>.



TEST: 1

$\rho_s = 1.39 \text{ grams/cc}$

$\omega_s = 31.7 \%$

$\eta_s = 0.442$

$\omega = 25.6 \%$

$\Delta\omega = 0.061$

$i = 0.54 \text{ in/hr}$

$k = 1.42 \times 10^{-10} \text{ cm}^2$

Sample	$\Delta t$ Hours since runoff begin	Conduct- ance $\mu\text{mhos/cm}$ 25°C	Sediment g/l	pH 25°C	Dissolved Solids milliequivalent/l / mg/l					
					Na <sup>+</sup>	Ca <sup>++</sup>	Mg <sup>++</sup>	SO <sub>4</sub> <sup>=</sup>	HCO <sub>3</sub> <sup>-</sup>	Total
1-1	0.00	---	---	----	---	---	---	---	---	---
1-2	0.25	410	5.5	8.14	1.84 42.3	2.50 50.1	0.21 2.5	4.37 210	0.39 23.8	-0.21 328.5
1-3	0.50	278	4.9	8.20	1.68 38.6	1.75 35.1	<0.05 0.6	3.02 145	0.30 18.3	+0.11 237.0
1-4	0.75	216	4.8	8.29	0.51 11.7	1.40 28.1	0.51 6.2	2.04 98.1	0.31 18.9	+0.07 163.0
1-5	1.25	191	4.9	8.36	0.21 4.8	1.25 25.1	<0.05 0.6	1.06 51.0	0.35 21.4	+0.05 102.3
1-6	1.75	131	4.3	8.27	0.15 3.4	1.19 23.8	<0.05 0.6	0.87 41.8	0.40 24.4	+0.07 93.4
1-7	2.25	137	3.0	8.40	0.13 3.0	0.70 14.0	<0.05 0.6	0.60 28.8	0.35 21.4	-0.12 67.2
1-8	2.75	124	2.5	8.48	0.07 1.6	0.82 16.4	<0.05 0.6	0.52 25.0	0.36 22.0	+0.01 65.0
1-9	3.50	137	2.1	8.48	0.09 2.1	0.70 14.0	<0.05 0.6	0.42 20.2	0.32 19.5	+0.05 55.8
1-10	rainwater	80		7.20	<0.05 <1.1	0.48 9.6	<0.05 0.6	<0.10 4.8	0.46 29.9	-0.01 39.5

TEST: 2

$\rho_s = 1.39$  grams/cc

$\omega_s = 31.7\%$

$n_s = 0.442$

$\omega = 21.1\%$

$\Delta\omega = 0.106$

$i = 0.46$  in/hr

$k = 1.42 \times 10^{-10}$  cm<sup>2</sup>

Sample	$\Delta t$ Hours since runoff begin	Conduct- ance $\mu\text{mhos/cm}$ 25°C	Sediment g/l	pH 25°C	Dissolved Solids milliequivalent/l / mg/l					
					Na <sup>+</sup>	Ca <sup>++</sup>	Mg <sup>++</sup>	SO <sub>4</sub> <sup>=</sup>	HCO <sub>3</sub> <sup>-</sup>	Total
2-1	0	917	2.07	7.87	2.20	7.20	1.31	10.41	0.40	-0.10
					50.6	144.3	15.7	500.5	24.4	735.5
2-2	0.167	1415	2.9	8.02	2.40	15.1	2.91	19.23	0.44	+0.74
					55.2	302.6	35.4	924.5	26.8	1344.5
2-3	0.317	1095	2.5	7.99	2.10	11.7	1.32	15.04	0.45	-0.37
					48.3	234.5	16.0	723.1	27.5	1048.4
2-4	0.580	788	2.1	8.05	1.38	8.08	1.49	10.20	0.38	+0.38
					31.7	161.9	18.1	490.4	23.2	725.3
2-5	1.17	340	3.1	7.82	0.52	2.80	0.34	3.42	0.40	-0.16
					12.0	56.1	4.1	164.4	24.4	261.0
2-6	1.61	248	2.6	8.19	0.35	1.90	0.40	2.02	0.45	+0.18
					8.0	38.1	4.7	97.1	27.5	175.4
2-7	2.42	196	1.6	8.38	0.20	1.09	0.34	1.08	0.46	+0.09
					4.6	21.8	4.1	51.9	28.1	110.5
2-8	3.42	184	1.3	8.34	0.11	0.80	< 0.05	0.60	0.36	-0.05
					2.5	16.0	< 0.6	28.8	22.0	69.3

TEST: 3

$\rho_s = 1.39$  grams/cc

$\omega_s = 31.7$

$\eta_s = 0.442$

$\omega = 23.0\%$

$\Delta\omega = .087$

$i = 1.00$  in/hr

$k = 1.42 \times 10^{-10}$  cm<sup>2</sup>

Sample	$\Delta t$ Hours since runoff begin	Conduct- ance $\mu$ mhos/cm 25°C	Sediment g/l	pH 25°C	Dissolved Solids milliequivalent/l / mg/l					
					Na <sup>+</sup>	Ca <sup>++</sup>	Mg <sup>++</sup>	SO <sub>4</sub> <sup>=</sup>	HCO <sub>3</sub> <sup>-</sup>	Total
3-1	-----	1265	1.5	7.85	3.20 73.6	11.6 232	0.82 10.0	15.1 726	0.41 25.0	+0.11 1066.6
3-2	0.0833	930	4.4	7.74	1.70 39.1	7.64 153	0.40 4.9	9.10 437	0.42 25.6	+0.22 659.6
3-3	0.250	470	4.1	7.88	1.22 28.0	4.02 80.6	0.61 7.4	5.32 256	0.46 28.0	+0.07 400.0
3-4	0.583	248	3.5	7.96	1.02 23.4	1.56 31.2	0.30 3.6	2.83 121	0.39 23.8	-0.14 203.0
3-5	1.083	163	3.3	8.21	0.31 7.1	1.28 25.6	0.18 2.2	1.14 54.8	0.43 26.2	+0.20 115.9
3-6	1.583	125	2.9	8.19	0.25 5.7	0.70 14.0	0.10 1.2	0.89 33.2	0.44 26.8	-0.08 80.9
3-7	2.583	106	2.8	8.46	0.07 1.6	0.61 12.2	0.06 0.7	0.31 14.9	0.43 26.2	0.00 55.6
3-8	3.583	88	1.6	8.52	< 0.05 < 1.1	0.53 10.6	< 0.05 < 0.6	0.15 7.2	0.41 25.0	-0.03 42.8

TEST: 4  
 $\rho_s = 1.39 \text{ grams/cc}$   
 $\omega_s = 31.7 \%$

$\eta_s = 0.442$   
 $\omega = 16.1 \%$   
 $\Delta\omega = .156$

$i = 1.70 \text{ in/hr}$   
 $k = 1.42 \times 10^{-10} \text{ cm}^2$

Sample	$\Delta t$ Hours since runoff begin	Conductance umhos/cm 25°C	Sediment g/l	pH 25°C	Dissolved Solids milliequivalent/l / mg/l					
					Na <sup>+</sup>	Ca <sup>++</sup>	Mg <sup>++</sup>	SO <sub>4</sub> <sup>=</sup>	HCO <sub>3</sub> <sup>-</sup>	Total
4-1	-----	3130	7.7	---	33.8 777	6.51 130	10.1 123	50.6 2435	0.41 25.0	-0.60 3490
4-2	0.0833	1830	4.6	8.01	10.1 232	8.64 173	3.05 37.0	21.8 1048	0.40 24.4	-0.41 1614.4
4-3	0.333	735	3.7	8.21	4.21 96.8	5.83 117	1.32 16.0	11.4 548	0.42 25.6	-0.46 803.4
4-4a*	0.833	414	-----	8.17	1.04 23.9	2.55 51.1	1.11 13.5	4.16 200	0.43 26.2	+0.11 314.7
4-4b**	0.853	383	-----	8.23	1.56 35.8	1.90 38.0	0.60 7.3	3.74 180	0.43 26.2	-0.11 287.3
4-4	0.873	292	3.5	8.41	1.02 23.4	1.51 30.2	0.51 6.2	2.71 130	0.41 25.0	-0.08 214.8
4-5a	1.33	242	-----	8.40	0.93 21.4	1.30 26.0	<.05 <0.6	1.81 87.0	0.39 23.8	+0.03 158.2
4-5b	1.35	192	-----	8.12	0.85 19.5	0.70 14.0	0.42 5.1	1.68 80.7	0.35 21.4	-0.06 140.7
4-5	1.37	164	2.9	8.22	0.35 8.0	0.90 18.0	0.20 2.4	1.10 52.8	0.42 25.6	-0.07 106.8
4-6a	2.33	163	-----	8.34	0.32 7.3	0.72 15.4	0.34 4.1	0.88 42.7	0.41 25.0	+0.08 94.5
4-6b	2.35	139	-----	8.39	0.36 8.3	0.61 12.2	0.19 2.3	0.83 39.9	0.44 26.8	-0.11 89.5
4-6	2.37	120	1.2	8.23	0.13 3.0	0.70 14.0	0.11 1.3	0.60 28.8	0.38 23.2	-0.04 70.3
4-7a	3.08	137	-----	8.12	0.23 5.3	0.83 16.6	<0.05 <0.6	0.58 27.9	0.41 25.0	+0.07 74.8
4-7b	3.10	100	-----	8.41	0.12 2.8	0.65 13.0	<0.05 <0.6	0.48 23.1	0.39 23.8	-0.10 62.7
4-7	3.12	153	0.7	8.11	0.24 5.5	0.85 17.0	<0.05 <0.6	0.62 29.8	0.47 28.7	0.00 81.0

\* Refers to station 30 feet downstream  
 \*\* Refers to station 50 feet downstream

TEST: 5

$\rho_s = 1.39$  grams/cc

$\omega_s = 31.7\%$

$n_s = 0.442$

$\omega = 11.5\%$

$\Delta\omega = .202$

$i = 2.25$  in/hr

$k = 1.42 \times 10^{-10}$  cm<sup>2</sup>

Sample	$\Delta t$ Hours since runoff begin	Conduct- ance $\mu$ mhos/cm 25°C	Sediment g/l	pH 25°C	Dissolved Solids milliequivalent/l/ mg/l					
					Na <sup>+</sup>	Ca <sup>++</sup>	Mg <sup>++</sup>	SO <sub>4</sub> <sup>=</sup>	HCO <sub>3</sub> <sup>-</sup>	Total
5-1	-----	5060	20.4	-----	58.7	6.82	11.8	79.0	0.37	-2.05
					1350	137	143	3795	22.6	5447.6
5-2	0.10	1390	18.2	8.24	10.8	4.04	1.62	16.1	0.42	-0.06
					248	81.0	19.7	774	25.6	1148.3
5-3	0.35	470	8.5	8.13	2.82	2.33	0.52	5.27	0.42	-0.02
					64.8	46.7	6.3	254	25.6	397.4
5-4	0.85	235	7.7	8.24	1.10	1.10	0.21	1.91	0.42	+0.08
					25.2	22.0	2.6	91.8	25.6	167.2
5-5a*	1.85	148	-----	8.23	0.50	0.81	0.30	1.14	0.42	+0.05
					11.5	16.2	3.6	54.8	25.6	111.7
5-5b**	1.86	139	-----	8.34	0.31	0.70	0.23	0.75	0.41	+0.08
					7.1	14.0	2.8	36.1	25.0	85.0
5-5	1.87	110	4.1	8.12	0.32	0.64	0.10	0.77	0.33	-0.04
					7.4	12.8	1.2	37.0	20.2	78.6
5-6a	2.35	161	-----	8.01	0.25	0.85	0.32	0.94	0.42	+0.06
					5.8	17.0	3.9	45.2	25.6	97.5
5-6b	2.36	121	-----	8.11	0.10	0.60	0.24	0.46	0.46	+0.02
					2.3	12.0	2.9	22.1	28.1	67.4
5-6	2.37	87	4.1	8.36	0.10	0.52	0.11	0.31	0.45	-0.03
					2.3	10.4	1.3	14.9	27.5	56.4
5-7a	2.85	151	----	8.19	0.21	0.86	0.42	0.79	0.47	+0.23
					4.8	17.4	5.1	38.0	28.7	94.0
5-7b	2.86	112	----	8.23	0.17	0.61	0.27	0.54	0.48	+0.03
					3.9	12.2	3.3	25.9	29.3	74.6
5-7	2.87	100	3.2	8.00	0.19	0.61	0.20	0.52	0.46	+0.02
					4.4	12.2	2.4	25.0	28.1	72.1
5-8a	3.85	109	----	8.12	0.05	0.73	0.09	0.33	0.37	+0.12
					1.1	14.6	1.1	15.8	22.6	54.1
5-8b1	3.86	96	----	8.11	0.05	0.74	0.05	0.33	0.39	+0.02
					1.1	14.8	0.6	15.8	23.8	54.4
5-8	3.87	105	2.4	8.05	0.05	0.71	0.11	0.37	0.38	+0.09
					1.1	14.2	1.3	18.3	23.2	57.0

\* Refers to station 30 feet downstream  
 \*\* Refers to station 50 feet downstream

TEST: 6

$\rho_s = 1.39$  grams/cc

$\omega_s = 31.7\%$

$n_s = 0.442$

$\omega = 18.7\%$

$\Delta\omega = .130$

$i = 0.94$  in/hr

$k = 1.42 \times 10^{-10}$  cm<sup>2</sup>

Sample	$\Delta t$ Hours since runoff begin	Conductance $\mu\text{mhos/cm}$ 25°C	Sediment g/l	pH 25°C	Dissolved Solids milliequivalent/l / mg/l					
					Na <sup>+</sup>	Ca <sup>++</sup>	Mg <sup>++</sup>	SO <sub>4</sub> <sup>=</sup>	HCO <sub>3</sub> <sup>-</sup>	Total
6-1	-----	4100	14.1	8.01	58.4	7.21	4.18	68.6	0.39	0.80
					1342	144	50.8	3300	23.8	4860.6
6-2	0.0833	1110	12.3	7.82	7.53	5.54	1.57	14.6	0.38	-0.34
					173	111	19.1	702	23.2	1028.4
6-3	0.250	627	11.3	8.09	4.52	3.37	0.70	8.58	0.42	-0.41
					104	67.4	8.5	413	25.6	618.5
6-4	0.500	300	9.6	8.11	1.31	1.92	0.31	3.26	0.44	-0.16
					30.1	38.4	4.4	157	26.8	256.7
6-5	0.750	211	9.7	8.13	1.12	1.17	0.41	2.07	0.42	+0.21
					25.7	23.4	5.0	99.5	25.6	179.2
6-6	1.25	184	7.6	8.24	0.50	1.01	0.20	1.20	0.43	+0.08
					11.5	20.1	2.4	57.7	26.2	117.9
6-7	2.00	125	6.8	8.15	0.30	0.71	0.16	0.77	0.41	-0.01
					6.9	14.2	1.9	37.0	25.0	85.0
6-8	2.25	121	3.8	8.20	0.21	0.69	0.16	0.66	0.41	-0.01
					4.8	13.8	1.9	31.7	25.0	77.2
6-9	3.00	115	3.4	8.07	0.12	0.61	0.16	0.56	0.38	0.05
					2.8	12.2	1.9	26.9	23.2	67.0

TEST: 7

$\rho_B = 1.63 \text{ grams/cc}$

$\omega_s = 21.2 \%$

$\eta_s = 0.345$

$\omega = 15.4 \%$

$\Delta\omega = 0.058$

$i = 0.40 \text{ in/hr}$

$k = 6.11 \times 10^{-11} \text{ cm}^2$

Sample	$\Delta t$ Hours since runoff begin	Conduct- ance $\mu\text{mhos/cm}$ 25°C	Sediment g/l	pH 25°C	Dissolved Solids milliequivalent/l / mg/l					
					Na <sup>+</sup>	Ca <sup>++</sup>	Mg <sup>++</sup>	SO <sub>4</sub> <sup>=</sup>	HCO <sub>3</sub> <sup>-</sup>	Total
7-1	-----	2310	4.2	8.21	16.3 375	4.87 97.4	12.6 153	32.2 1548	0.38 23.2	+1.19 2196.6
7-2	0.0833	664	2.3	8.01	4.08 93.8	2.10 42.0	1.01 12.3	6.86 330	0.41 25.0	-0.08 503.1
7-3	0.333	1560	3.2	8.11	10.1 232	4.83 96.6	4.37 53.2	18.7 898	0.43 26.2	+0.17 1306
7-4	0.583	855	2.3	8.13	5.72 132	3.69 73.8	1.53 18.6	10.6 509	0.43 26.2	-0.09 759.6
7-5	1.08	487	2.0	8.36	2.46 56.6	2.38 47.6	0.69 8.4	5.00 240	0.45 27.5	+0.08 380.1
7-6	1.58	372	2.0	8.42	1.75 40.2	1.81 36.2	0.70 8.5	3.96 191	0.39 23.8	-0.09 299.7
7-7	2.08	323	1.5	8.22	1.51 34.7	1.40 28.0	0.51 6.2	3.12 150	0.41 25.0	-0.11 243.9
7-8	2.58	278	2.0	8.09	1.30 29.9	1.26 25.2	0.49 6.0	2.70 130	0.36 22.0	-0.01 213.1
7-9	3.08	273	1.7	8.09	1.25 28.7	1.18 23.6	0.40 4.9	2.50 120	0.39 23.8	-0.06 261.0
7-10	3.58	243	2.5	8.19	0.77 17.7	1.17 23.4	0.19 2.3	1.62 77.8	0.44 26.8	+0.07 148.0

TEST: 8

$\rho_s = 1.63 \text{ grams/cc}$

$\omega_s = 21.2 \%$

$n_s = 0.345$

$\omega = 11.0 \%$

$\Delta\omega = 0.102$

$i = 1.20 \text{ in/hr}$

$k = 6.11 \times 10^{-11} \text{ cm}^2$

Sample	$\Delta t$ Hours since runoff begin	Conduct- ance $\mu\text{mhos/cm}$ 25°C	Sediment g/l	pH 25°C	Dissolved Solids milliequivalent/l / mg/l					
					Na <sup>+</sup>	Ca <sup>++</sup>	Mg <sup>++</sup>	SO <sub>4</sub> <sup>=</sup>	HCO <sub>3</sub> <sup>-</sup>	Total
8-1	-----	290	8.0	8.10	0.30	1.01	0.50	1.23	0.41	+0.17
8-2	0.117	2800	8.2	8.08	25.2	6.47	4.03	37.0	0.41	-1.71
8-3	0.367	805	4.7	8.21	4.81	3.78	1.21	9.05	0.43	+0.32
8-4	0.534	605	3.7	8.00	3.82	3.04	0.90	7.29	0.39	+0.08
8-5	1.62	340	4.0	8.31	1.78	1.42	0.47	3.29	0.45	-0.07
8-6	1.79	210	3.9	8.12	0.52	1.17	0.26	1.46	0.41	+0.09
8-7	2.29	174	3.3	7.99	0.24	0.92	0.33	1.04	0.38	+0.07
8-8	2.79	173	3.6	8.22	0.10	1.0	0.30	0.83	0.44	+0.13
8-9	3.62	169	3.5	8.14	0.11	0.91	0.20	0.75	0.37	+0.10



TEST: 9

$\rho_s = 1.63$  grams/cc

$\omega_s = 21.2\%$

$n_s = 0.345$

$\omega = 13.2\%$

$\Delta\omega = 0.080$

$i = 2.12$  in/hr

$k = 6.11 \times 10^{-11}$  cm<sup>2</sup>

Sample	$\Delta t$ Hours since runoff begin	Conduct- ance $\mu\text{mhos/cm}$ 25°C	Sediment g/l	pH 25°C	Dissolved Solids milliequivalent/l / mg/l					
					Na <sup>+</sup>	Ca <sup>++</sup>	Mg <sup>++</sup>	SO <sub>4</sub> <sup>=</sup>	HCO <sub>3</sub> <sup>-</sup>	Total
9-1	-----	1860	14.2	8.32	15.1 347	4.02 80.4	7.42 90.2	27.0 1297	0.43 26.2	-0.89 1840.8
9-2	0.0833	3640	5.5	8.21	43.2 994	4.88 97.6	12.4 151	58.2 2795	0.38 23.2	+1.90 4060.8
9-3	0.167	1160	5.5	8.26	3.25 74.7	4.29 85.8	1.81 22.0	9.15 440	0.41 25.0	-0.21 647.5
9-4	0.333	714	4.6	8.14	1.60 36.8	2.93 58.6	1.23 15.0	5.17 249	0.41 25.0	+0.18 384.4
9-5	0.580	320	4.8	8.20	0.87 20.0	1.77 35.4	0.49 6.0	2.83 136	0.42 25.6	-0.12 223.0
9-6	0.830	222	3.0	8.19	0.37 8.5	1.24 24.8	0.55 6.7	1.67 80.4	0.43 26.2	+0.06 146.6
9-7	1.330	182	2.5	8.19	0.30 6.9	1.09 21.8	0.28 3.4	0.96 46.2	0.39 23.8	+0.32 102.1
9-8	1.83	128	4.4	8.02	0.15 3.4	0.91 18.2	0.21 2.5	0.76 36.6	0.42 25.6	+0.09 86.3
9-9	2.33	129	3.6	8.11	0.09 2.1	0.99 19.8	0.19 2.3	0.79 38.0	0.40 24.4	+0.08 86.6
9-10	2.83	116	2.4	8.17	0.10 2.3	0.74 14.8	0.15 1.8	0.52 25.0	0.37 22.6	+0.10 66.5
9-11	3.83	117	3.2	8.13	0.07 1.6	0.75 15.0	0.08 1.0	0.48 23.1	0.41 25.0	+0.01 65.7
9-12	-----	83	-----	7.41	< 0.05 < 1.1	0.52 10.4	< 0.05 < 0.60	< 0.10 < 4.8	0.53 32.3	-0.01 42.7

TEST: 10

$\rho_s = 1.63 \text{ grams/cc}$

$\omega_s = 21.2 \%$

$\eta_s = 0.345$

$\omega = 16.5 \%$

$\Delta\omega = 0.047$

$i = 1.72 \text{ in/hr}$

$k = 6.11 \times 10^{-11} \text{ cm}^2$

Sample	$\Delta t$ Hours since runoff begin	Conduct- ance $\mu\text{mhos/cm}$ 25°C	Sediment g/l	pH 25°C	Dissolved Solids milliequivalent/l / mg/l					
					Na <sup>+</sup>	Ca <sup>++</sup>	Mg <sup>++</sup>	SO <sub>4</sub> <sup>=</sup>	HCO <sub>3</sub> <sup>-</sup>	Total
10-1	-----	473	12.0	8.26	0.57 13.2	2.87 59.5	0.69 8.4	3.35 161	0.42 25.6	+0.46 267.7
10-2	0.150	643	7.8	8.07	3.36 17.2	2.89 57.7	1.56 19.0	7.65 368	0.37 22.6	-0.21 544.5
10-3	0.350	322	6.1	8.02	0.70 16.1	1.46 29.2	0.81 10.2	2.74 132	0.37 22.6	-0.14 210.1
10-4	0.600	211	5.6	8.15	0.15 3.4	1.09 21.8	0.16 1.9	0.98 47.0	0.41 25.0	+0.01 99.1
10-5	0.850	203	5.3	8.21	0.11 2.6	1.05 21.0	0.26 3.2	1.00 48.0	0.36 22.0	+0.06 96.8
10-6	1.350	189	3.1	8.19	0.08 1.8	1.02 20.5	0.20 2.4	0.78 37.1	0.41 25.0	+0.11 86.8
10-7	1.85	179	2.7	8.24	<0.05 <1.1	0.00 18.0	0.11 1.3	0.68 32.6	0.42 25.6	-0.09 77.5

## APPENDIX D

### COMPUTER PROGRAM

This is the computer program used to predict the concentration of  $Mg^{++}$ ,  $SO_4^{=}$ ,  $Na^+$ ,  $Ca^{++}$ , and total dissolved solids (see Figures 22 and 23) in the percolation water (for a CDC 6400 computer), as discussed in Section VI.

```

PROGRAM MAIN(INPUT,OUTPUT,TAPE5=INPUT,TAPE6=OUTPUT)
DIMENSION C(11),RR(10),RI(10),R1(4),R2(4),DCA(50),DMG(50),DNA(50)
READ(5,30) SCA,SMG,SNA,SS04,SCL,CK1,CK2,CK3
30 FORMAT(RF10,9)
READ(5,31) ACA,AMG,ANA,BMG,BCA,BNA,BS04,UU,UUU
31 FORMAT(5F9.9,2F9.8,2F8.8)
I=R
BETA=2R40.0
MM=0
J=0
SSCA=SCA
SSNA=SNA
SSMG=SMG
SSS04=SS04
SANA=ANA
SACA=ACA
SAMG=AMG
SCA=SCA
SNA=SNA
SMG=SMG
SS04=SS04
U=UU
L=2
12 GO TO (201,202),L
202 SCA=SCA+BCA
SMG=SMG+BMG
SNA=SNA+BNA
SS04=SS04+BS04
ANA=SANA
ACA=SACA
AMG=SAMG
U=U+UUU
13 CALL EQUIL(SCA,SMG,SS04,SNA,ACA,AMG,ANA,CK3,U,CK1,CK2,BETA)
J=J+1
DCA(J)=ACA
DNA(J)=ANA
DMG(J)=AMG
IF(J-I) 12,10,10
10 WRITE(6,87) MM,SCA,SMG,SS04,SNA
87 FORMAT(1H0,13,20X*SCA*26X*SMG*27X*SS04*26X*SNA*/(4F30,10))
MM=MM+1
J=0
SSCA=SSCA
SSMG=SSMG
SSNA=SSNA
SSS04=SSS04
U=UU
201 J=J+1
IF(MM-10) 23,23,51
23 CONTINUE
L=1
ACA=DCA(J)
AMG=DMG(J)
ANA=DNA(J)
J=J-1
GO TO 13
51 CONTINUE
END

```

```

SUBROUTINE EQUIL (SCA,SMG,SSO4,SNA,ACA,AMG,ANA,CK1,CK2,BETA)
DIMENSION C(11),RR(10),RI(10),R1(4),R2(4),DCA(50),DMG(50),DNA(50)
IFLAG=0
1 C(1)=250.0*BETA**2*CK2**2
C(2)=-1000.0*BETA*CK2**2*(BETA*ACA+BETA*AMG+0.5*SNA)-0.5*BETA
C(3)=1000.0*BETA*CK2**2*(BETA*ACA**2+2.0*SNA*ACA+2.0*BETA*ACA*AMG+
72.0*SNA*AMG+BETA*AMG**2)-SCA-SMG-BETA*ANA+250.0*CK2**2*SNA**2
C(4)=-2000.0*BETA*CK2**2*(SNA*ACA**2+2.0*SNA*ACA*AMG+SNA*AMG**2)-A
4NA*(2.0*SCA+2.0*SMG+0.5*BETA*ANA)-1000.0*CK2**2*SNA**2*(AMG+ACA)
C(5)=1000.0*CK2**2*SNA**2*(ACA**2+2.0*ACA*AMG+AMG**2)-ANA**2*(SCA+
2SMG)
CALL RTSLV(C,4,RR,RI)
N=0
DO 50 I=1,4
WRITE(6,49) RR(I),RI(I)
49 FORMAT(1H0,25X*RR(I)*25X*RI(I)/(2F30.10))
IF (ABS(RI(I)).GT.1.E-05) GO TO 50
N=N+1
RI(N)=RR(I)
50 CONTINUE
IF(N.LT.1) GO TO 500
IF(IFLAG.GT. 0) GO TO 200
IFLAG = 1
XMIN=100.0
DO 70 I=1,N
70 XMIN = AMINJ (XMIN,R1(I))
X=XMIN
HOLD = X
GO TO 300
200 XMIN=100.0
DO 90 I=1,N
IF (ABS(R1(I)-HOLD).LT.XMIN) GO TO 80
XMIN = XMIN
GO TO 90
80 XMIN=ABS(R1(I)-HOLD)
M=I
90 CONTINUE
X=R1(M)
WRITE(6,48)X
48 FORMAT(1H0,25X*X*2X*:=*2X1F30.10)
HOLD=X
300 CONTINUE
A = BETA*(1.-CK1)
B=SCA+BETA*(AMG+CK1*ACA-0.5*CK1*X+0.5*X)+CK1*SMG
V=SCA*AMG-SMG*ACA*CK1+0.5*BETA*X*AMG+0.5*CK1*X*SMG
ARG= B**2-4.*A*V
Y=(-B+SQRT(ARG))/(2.*A)
SCA=SCA+BETA*(X/2.0 +Y)
SMG=SMG-BETA*Y
SNA=SNA-BETA*X
ACA=ACA-(X/2.0+Y)
AMG=AMG+Y
ANA=ANA+X
Z=0.
4 SCA1=SCA+Z
SSO41=SSO4+Z
UH=SQRT(2.*(SCA1+SSO41+SMG+0.25*SNA)+U)
II=1

```

```

100 BB=SCA+SS04
    CC=SCA*SS04-CKS*EXP(9.336*UH/(1.+UH))
    Z=(-BB+SQRT(BB*BB-4.*CC))*0.5
    IF(II.EQ.2) GO TO 102
101 AACA=SCA+Z
    SCA2=SCA+Z
    SS042=SS04+Z
    UH=SQRT(2.*(SCA2+SS042+SMG+0.25*SNA)+U)
    II=2
    GO TO 100
102 SCA2=SCA+Z
    IF(ABS(SCA2-AACA).GT.1.E-05) GO TO 4
    AAASCA=SCA
    SCA=SCA+Z
    SS04=SS04+Z
    17 IF(ABS(SCA2-AAA SCA).GT.1.E-04) GO TO 1
    GO TO 9050
500 WRITE(6,5001)
500) FORMAT(1H0,* NO REAL QUARTIC ROOTS*)
9050 CONTINUE
    RETURN
    END
    SUBROUTINE RTSLV (COE,N1,ROOTR,ROOTI)
    DIMENSION COE(11),ROOTR(10),ROOTI(10)
    N2=N1+1
    N4=0
    I=N1+1
19 IF(COE(I))9.7.9
    7 N4=N4+1
    ROOTR(N4)=0.
    ROOTI(N4)=0.
    I=I-1
    IF(N4-N1)19.37.19
    9 CONTINUE
10 AXR=0.8
    AXI=0.
    L=1
    N3=1
    ALP1R=AXR
    ALP1I=AXI
    M=1
    GOT099
11 BET1R=TEMR
    BET1I=TEMI
    AXR=0.85
    ALP2R=AXR
    ALP2I=AXI
    M=2
    GOT099
12 BET2R=TEMR
    BET2I=TEMI
    AXR=0.9
    ALP3R=AXR
    ALP3I=AXI
    M=3
    GOT099
13 BET3R=TEMR
    BET3I=TEMI

```

```

14 TE1=ALP1R-ALP3R
   TE2=ALP1I-ALP3I
   TE5=ALP3R-ALP2F
   TE6=ALP3I-ALP2I
   TEM=TE5*TE5+TE6*TE6
   TE3=(TE1*TE5+TE2*TE6)/TEM
   TE4=(TE2*TE5-TE1*TE6)/TEM
   TE7=TE3+1.
   TE9=TE3*TE3-TE4*TE4
   TE10=2.*TE3*TE4
   DE15=TE7*BET3R-TE4*BET3I
   DE16=TE7*BET3I+TE4*BET3R
   TE11=TE3*BET2R-TE4*BET2I+BET1R-DE15
   TE12=TE3*BET2I+TE4*BET2R+BET1I-DE16
   TE7=TE9-1.
   TE1=TE9*BET2R-TE10*BET2I
   TE2=TE9*BET2I+TE10*BET2R
   TE13=TE1-BET1R-TE7*BET3R+TE10*BET3I
   TE14=TE2-BET1I-TE7*BET3I-TE10*BET3R
   TE15=DE15*TE3-DE16*TE4
   TE16=DE15*TE4+DE16*TE3
   TE1=TE13*TE13-TE14*TE14-4.*(TE11*TE15-TE12*TE16)
   TE2=2.*TE13*TE14-4.*(TE12*TE15+TE11*TE16)
   TEM=SQRT (TE1*TE1+TE2*TE2)
   IF (TE1) 113,113,112
113 TE4=SQRT (.5*(TEM-TE1))
   TE3=.5*TE2/TE4
   GO TO 111
112 TE3=SQRT (.5*(TEM+TE1))
   IF (TE2) 110,200,200
110 TE3=-TE3
200 TE4=.5*TE2/TE3
111 TE7=TE13+TE3
   TE8=TE14+TE4
   TE9=TE13-TE3
   TE10=TE14-TE4
   TE1=2.*TE15
   TE2=2.*TE16
   IF (TE7*TE7+TE8*TE8-TE9*TE9-TE10*TE10) 204,204,205
204 TE7=TE9
   TE8=TE10
205 TEM=TE7*TE7+TE8*TE8
   TE3=(TE1*TE7+TE2*TE8)/TEM
   TE4=(TE2*TE7-TE1*TE8)/TEM
   AXR=ALP3R+TE3*TE5-TE4*TE6
   AXI=ALP3I+TE3*TE6+TE4*TE5
   ALP4R=AXR
   ALP4I=AXI
   M=4
   GO TO 99
15 N6=1
38 IF (ABS (HELL)+ABS (BELL)-1.E-10) 18,18,16
16 TE7=ABS (ALP3R-AXR)+ABS (ALP3I-AXI)
   IF (TE7/(ABS (AXR)+ABS (AXI))-1.E-7) 18,18,17
17 N3=N3+1

```

```

ALP1R=ALP2R
ALP1I=ALP2I
ALP2R=ALP3R
ALP2I=ALP3I
ALP3R=ALP4R
ALP3I=ALP4I
BET1R=BET2R
BET1I=BET2I
BET2R=BET3R
BET2I=BET3I
BET3R=TEMR
BET3I=TEMI
IF(N3-100)14,18,18
18 N4=N4+1
   ROOTR(N4)=ALP4R
   ROOTI(N4)=ALP4I
   N3=0
41 IF(N4-N1)30,37,37
37 RETURN
30 IF(ABS(ROOTI(N4))-1.E-5)10,10,31
31 GO TO(32,10),L
32 AXR=ALP1R
   AXI=-ALP1I
   ALP1I=-ALP1I
   M=5
   GO TO 99
33 BET1R=TEMR
   BET1I=TEMI
   AXR=ALP2R
   AXI=-ALP2I
   ALP2I=-ALP2I
   M=6
   GO TO 99
34 BET2R=TEMR
   BET2I=TEMI
   AXR=ALP3R
   AXI=-ALP3I
   ALP3I=-ALP3I
   L=2
   M=3
99 TEMR=COE(1)
   TEMI=0.0
   DO100I=1,N1
   TE1=TEMR*AXR-TEMI*AXI
   TEMI=TEMI*AXR+TEMR*AXI
100 TEMR=   TE1+COE(I+1)
   HELL=TEMR
   BELL=TEMI
42 IF(N4)102,103,102
102 DO101I=1,N4
   TEM1=AXR-ROOTR(I)
   TEM2=AXI-ROOTI(I)
   TE1=TEM1*TEM1+TEM2*TEM2
   TE2=(TEMR*TEM1+TEMI*TEM2)/TE1
   TEMI=(TEMI*TEM1-TEMR*TEM2)/TE1
101 TEMR=TE2
103 GO TO(11,12,13,15,33,34),M
END

```



<b>1</b> Accession Number	<b>2</b> Subject Field & Group 05E	<b>SELECTED WATER RESOURCES ABSTRACTS INPUT TRANSACTION FORM</b>
---------------------------	---------------------------------------	----------------------------------------------------------------------

<b>5</b> Organization	Sanitary Engineering Program, Department of Civil Engineering, Colorado State University, Fort Collins, Colorado 80521
-----------------------	------------------------------------------------------------------------------------------------------------------------

<b>6</b> Title	WATER POLLUTION POTENTIAL OF RAINFALL ON SPENT OIL SHALE RESIDUES
----------------	-------------------------------------------------------------------

<b>10</b> Author(s) Ward, John C. Margheim, Gary A. L8f, George O. G.	<b>16</b> Project Designation EPA, WQO Grant No. 14030EDB	<b>21</b> Note A companion report to this report entitled, "Water Pollution Potential of Snowfall on Spent Oil Shale Residues," is in preparation.
--------------------------------------------------------------------------------	--------------------------------------------------------------	-------------------------------------------------------------------------------------------------------------------------------------------------------

<b>22</b> Citation	Water Pollution Control Research Series, Water Quality Office, Environmental Protection Agency, 1971
--------------------	------------------------------------------------------------------------------------------------------

<b>23</b> Descriptors (Starred First)	*Salinity, *Oil Shale, *Colorado River, *Colorado, *Sodium Sulfate, *Rainfall Simulators, Capillary action, Snowfall, Erosion Control, Soil Temperature, Water Analysis, Soil Chemistry, Soil Water Movement, Overland Flow, Rainfall Intensity, Porous Media
---------------------------------------	---------------------------------------------------------------------------------------------------------------------------------------------------------------------------------------------------------------------------------------------------------------

<b>25</b> Identifiers (Starred First)	*Water Quality Hydrology, *Ion Activity Electrodes, Specific Conductance, Soil Evaporation, TOSCO II Process, Piceance Basin, Parachute Creek
---------------------------------------	-----------------------------------------------------------------------------------------------------------------------------------------------

<b>27</b> Abstract	Physical properties, including porosity, permeability, particle size distribution, and density of spent shale from three different retorting operations, (TOSCO, USBM, and UOC) have been determined. Slurry experiments were conducted on each of the spent shales and the slurry analyzed for leachable dissolved solids. Percolation experiments were conducted on the TOSCO spent shale and the quantities of dissolved solids leachable determined. The concentrations of the various ionic species in the initial leachate from the column were high. The major constituents, $SO_4^{=}$ and $Na^+$ , were present in concentrations of 90,000 and 35,000 mg/l in the initial leachate; however the succeeding concentrations dropped markedly during the course of the experiment. A computer program was utilized to predict equilibrium concentrations in the leachate from the column. The extent of leaching and erosion of spent shale, and the composition and concentration of natural drainage from spent shale has been determined using oil shale residue and simulated rainfall.
--------------------	----------------------------------------------------------------------------------------------------------------------------------------------------------------------------------------------------------------------------------------------------------------------------------------------------------------------------------------------------------------------------------------------------------------------------------------------------------------------------------------------------------------------------------------------------------------------------------------------------------------------------------------------------------------------------------------------------------------------------------------------------------------------------------------------------------------------------------------------------------------------------------------------------------------------------------------------------------------------------------------------------------------------------------------------------------------------------------------------------

Concentrations in the runoff from the spent shale have been correlated with runoff rate, precipitation intensity, flow depth, application time, slope, and water temperature. This report was submitted in fulfillment of Grant No. 14030EDB under the sponsorship of the Water Quality Office, Environmental Protection Agency.

Abstractor John C. Ward	Institution Colorado State University
----------------------------	------------------------------------------